ELASTIC FLEXURAL-TORSIONAL BUCKLING ANALYSIS OF DOUBLY-SYMMETRICAL WEB-TAPERED I-BEAMS

by

Shuai Zhu

B.S., Wuhan University, 2007

Submitted to the Graduate Faculty of the

Swanson School of Engineering in partial fulfillment

of the requirements for the degree of

Master of Science

University of Pittsburgh

2009

UNIVERSITY OF PITTSBURGH

SWANSON SCHOOL OF ENGINEERING

This thesis was presented

by

Shuai Zhu

It was defended on

Oct. 5, 2009

and approved by

Kent A. Harries, Associate Professor,
Department of Civil and Environmental Engineering

John F. Oyler, Adjunct Associate Professor,
Department of Civil and Environmental Engineering

Morteza A. M. Torkamani, Associate Professor,
Department of Civil and Environmental Engineering,
Thesis Advisor

ELASTIC FLEXURAL-TORSIONAL BUCKLING ANALYSIS OF DOUBLY-SYMMETRICAL WEB-TAPERED I-BEAMS

Shuai Zhu, M.S.

University of Pittsburgh, 2009

In structural steel design, flexural-torsional buckling (FTB) is an important limit state that must be considered, especially in thin-walled members. A thin-walled beam loaded in its plane of symmetry bends in-plane of loading, however, it may fail because of the flexural-torsional buckling, where the beam suddenly deflects and twists out of the loading plane. This type of failure occurs suddenly in members with a much greater in-plane bending stiffness than torsional or lateral bending stiffness. In this paper, the finite element approach in conjunction with the energy method is employed to predict the flexural-torsional buckling loads of a doubly symmetric and web-tapered I-beam.

The total potential energy of the flexural-torsional buckling of a beam element is formulated by adding the strain energy to the potential energy of the external forces. To apply the finite element approach, the displacement function of an element is assumed to be cubic polynomials, the variational principle is then applied to the total potential energy equation. Rearrangement of the energy equation leads to the elastic and geometric stiffness matrices. To apply this methodology to the analysis of plane structures, the rotation transportation matrix is applied to both element elastic and geometric stiffness matrices to convert them from the local to a global coordinate system. Through the assembly process of

stiffness matrices of each element, with respect to the global degree of freedom, the equilibrium equation of the whole structure is formed, which leads to a generalized eigenvalue problem.

In out-of-plane stability problems, in-plane deflections are normally assumed to be neglected if the ratio of the minor axis flexural and torsional stiffness to the major axis flexural stiffness is small. The effects of prebuckling are also required when accurate solutions are needed.

Due to the compatibility between the finite element approach and programming, computer technology is utilized in the analysis to extend the application of the method developed in this paper to much more complex structures, which involves enormous computations. Object-oriented technology in C++ is employed to help organize the programming process. Several examples are presented to compare the results to show the efficiency of developed principles.

TABLE OF CONTENTS

LIST OF TABLES

LIST OF FIGURES

NOMENCLATURE

Symbol	Description
A	Area of member
a	distributed load height
$[C]$	Cholesky matrix
$\{D\}$	global nodal displacement vector for the structure
$\{D_e\}$	global nodal displacement vector for an element
$\{d_e\}$	local nodal displacement vector for an element
E	modulus of elasticity
e	concentrated load height
F	axial load
F_i	axial loads at node i
F_j	axial loads at node j
G	*sh*ear modulus
h	depth of the member
h_i	depth of the member at node i
h_j	depth of the member at node j
$[I]$	identity matrix
I_x	moment of inertia about the *x*- axis

I_n	moment of inertia about the *n*- axis
I_y	moment of inertia about the *y*- axis
I_ω	warping moment of inertia
J	torsional constant
k_z	torsional curvature of the deformed element
$[K_e]_{web}$	web global elastic stiffness matrix
$[K_e]_{flange}$	flange global elastic stiffness matrix
$[K_e]$	structure global elastic stiffness matrix
$[K_g]$	structure global geometric stiffness matrix
L	member length
L_f	member length of the flange
M_x	bending moment about *x*- axis
M_i	moment at node i of the web
M_{if}	moment at node i of the flange
M_j	moment at node j of the web
M_{jf}	moment at node j of the flange
$[N]$	shape function matrix
P	concentrated load
q	distributed load
$[T_e]$	transformation matrix
t_p	perpendicular distance to P from the mid-thickness surface
U	strain energy
U_e	strain energy for each finite element
u	out-of-plane lateral displacement
u_p	out-of-plane lateral displacement

	of point P
u_q	out-of-plane lateral displacement of point Q
u_i ,u_j	out-of-plane lateral displacements at nodes i and j
u'	out-of-plane rotation
V_i	shear at node i of the web
V_{if}	shear at node i of the flange
V_j	shear at node j of the web
V_{jf}	shear at node j of the flange
v	in-plane bending displacement
v_P	displacement through which the concentrated load acts
v_q	displacement through which the distributed load acts
v'	in-plane rotation
w	axial displacement
w_F	longitudinal displacement through which the axial load acts
w_p	longitudinal displacement of point P_o
z_P	concentrated load location from left support
α_0	tapered angle
ε_p	longitudinal strain of point P_o
ϕ	out-of-plane twisting rotation
ϕ'	out-of-plane torsional curvature
γ_p	shear strain of point P_o
λ	buckling parameter
Π	total potential energy

σ_p	longitudinal stress of point P_o
τ_p	shear stress of point P_o
ω	warping function
Ω	potential energy of the loads
θ	rotation of the member cross section

1.0 INTRODUCTION

Thin-walled structural elements having cross sections such as I, T, L, and C, with isotropic or anisotropic composite materials are extensively used as beams, columns, and beam-columns in engineering applications, ranging from buildings, bridges to aerospace and many other engineering fields where requirements of a high performance in terms of minimum weight for a given strength are of importance. Due to their particular shapes resulting from the fabrication process, these elements always have open cross sections that make their behavior highly sensitive to torsion, instabilities and imperfections (Mohri et al. 2003 and 2008). The buckling behavior of thin-walled structures and structural elements is very complex due to the coupling effect of compression, bending, and torsional deformations.

Presently, web-tapered thin-walled I-beams are used extensively in engineering construction due to their structural and economic efficiency. The stability issue concerning this type of structure has been receiving increased attention from engineers and researchers. To take full advantage of the benefits of tapered beams, a design engineer has to be equipped with reliable and efficient methods of analysis to give accurate predictions of the tapered structure behavior. Lee et al. (1975) studied the behavior of tapered members extensively, and their work was adopted in Appendix F3 of the AISC specification (Manual 1994). At present, the general design approach used in the AISC Specification (Manual 2009) for the

design of web-tapered beams is to apply modification factors to convert the tapered members into appropriately proportioned prismatic members in order that the prismatic LRFD beam equations may be applied. This procedure is mostly applicable to a simple analysis of tapered members. Therefore, there is a need to investigate and understand the behavior of tapered beams to develop a method that aids engineers to use numerical methods to analyze more complex tapered structures.

With recent advances and new development in computing technologies, complex problems that were almost impossible to solve by the classical methods now can effectively be solved using the numerical approach. Among many numerical methods, the finite element method is one of the most powerful in handling complicated loadings, boundary conditions and geometry. Furthermore, the finite element method is compatible with the software development, because it implements in the matrix form that is suitable to use in the discretized calculation.

The intent of this paper is to illustrate the practical application of the finite element method in the flexural-torsional buckling analysis of doubly symmetric web-tapered I-beams. A tapered I-beam is synthesized from two rectangular flat plates for flanges and a tapered flat plate for the web, these plates form a rigid cross-section for the beam. The total potential energy equation of the tapered I-beam is directly formulated from summing all the sub-potential energy equations of these narrow beams.

2.0 LITERATURE REVIEW

2.1 FLEXURAL-TORSIONAL BUCKLING

The first theoretical research into elastic flexural-torsional buckling problem was preceded by Euler's 1759 treatise on column flexural buckling, which gave the first analytical method to predict the reduced strengths of slender columns, and by Saint Venant's 1855 memoir on uniform torsion, which gave the first reliable description of twisting response of members to torsion (Trahair 1993). However, it was not until 1899 that the first published discussions of flexural-torsional buckling were made by Prandtl (1899) and Michell (1899), who considered the lateral buckling of beams with narrow rectangular cross-sections.

Subsequent work by Wagner (1929) and later work by Bleich (1952) and also by Timoshenko and Gere (1961) led the development of a general theory of flexural-torsional buckling. They provided the classical energy equation for calculating the elastic flexural-torisonal buckling loads of thin-walled beams.

Galambos (1963) introduced inelastic behavior of the flexural-torsional buckling; similar research was also presented by Lee (1960), White (1956), Wittrick (1952), and Horne (1950). All of these researches were done using the classical method, which provided exact solutions, yet it is limited by the necessity to make extensive calculations by hand.

This situation changed dramatically with the advent of digital computers in the 1960's. Researchers used numerical approaches that worked well with computers. There were many publications on various numerical approaches, such as Rayleigh Ritz method by Wang (1994), the finite difference method by Bleich (1952), Assadi and Roeder (1985), and Chajes (1993), and the finite integral method by Trahair (1968), Anderson and Trahair (1972), and Kitipornchai and Trahair (1975).

The finite element method was introduced by Barsoum and Gallagher (1970), in which they derived the stiffness equations for flexural-torsional instabilities of one-dimensional members with constant cross sections. During the later research, Powell and Klingner (1970) presented a lateral buckling analysis of an I-section beam, Hancock and Trahair (1978) considered the lateral buckling analysis of a monosymmetric cross-section beam with continuous restraints, Sallstrom (1996), Bradford and Ronagh (1997), and Papangelis et al. (1998) calculated the flexural-torsional buckling loads of beams, beam-columns, and plane frames, and Bazeos and Xykis (2002) presented research using the finite element method to analyze three dimensional trusses and frames.

More recent research on the theory of flexural-torsional buckling has been presented by Tong and Zhang (2003a) and (2003b) with their investigations of a new theory to clarify the inconsistencies of existing theories of the flexural-torsional buckling of thin-walled members. Torkamani and Roberts (2009) studied the elastic flexural-torsional buckling analysis of plane structures by considering second variation of the total potential energy of beam-column element and finite element method.

Many of the developments of the flexural-torsional buckling theory have been made by extensions of the previously accepted theories, as expressed either by the differential equations of elastic bending and torsion or by energy equation for buckling. The classical energy equations for calculating the elastic flexural-torsional buckling load of thin-walled beams are usually assumed to be independent of the prebuckling deflections.

2.2 FLEXURAL-TORSIONAL BUCKLING OF TAPERED STRUCTURES

The static analysis of thin-walled beams with variable cross-section can be dated back to the early works in 1960s by Cywinski (1964), Bazant (1965), Lee (1967) and Wilde (1968). During that period, researchers carried out extensive analytical works for the torsional response of tapered beams.

Later on, the first study on the flexural-torsional buckling of doubly and singly symmetric tapered I beams was conducted by Kitipornchai and Trahair (1972, 1975), who described the tapering effect of web-depth on the lateral buckling of tapered I-beams due to the transverse loads that their positions of application are above and below the shear centers. In recent years, with the rapid growth of high-performance computers, the finite element method has primarily become an efficient tool for dealing with the numerical analysis of complex structural problems. Yang and Yau (1987), Bradford and Cuk (1988) developed a general finite element model to investigate the instability of a doubly symmetric tapered I-beam subjected to various loads. Taking account of the rotational nature of applied end

torques, Yau et al. (1992) derived some closed form solutions for the buckling of torsionally loaded bars with various variable circular cross-sections by an analytical method. Starting from Yang and Kuo's elasticity approach (1994), Yang et al. (1996) presented an incremental equation of equilibrium for a straight tapered solid beam, in which the effects of instability caused by the initial forces acting on the beam element in deformed position have all been taken into consideration. One feature of Yang et al.'s buckling theory (1994, 1996) is that no assumption concerning the retaining and omission of higher-order terms was made in the expression of potential energy. Based on the membrane theory of shell and Valsov's (1961) assumption of negligible shear strain in the middle surface of thin-walled section, Wekezer (1985) and Rajasekaran (1994) derived the nonlinear equations for the buckling and dynamic stability analyses of tapered beams with general thin-walled open cross-section. However, such formulations were shown to be inconsistent, because either the shear center locations were not adequately handled or the derivation of the nonlinear strain and displacement relations omitted relevant terms (Andrade et al. 2005).

Pasquino and Marotti-de-Sciarra (1992) and Ronagh et al. (2000) adopted variational principle to develop a finite element model of thin-walled members with variable open cross-section for lateral stability analysis and obtained expressions for the first and second variations of the beam total potential energy. This theory was solely specified and numerically implemented for doubly symmetric cross-sections and then applied to study the flexural-torsional buckling of webs and flange-tapered simply supported I-beams and cantilevers acted by point loads (Andrade et al. 2005). Andrade and Camotim (2007) extend

this application of the general variational formulation to the study of the lateral-torsional buckling of singly symmetric thin-walled tapered beams using the finite element method. They presented derivation, and validate and illustrate the application. And recently, Zhang and Tong (2008) analyzed the lateral buckling of web-tapered I-beams and developed the total potential energy equations based on the classical variational principle for buckling analysis.

In this work, a tapered I-beam is synthesized from three flat plates: the top flange, the web, and the bottom flange. As a result, the total potential energy equation of a tapered I-beam can be formulated by summing up all the sub-potential energy equations of the three flat plates. The elastic and geometric stiffness matrices of a tapered I-beam element may be obtained from the total potential energy equation derived using finite element method.

3.0 FLEXURAL-TORSIONAL BUCKLING THEORY

Beams, which are loaded in their minor principal plane and have smaller lateral and torsional stiffness compared to their in-plane of loading stiffness or that have inadequate lateral restraints, may buckle out of plane of the transverse load. For a perfectly straight, elastic beam, there are no out-of-plane deformations until the load reaches a critical value, at which point the beam buckles by deflecting laterally and twisting. The lateral deflection and twisting are interdependent. When the beam deflects laterally, the induced moment exerts a component torque about the deflected longitudinal axis which causes the beam to twist. Such buckling behavior has been referred to as flexural-torsional buckling. Flexural-torsional buckling may significantly decrease the load capacity of a member; therefore, it is important to obtain the flexural-torsional buckling loads of a member to provide an upper limit on the member's strength.

To solve the problem effectively, a mathematical model is created based on the following assumptions.

1. The entire structure remains elastic prior buckling. In order to achieve this, we assume that the members are long and slender. It is assumed that $I_x > I_y$ for entire length of the beam.

2. The cross-sections of the members of the structure are doubly symmetric.

3. The member of the structure is perfectly straight and free of imperfection. The plane of the cross section does not distort after buckling.

4. The axial displacement and the bending displacements are small and are thus neglected.

5. The material properties do not change.

6. Local buckling of any member of the structure is not considered.

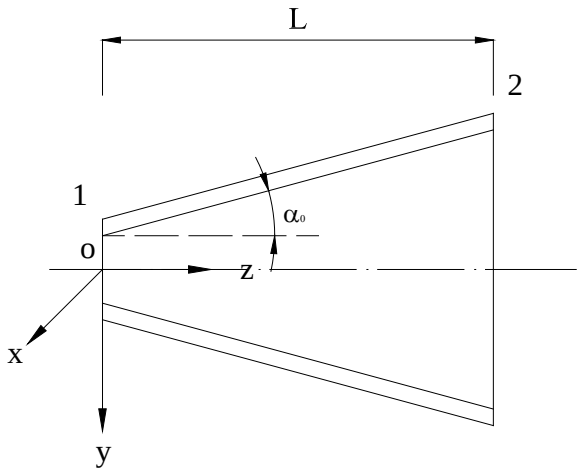

Figure 3.1 Coordinate System

A member loaded in the yz plane will have an in-plane displacement, v, and in-plane rotation v'. If the member is loaded along the z axis it will also have an axial displacement, w. Flexural-torsional buckling will cause an out-of-plane displacment of the member, u, an out-of-plane rotation, u', an out-of-plane twisting rotation, φ, and an out-of-plane torsional curvature, ϕ'. The prime indicates the first derivative with respect to

z. Figure 3.1 shows the elevation view of a doubly-symmetric web-tapered I-beam with its coordinate system, and Figure 3.2 shows the cross section and displacements u, v, and φ. Figure 3.3 (a) shows the out-of-plane lateral displacement and rotation. Figure 3.3 (b) shows the in-plane displacements, in-plane rotations, and out-of-plane twisting rotation.

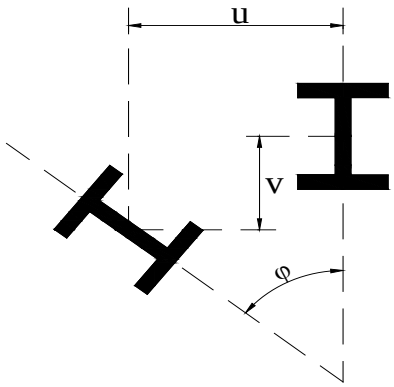

Figure 3.2 Cross Section View Displacements

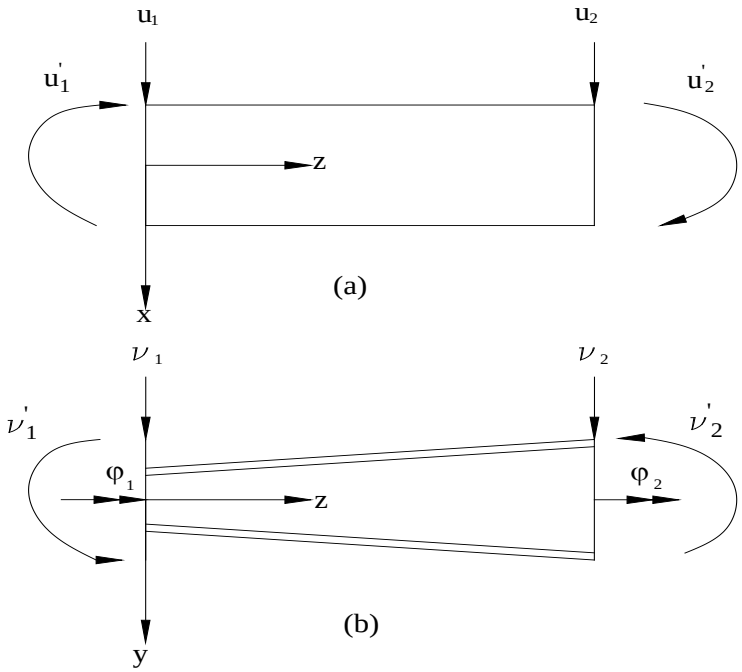

Figure 3.3 Displacements, (a) Top View Displacements, (b) Side View Displacements

It is assumed that the axial displacement, w, the in-plane bending displacement, v, and in-plane bending rotation, v', are small and neglected in buckling load calculations. Only the out-of-plane displacements, u, out-of-plane rotations, u', out-of-plane twisting rotation, φ, and out-of-plane torsional curvature, φ', will be considered to derive the energy equation.

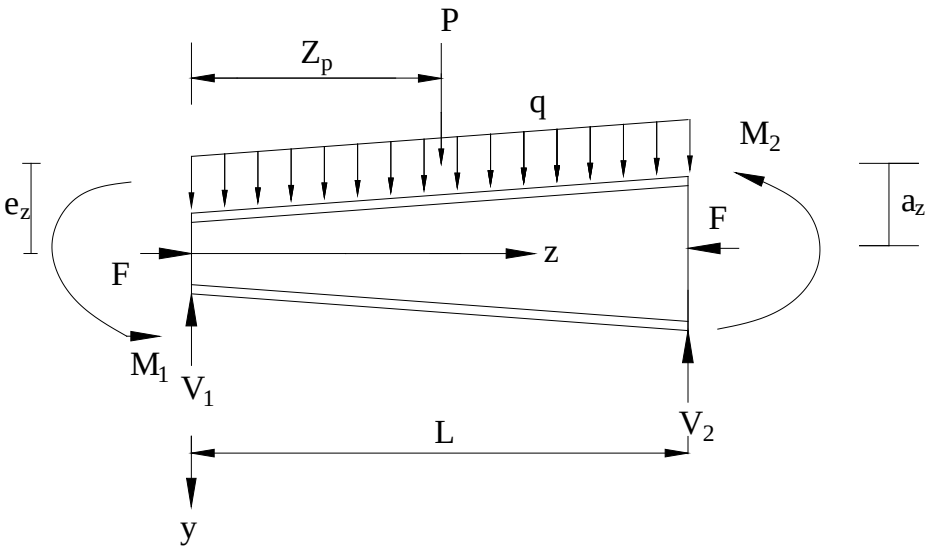

Figure 3.4 External Loads and Member End Actions of the Beam Element

Figure 3.4 shows the loading conditions and corresponding end actions of a web-tapered I-beam element. The element has three applied loads: (1) a distributed load, q, (2) a concentrated load, P, and (3) an axial load F. The distributed load is applied at a height a_z from the centroid of the cross section, which is a function of z; and the concentrated load is applied at a height of e_z from the centroid of the cross section with a distance z_p from the left end of this beam element. The element experiences four end actions: the shears V_1, V_2, and the moments M_1, M_2.

3.1 DERIVATION OF ENERGY EQUATIONS

The total potential energy, $\prod$, of a structure is the sum of the strain energy, U, and the potential energy of the external loads, Ω, which leads to the energy equation given by

$$\prod = U + \Omega \tag{3-1}$$

The theorem of stationary total potential energy states that of all kinematically admissible deformations, the actual deformations (those which correspond to stresses which satisfy equilibrium) are the ones for which the total potential energy assumes a stationary value, i.e., the extreme value (Pilkey et al. 1994)

$$\delta \prod = 0 \tag{3-2}$$

The second variation of the total potential energy equals to zero indicates the transition from a stable state to an unstable state (Pi et al. 1992(a)), which is the critical condition for buckling and can be expressed as

$$\frac{1}{2}\delta^2 \prod = 0 \tag{3-3a}$$

therefore, the equilibrium position is stable when

$$\frac{1}{2}\delta^2 \prod \geq 0 \tag{3-3b}$$

And the equilibrium position is unstable when

$$\frac{1}{2}\delta^2 \prod \leq 0 \tag{3-3c}$$

Substituting in for the strain energy and the potential energy of the external loads from Eq. (3-3a) gives

$$\frac{1}{2}(\delta^2 U + \delta^2 \Omega) = 0 \tag{3-4}$$

3.1.1 Strain Energy

An arbitrary point P_0 on a cross section of the member is considered, and the strain energy, U, in total potential energy equation of Eq. (3-1) can be expressed as

$$U = \frac{1}{2}\iint_{LA} (\varepsilon_P \sigma_P + \gamma_P \tau_P) dA dz \tag{3-5}$$

Where

ε_P = longitudinal strain of point P_0

σ_P = longitudinal stress of point P_0

γ_P = shear strain of point P_0

τ_P = shear stress of point P_0

The second variation of Eq. (3-5) is

$$\frac{1}{2}\delta^2 U = \frac{1}{2}\iint_{LA} (\delta\varepsilon_P \delta\sigma_P + \delta\gamma_P \delta\tau_P + \delta^2\varepsilon_P \sigma_P + \delta^2\gamma_P \tau_P) dA dz \tag{3-6}$$

The strains of point P_0 are defined in terms of the deformations of this point. The longitudinal finite normal strain may be expressed as (Boresi et al. 1993)

$$\varepsilon_P = \frac{dw_p}{dz} + \frac{1}{2}[(\frac{du_p}{dz})^2 + (\frac{dv_p}{dz})^2 + (\frac{dw_p}{dz})^2] \tag{3-7}$$

Where

u_P = the out-of-plane of loading lateral displacement at point P_0 on the cross section.

v_P = the in-plane of loading bending displacement at point P_0 on the cross section

w_P = the longitudinal displacement at point P_0 on the cross section

The longitudinal displacement w_P is assumed to be small compared to the other displacements, that is, $(\frac{dw_p}{dz})^2$ is small compared to $(\frac{du_p}{dz})^2$ and $(\frac{dv_p}{dz})^2$. Therefore, Eq. (3-7) can be simplified to

$$\varepsilon_P = \frac{dw_p}{dz} + \frac{1}{2}[(\frac{du_p}{dz})^2 + (\frac{dv_p}{dz})^2] \tag{3-8}$$

The shear strain due to bending and warping of the thin-walled section may be disregarded. The shear strain at point P_0 of the cross section due to St. Venant torsion can be defined as (Vlasov 1961)

$$\gamma_P = \gamma_{st} = -2t_P \frac{d\phi}{dz} \tag{3-9}$$

The term t_P is the perpendicular distance of point P_0 from the mid-thickness line of the cross-section. The first and the second variation of the shear strain are

$$\delta\gamma_P = -2t_P \frac{d\delta\phi}{dz} \tag{3-10}$$

$$\delta^2\gamma_P = 0 \tag{3-11}$$

3.1.2 Displacements

The displacements u_P, v_P, and w_P of point P_0 on the cross section need to be defined in terms of the centroidal deformations u, v, and w. The deformation of an element is shown in Figure 3.5. The coordinates $oxyz$ represents a fixed global coordinate system where point o is located at the beginning of the undeformed element. The ox and oy axes coincide with the principal axes of the undeformed element. The oz axis is oriented along the length of the element and passes through the element's centroid. The point P_0 is defined as an arbitrary point on the cross section of the element. The coordinate $\hat{o}\hat{x}\hat{y}\hat{z}$ represents a moving, right-handed, local coordinate system which is fixed at a point $\hat{o}$ on the centroidal axis of the beam and moves with the beam as it deforms. The axis $\hat{o}\hat{z}$ corresponds to the tangent at $\hat{o}$ to the deformed centroidal axis. The $\hat{o}\hat{x}$ and $\hat{o}\hat{y}$ axes are the principal axes of the deformed element. The coordinates of point P_0 are $(\hat{x}, \hat{y}, 0)$ with respect to the local coordinate system.

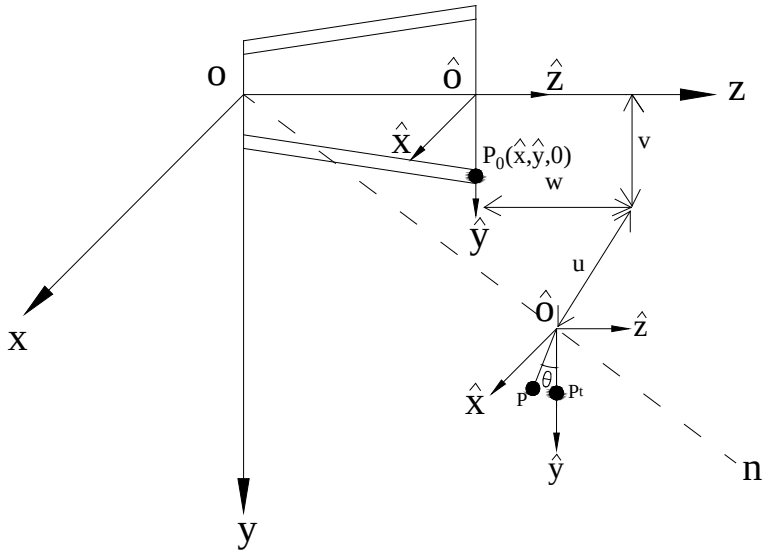

Figure 3.5 Deformed Element

When the element buckles, point P_0 moves to the point P. This deformation occurs in two pages: (1) the point P_0 translates to point P_t, and (2) the point P_t rotates through the angel θ to point P. The point P_0 translates to point P_t by the displacements u, v and w. This translation takes the local coordinate system $\hat{o}\hat{x}\hat{y}\hat{z}$ to a new location as shown in Figure 3.5. The point P_t then rotates through an angle θ to the point P about the line on where on is a line passing through the points o and $\hat{o}$. The rotation takes the local coordinate system $\hat{o}\hat{x}\hat{y}\hat{z}$ to its final location. The direction cosines of the axes $\hat{o}\hat{x}$, $\hat{o}\hat{y}$, and $\hat{o}\hat{z}$ relative to the fixed global coordinate $oxyz$ can be determined by considering a rigid body rotation.

The equation expressing the relationship between the displacements of an arbitrary point P_0 on the cross section and the displacements at the centroid of the cross section is (Torkamani 1998)

$$\begin{Bmatrix} u_p \\ v_p \\ w_p \end{Bmatrix} = \begin{Bmatrix} u \\ v \\ w \end{Bmatrix} + [T_R] \begin{Bmatrix} \hat{x} \\ \hat{y} \\ -\omega k_z \end{Bmatrix} - \begin{Bmatrix} x \\ y \\ 0 \end{Bmatrix} \tag{3-12}$$

Where

u = the out-of-plane of loading displacement at the centroid of the cross section.

v = in-plane of loading displacement at the centroid of the cross section

w = longitudinal displacement at the centroid of the cross section

$\hat{x}$ = x-coordinate of the point P_0

$\hat{y}$ = y-coordinate of the point P_0

k_z = torsional curvature of the deformed element

ω = warping function (Pi et al. 1992(b))

$[T_R]$ = rotation transformation matrix

The first term on the right side in Eq. (3-12) stands for the translation from the point P_0 to P_t. The combination of the second and the third term represents the rotation part of the total displacement due to the rotation θ. $-\omega k_z$ is the warping displacement defined as the deformation in z direction. $[T_R]$ is the rotation transformation matrix giving the direction cosines of the rotated axes $\hat{o}\hat{x}$, $\hat{o}\hat{y}$, and $\hat{o}\hat{z}$ relative to the fixed axes ox, oy, and oz by considering a rigid body rotation of the axes through an angle θ about the axis on.

From Appendix A, the rotation transformation matrix $[T_R]$ can be expressed for small angles of rotation as

$$[T_R]=\begin{bmatrix} 1-\frac{\theta_y^{\,2}}{2}-\frac{\theta_z^{\,2}}{2} & -\theta_z+\frac{\theta_x\theta_y}{2} & \theta_y+\frac{\theta_x\theta_z}{2} \\ \theta_z+\frac{\theta_x\theta_y}{2} & 1-\frac{\theta_x^{\,2}}{2}-\frac{\theta_z^{\,2}}{2} & -\theta_x+\frac{\theta_y\theta_z}{2} \\ -\theta_y+\frac{\theta_x\theta_z}{2} & \theta_x+\frac{\theta_y\theta_z}{2} & 1-\frac{\theta_x^{\,2}}{2}-\frac{\theta_y^{\,2}}{2} \end{bmatrix} \tag{3-13}$$

where θ_x, θ_y, and θ_z are the components of the rotation θ in the x-, y-, and z- axes, respectively.

$$\theta_x=\theta\cos\alpha \tag{3-14}$$

$$\theta_y=\theta\cos\beta \tag{3-15}$$

$$\theta_z=\theta\cos\gamma \tag{3-16}$$

where α, β, and γ are the angles between the rotational axis and x-, y-, and z- axes, respectively; θ is the rotation of the cross-section about the rotational axis.

Considering the undeformed element Δz and the deformed element $\Delta z(1+\varepsilon)$, where ε is the strain. The deformed element $\Delta z(1+\varepsilon)$ has components Δu, Δv, and $(\Delta z+\Delta w)$ on the ox, oy, and oz axes, respectively, as shown in Figure 3.6.

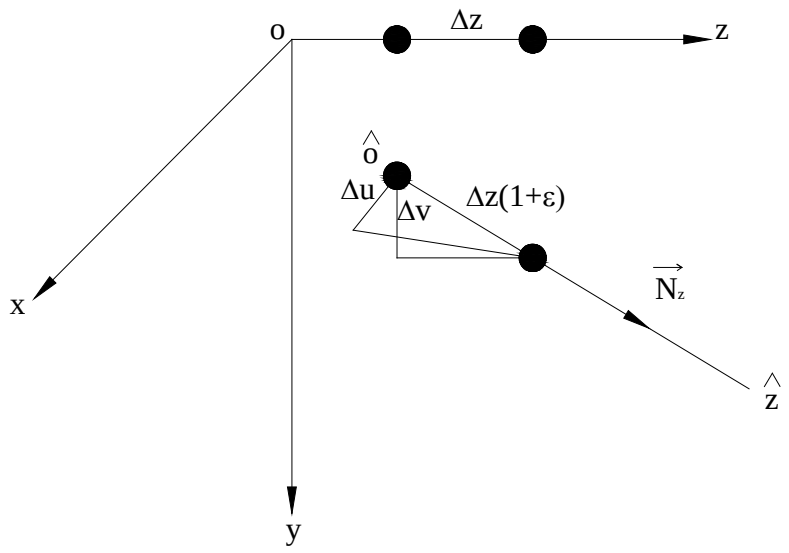

Figure 3.6 Undeformed Element Δz and Deformed Element $\Delta z(1+\varepsilon)$

If $\vec{N}_z$ is a unit vector in the $\hat{o}\hat{z}$ direction and l_z, m_z, and n_z are the directional cosines of the $\hat{o}\hat{z}$ axis with respect to the *oxyz* coordinate system, then the deformed element may be expressed as

$$\Delta z(1+\varepsilon)\vec{N}_z = \Delta u \cdot \vec{i} + \Delta v \cdot \vec{j} + (\Delta z + \Delta w) \cdot \vec{k} \tag{3-17}$$

The projections of vector $\Delta z(1+\varepsilon)\vec{N}_z$ on the x- and y- axes are

$$\Delta u = \Delta z(1+\varepsilon)\vec{N}_z \cdot \vec{i} = \Delta z(1+\varepsilon)l_z \tag{3-18}$$

$$\Delta v = \Delta z(1+\varepsilon)\vec{N}_z \cdot \vec{j} = \Delta z(1+\varepsilon)m_z \tag{3-19}$$

Divide Eqs. (3-17) and (3-18) by Δz, and take the limit as Δz approaching zero, these equations become

$$\frac{du}{dz} = \lim_{\Delta z \to 0} \frac{\Delta u}{\Delta z} = \lim_{\Delta z \to 0} \frac{\Delta z(1+\varepsilon)l_z}{\Delta z} = (1+\varepsilon)l_z \tag{3-20}$$

$$\frac{dv}{dz} = \lim_{\Delta z \to 0} \frac{\Delta v}{\Delta z} = \lim_{\Delta z \to 0} \frac{\Delta z(1+\varepsilon)m_z}{\Delta z} = (1+\varepsilon)m_z \tag{3-21}$$

From Appendix A, we have $l_z = \theta_y + \frac{\theta_x \theta_z}{2}$ and $m_z = -\theta_x + \frac{\theta_y \theta_z}{2}$

Therefore, the out-of-plane of loading rotation $\frac{du}{dz}$ and the in-plane of loading rotation $\frac{dv}{dz}$ can be defined as

$$\frac{du}{dz} = (\theta_y + \frac{\theta_x \theta_z}{2})(1+\varepsilon) \tag{3-22}$$

$$\frac{dv}{dz} = (-\theta_x + \frac{\theta_y \theta_z}{2})(1+\varepsilon) \tag{3-23}$$

By disregarding higher order term ε, Eqs. (3-21) and (3-22) simplify to

$$\frac{du}{dz} = \theta_y + \frac{\theta_x \theta_z}{2} \tag{3-24}$$

$$\frac{dv}{dz} = -\theta_x + \frac{\theta_y \theta_z}{2} \tag{3-25}$$

Solving Eqs. (3-23) and (3-24) for θ_x and θ_y gives

$$\theta_x = -\frac{dv}{dz} + \frac{1}{2}\theta_z \frac{du}{dz} \tag{3-26}$$

$$\theta_y = \frac{du}{dz} + \frac{1}{2}\theta_z \frac{dv}{dz} \tag{3-27}$$

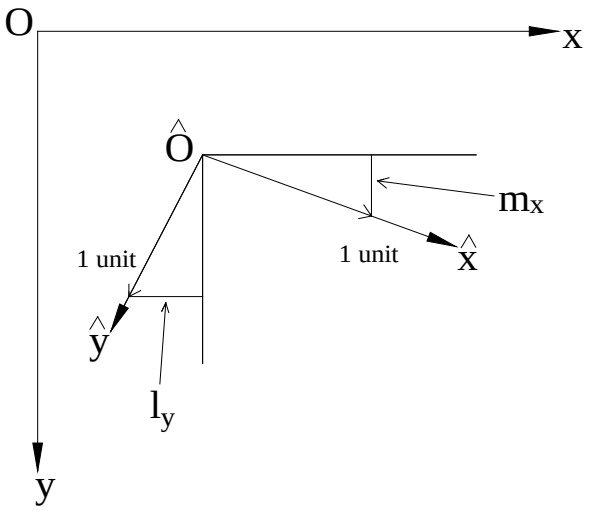

Figure 3.7 Twist Rotation

The projections of unit lengths along the $\hat{o}\hat{x}$ axis onto the oy axis and $\hat{o}\hat{y}$ axis onto the ox axis are m_x and l_y, respectively. l_y and m_x are used to define the mean twisting rotation, ϕ, of the $\hat{o}\hat{x}$ and $\hat{o}\hat{y}$ axes about the oz axis as shown in Figure 3.7. From Appendix A, we have $l_y = -\theta_z + \frac{\theta_x \theta_y}{2}$ and $m_x = \theta_z + \frac{\theta_x \theta_y}{2}$, therefore,

$$\phi = \frac{1}{2}[(\theta_z + \frac{\theta_x \theta_y}{2}) - (-\theta_z + \frac{\theta_x \theta_y}{2})] = \theta_z \tag{3-28}$$

Substituting Eqs. (3-26) to (3-28) into Eq. (3-16) gives

$$[T_R] = \begin{bmatrix} l_x & l_y & l_z \\ m_x & m_y & m_z \\ n_x & n_y & n_z \end{bmatrix} \tag{3-29}$$

Where

$$l_x = 1 - \frac{1}{2}(\frac{du}{dz})^2 - \frac{1}{2}\phi^2 - \frac{1}{2}\frac{du}{dz}\frac{dv}{dz}\phi \tag{3-30}$$

$$l_y = -\phi - \frac{1}{2}\frac{du}{dz}\frac{dv}{dz} + \frac{1}{4}(\frac{du}{dz})^2\phi - \frac{1}{4}(\frac{dv}{dz})^2\phi \tag{3-31}$$

$$l_z = \frac{du}{dz} \tag{3-32}$$

$$m_x = \phi - \frac{1}{2}\frac{du}{dz}\frac{dv}{dz} - \frac{1}{4}(\frac{dv}{dz})^2\phi + \frac{1}{4}(\frac{du}{dz})^2\phi \tag{3-33}$$

$$m_y = 1 - \frac{1}{2}(\frac{dv}{dz})^2 - \frac{1}{2}\phi^2 + \frac{1}{2}\frac{du}{dz}\frac{dv}{dz}\phi \tag{3-34}$$

$$m_z = \frac{dv}{dz} \tag{3-35}$$

$$n_x = -\frac{du}{dz} - \frac{dv}{dz}\phi + \frac{1}{4}\frac{du}{dz}\phi^2 \tag{3-36}$$

$$n_y = -\frac{dv}{dz} + \frac{du}{dz}\phi + \frac{1}{4}\frac{dv}{dz}\phi^2 \tag{3-37}$$

$$n_z = 1 - \frac{1}{2}(\frac{du}{dz})^2 - \frac{1}{2}(\frac{dv}{dz})^2 \tag{3-38}$$

The torsional curvature of the deformed cross section axes is (Love 1944)

$$k_z = \frac{dl_x}{dz}l_y + \frac{dm_x}{dz}m_y + \frac{dn_x}{dz}n_y \tag{3-39}$$

Substituting Eqs. (3-30) to (3-38) into Eq. (3-39) gives

$$k_z = \frac{d\phi}{dz} + \frac{1}{2}(\frac{d^2u}{dz^2}\frac{dv}{dz} + \frac{d^2v}{dz^2}\frac{du}{dz}) \tag{3-40}$$

The second and third term in this equation are small compared to the first term because of the higher order effects. Eq. (3-40) may be approximated by

$$k_z = \frac{d\phi}{dz} \tag{3-41}$$

Substitue Eqs. (3-30) to (3-41) into Eq. (3-12), the displacement of an arbitrary point on the cross section may be expressed in terms of the centroidal deformations as

$$\begin{bmatrix} u_p \\ v_p \\ w_p \end{bmatrix} = \begin{bmatrix} u - \hat{y}\phi \\ v + \hat{x}\phi \\ w - \hat{x}\frac{du}{dz} - y\frac{dv}{dz} - \omega\frac{d\phi}{dz} \end{bmatrix}$$

$$+ \begin{bmatrix} -\frac{1}{2}\hat{x}\left[(\frac{du}{dz})^2 + \phi^2 + \frac{du}{dz}\frac{dv}{dz}\phi\right] - \frac{1}{2}y\left[\frac{du}{dz}\frac{dv}{dz} - \frac{1}{2}(\frac{du}{dz})^2\phi + \frac{1}{2}(\frac{dv}{dz})^2\phi\right] - \omega\frac{du}{dz}\frac{d\phi}{dz} \\ -\frac{1}{2}\hat{x}\left[\frac{du}{dz}\frac{dv}{dz} + \frac{1}{2}(\frac{dv}{dz})^2\phi - \frac{1}{2}(\frac{du}{dz})^2\phi\right] - \frac{1}{2}y\left[(\frac{dv}{dz})^2 + \phi^2 - \frac{du}{dz}\frac{dv}{dz}\phi\right] - \omega\frac{dv}{dz}\frac{d\phi}{dz} \\ -\hat{x}(\frac{dv}{dz}\phi - \frac{1}{4}\frac{du}{dz}\phi^2) + y(\frac{du}{dz}\phi + \frac{1}{4}\frac{dv}{dz}\phi^2) + \frac{1}{2}\omega\frac{d\phi}{dz}\left[(\frac{du}{dz})^2 + (\frac{dv}{dz})^2\right] \end{bmatrix}$$

(3-42)

The first bracket on the right side of Eq. (3-42) contains the linear terms of the displacements, and the second bracket contains the nonlinear terms of the displacements. The derivatives of u_p, v_p, and w_p with respect to z are

$$\frac{du_p}{dz} = \frac{du}{dz} - \hat{y}\frac{d\phi}{dz} + \mathrm{O}_x(\frac{du}{dz}, \frac{dv}{dz}, \phi) \tag{3-43}$$

$$\frac{dv_p}{dz} = \frac{dv}{dz} + \hat{x}\frac{d\phi}{dz} + \mathrm{O}_y(\frac{du}{dz}, \frac{dv}{dz}, \phi) \tag{3-44}$$

$$\frac{dw_p}{dz} = \frac{dw}{dz} - \hat{x}\frac{du^2}{dz^2} - y\frac{d^2v}{dz^2} - \omega\frac{d^2\phi}{dz^2} - x\frac{d\phi}{dz}\frac{dv}{dz} - x\phi\frac{d^2v}{dz^2} + y\frac{d\phi}{dz}\frac{du}{dz} + y\phi\frac{d^2u}{dz^2} + \mathrm{O}_z(\frac{du}{dz}, \frac{dv}{dz}, \phi)$$

(3-45)

The terms O_x and O_y indicate functions of second and higher order in magnitude, and the term O_z indicates functions of third order and higher in magnitude, all of which are disregarded.

3.1.3 Strains

The longitudinal finite normal strain may be expressed as (Boresi 1993)

$$\varepsilon = \frac{dw_P}{dz} + \frac{1}{2}[(\frac{du_P}{dz})^2 + (\frac{dv_P}{dz})^2 + (\frac{dw_P}{dz})^2] \tag{3-46}$$

Since $\frac{dw_P}{dz}$ is small compared to $\frac{du_P}{dz}$ and $\frac{dv_P}{dz}$, we can simplify this equation into

$$\varepsilon = \frac{dw_P}{dz} + \frac{1}{2}[(\frac{du_P}{dz})^2 + (\frac{dv_P}{dz})^2] \tag{3-47}$$

Substituting in the derivatives of the displacements of point P_o from Eqs. (3-43) to (3-45), Eq. (3-47) becomes

$$\varepsilon_P = \frac{dw}{dz} - \tilde{x}\frac{d^2u}{dz^2} - y\frac{d^2v}{dz^2} - \omega\frac{d^2\phi}{dz^2} + \frac{1}{2}[(\frac{du}{dz})^2 + (\frac{dv}{dz})^2] - x\frac{d^2v}{dz^2}\phi + y\frac{d^2u}{dz^2}\phi + \frac{1}{2}(x^2+y^2)(\frac{d\phi}{dz})^2 \tag{3-48}$$

The first and second variations of the longitudinal strain are

$$\begin{aligned}\delta\varepsilon_P = {} & \frac{d\delta w}{dz} - \tilde{x}\frac{d^2\delta u}{dz^2} - y\frac{d^2\delta v}{dz^2} - \omega\frac{d^2\delta\phi}{dz^2} + \frac{d\delta u}{dz}\frac{du}{dz} + \frac{d\delta v}{dz}\frac{dv}{dz} - x\frac{d^2\delta v}{dz^2}\phi - x\frac{d^2v}{dz^2}\delta\phi \\ & + \tilde{y}\frac{d^2\delta u}{dz^2}\phi + y\frac{d^2u}{dz^2}\delta\phi + (x^2+y^2)\frac{d\delta\phi}{dz}\frac{d\phi}{dz}\end{aligned} \tag{3-49}$$

$$\delta^2\varepsilon_P = (\frac{d\delta u}{dz})^2 + (\frac{d\delta v}{dz})^2 - 2\tilde{x}\frac{d^2\delta v}{dz^2}\delta\phi + 2y\frac{d^2\delta u}{dz^2}\delta\phi + (x^2+y^2)(\frac{d\delta\phi}{dz})^2 \tag{3-50}$$

The second variations of the displacements in the above equations are assumed to vanish.

The strains contain the combination of the displacements before buckling and the displacements after buckling. The prebuckling displacements are defined as w, v, and their derivatives. The displacements at buckling are defined as δu and $\delta\phi$. As a result, the displacement u, ϕ, δw, δv, and their derivatives are meaningless for this problem (Pi et al. 1992). Based on the assumptions presented above, the longitudinal stain, the first, and the second variation of the longitudinal strain, may be presented as

$$\varepsilon_P = \frac{dw}{dz} - \hat{y}\frac{d^2v}{dz^2} + \frac{1}{2}(\frac{dv}{dz})^2 \tag{3-51}$$

$$\delta\varepsilon_P = -\hat{x}\frac{d^2\delta u}{dz^2} - \omega\frac{d^2\delta\phi}{dz^2} - x\frac{d^2v}{dz^2}\delta\phi \tag{3-52}$$

$$\delta^2\varepsilon_P = (\frac{d\delta u}{dz})^2 + 2\hat{y}\frac{d^2\delta u}{dz^2}\delta\phi + (x^2+y^2)(\frac{d\delta\phi}{dz})^2 \tag{3-53}$$

3.1.4 Stresses and Stress Resultants

The stresses at a point P_0 on the cross section are directly proportional to the strains by Hooke's Law

$$\begin{pmatrix}\sigma_P\\ \tau_P\end{pmatrix} = \begin{bmatrix}E & 0\\ 0 & G\end{bmatrix}\begin{pmatrix}\varepsilon_P\\ \gamma_P\end{pmatrix} \tag{3-54}$$

The stress resultants are

$$M_x = \int_A \sigma_P y dA \tag{3-55}$$

$$F = \int_A \sigma_P dA \tag{3-56}$$

3.1.5 Section Properties

For a member of length L with a doubly symmetric cross section, the $\hat{x}$ and $\hat{y}$ principal centroidal axes are defined by

$$\int_A \hat{x}\hat{d}A = \int_A ydA = 0 \tag{3-57}$$

$$\int_A \hat{x}\hat{y}dA = 0 \tag{3-58}$$

The section properties are defined as

$$A = \int_A dA \tag{3-59}$$

$$I_x = \int_A \hat{y}^2 dA \tag{3-60}$$

$$I_y = \int_A \hat{x}^2 dA \tag{3-61}$$

$$I_\omega = \int_A \hat{\omega}^2 dA \tag{3-62}$$

$$J = \int_A 4{t_P}^2 dA \tag{3-63}$$

The shear center of a doubly symmetric cross section coincides with the centroid, which satisfies the conditions

$$\int_A \hat{x}\omega dA = 0 \tag{3-64}$$

$$\int_A \hat{y}\omega dA = 0 \tag{3-65}$$

$$\int_A \omega dA = 0 \tag{3-66}$$

3.1.6 Strain Energy Equation

The second variation of the strain energy equation is developed by substituting ε_P, $\delta\varepsilon_P$, $\delta^2\varepsilon_P$, γ_P, $\delta\gamma_P$, and $\delta^2\gamma_P$ along with the stresses, stress resultants, and section properties from Sections 3.1.2 and 3.1.3 into Eq. (3-6). The second variation of the strain energy for the flexural-torsional buckling problem is

$$\frac{1}{2}\delta^2 U = \frac{1}{2}\int [EI_y(\frac{d^2(\delta u)}{dz^2})^2 + EI_\omega(\frac{d^2(\delta\phi)}{dz^2})^2 + GJ(\frac{d(\delta\phi)}{dz})^2 + 2M_x(\frac{d^2(\delta u)}{dz^2})\delta\phi + F(\frac{d(\delta u)}{dz})^2]dz \tag{3-67}$$

Where the stress resultants are linearized to

$$M_x = -EI_x\frac{d^2 v}{dz^2} \tag{3-68}$$

$$F = EA\frac{dw}{dz} \tag{3-69}$$

3.2 POTENTIAL ENERGY OF THE LOADS

The second part of the total potential energy equation, Eq. (3-1), is the potential energy of the external loads, may be expressed by the multiplication of the external loads with the corresponding displacements:

$$\Omega = -\int_L (v_q q)dz - \sum(v_p P - \frac{dv_M}{dz} M + w_F F) \tag{3-70}$$

where

v_q = vertical displacement through which the load q acts

q = the distributed load in the y - direction

v_p = vertical displacement through which the load P acts

P = the concentrated load in the y - direction

v_M = vertical displacement through which the moment M acts

$\frac{dv_M}{dz}$ = rotation due to the moment M

M = the applied moment about the x - axis

w_F = longitudinal displacement through which the load F acts

F = the concentrated load in the z - direction

The second variation of the potential energy of the loads is

$$\delta^2\Omega = -\int_L (\delta^2 v_q q)dz - \sum(\delta^2 v_p P - \frac{d\delta^2 v_M}{dz} M + \delta^2 w_F F) \tag{3-71}$$

3.2.1 Displacements

The longitudinal displacement is considered negligible due to its small quantity, therefore, $w_F = 0$. The displacement due to the concentrated load P at a height of e_z from the neutral axis may be found by using Eq. (3-42) ($x = 0, y = e_z, \omega = 0$)

$$v_P = v + m_y e_z - e_z \tag{3-72}$$

Substituting Eq. (3-34) into Eq. (3-72) gives

$$v_P = v - \frac{1}{2} e_z [(\frac{dv}{dz})^2 + \phi^2 - \frac{du}{dz}\frac{dv}{dz}\phi] \tag{3-73}$$

Likewise, the displacement due to the distributed load is

$$v_q = v - \frac{1}{2} a_z [(\frac{dv}{dz})^2 + \phi^2 - \frac{du}{dz}\frac{dv}{dz}\phi] \tag{3-74}$$

Also, the rotation about an axis parallel to the ox axis at a point with a concentrated moment M_x is

$$\frac{dv_M}{dz} = \frac{dv}{dz} \tag{3-75}$$

In this section, the effects of prebuckling deformations are neglected; therefore, the deformation v and its derivatives are disregarded. The displacements corresponding to the external loads become

$$v_q = \frac{1}{2} a_z \phi^2 \tag{3-76}$$

$$v_P = -\frac{1}{2} e_z \phi^2 \tag{3-77}$$

$$\frac{dv_M}{dz} = 0 \tag{3-78}$$

The second variations of Eqs. (3-76) to (3-78) are

$$\delta^2 v_q = a_z (\delta\phi)^2 \tag{3-79}$$

$$\delta^2 v_P = e_z (\delta\phi)^2 \tag{3-80}$$

$$\frac{d\delta^2 v_M}{dz} = 0 \tag{3-81}$$

3.2.2 Potential Energy of Loads Equation

Substituting in the displacements of Eqs. (3-79) to (3-81) into Eq. (3-71) gives the second variation of the potential energy of the loads

$$\frac{1}{2}\delta^2\Omega = \frac{1}{2}\int_L q a_z (\delta\phi)^2 dz + \frac{1}{2}\sum P e_z (\delta\phi)^2 \tag{3-82}$$

3.3 ENERGY EQUATION

The second variation of the total potential energy equation for the flexural-torsional buckling of a beam element is the sum of the second variation of the strain energy and the second variation of the potential energy of the loads. Therefore, the second variation of the total potential energy equation is given by

$$\frac{1}{2}\delta^2\prod=\frac{1}{2}\int\left[EI_y(\frac{d^2(\delta u)}{dz^2})^2+EI_\omega(\frac{d^2(\delta\phi)}{dz^2})^2+GJ(\frac{d(\delta\phi)}{dz})^2+2M_x(\frac{d^2(\delta u)}{dz^2})\delta\phi+F(\frac{d(\delta u)}{dz})^2\right]dz$$

$$+\frac{1}{2}\int_L qa_z(\delta\phi)^2dz+\frac{1}{2}\sum Pe_z(\delta\phi)^2=0 \tag{3-83}$$

Where

$$M_x=M_1+V_1z-q\frac{z^2}{2}\quad\text{for}\quad 0<z<z_P \tag{3-84}$$

$$M_x=M_1+V_1z-q\frac{z^2}{2}-P(z-z_P)\quad\text{for}\quad z_P<z<L \tag{3-85}$$

z_P = the location where the concentrated load applies.

4.0 DERIVATION OF SECTION PROPERTIES OF A DOUBLY-SYMMETRIC WEB-TAPERED I-BEAM

In uniform beams, calculation of the section properties such as cross section area, A, the second moment of inertia, I_x or I_y, the torsional constant, J, and etc., are standard procedure and can easily be determined from the characteristics of the cross section. However, because of the tapered effects, these calculations are more complex for a web-tapered I-beam. These section properties are changed along the length, and they are related to the tapered angle α_0, the web depth b_w and the height h (Figure 4.2). Figure 4.1 defines the longitudinal direction of the web the z-axis, and that of the flanges the s-axis, then α_0 is the angle between these two axes (Figure 4.1).

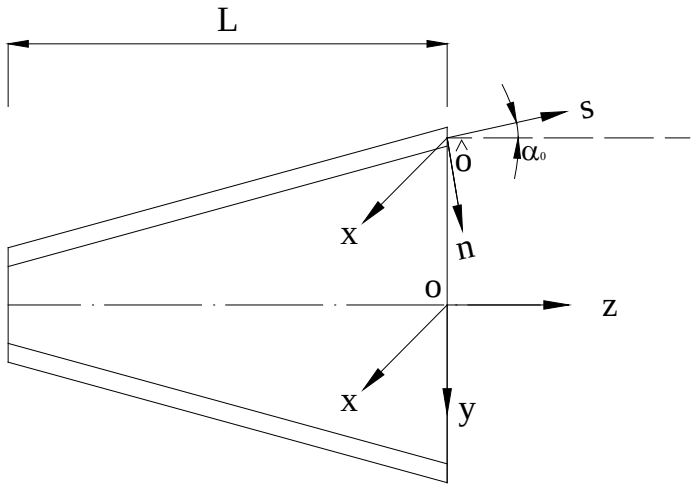

Figure 4.1 Coordinate Systems

In this chapter, the rotation transformation equation, Eq. (3-12), which is extracted from Torkamani (1998), will be employed to calculate section properties of a web-tapered I-beam. The results obtained will be shown to be consistent with the work by Zhang and Tong (2008), which are listed below:

$$A = 2A_f \cos^3 \alpha_0 + A_w \tag{4-1}$$

$$I_x = \frac{A_f \cos^3 \alpha_0 h^2}{2} + \frac{1}{12} t_w h^3 \tag{4-2}$$

$$I_y = \frac{t_f b_f{}^3 \cos^3 \alpha_0}{6} \tag{4-3}$$

$$J = \frac{2t_f{}^3 b_f}{3} \cos^3 \alpha_0 + \frac{t_w{}^3 b_w}{3} \tag{4-4}$$

$$I_\omega = 2I_{yf} \cos^3 \alpha_0 \left(\frac{h}{2}\right)^2 = \frac{h^2 I_y}{4} \tag{4-5}$$

where the area of the web, A_w, and the height, h, are function of z; the area of each flange, A_f, and the second moment of inertia of each flange with respect to the weak axis of a cross section, I_{yf}, are constants.

4.1 APPLICATION OF ROTATION TRANSFORMATION EQUATION IN A DOUBLY-SYMMETRIC WEB-TAPERED CROSS SECTION

Figure 4.2 shows a typical cross section of a doubly-symmetric web-tapered I-beam. In order to use Eq. (3-12) to calculate the cross section properties, the displacement functions of

an arbitrary point on the cross section, point P in Figure 4.3 and point Q in Figure 4.4, will be analyzed and formulated.

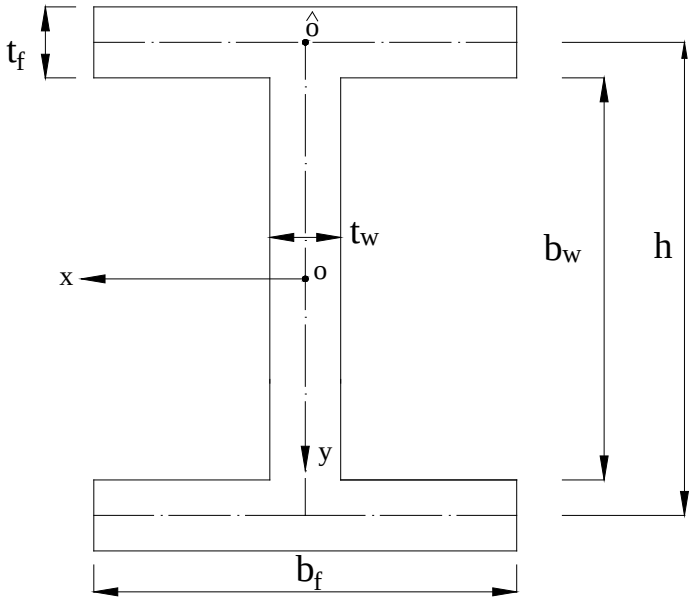

Figure 4.2 Cross-section Diameters

However, due to the tapered effects, the longitudinal direction of the web and that of the flanges depart from each other (Figure 4.1). Displacements of a point on the web and on the flanges are defined considering different coordinate systems— xyz coordinate system for the web and xns coordinate for the flanges. Thus, the cross section of a doubly-symmetric web-tapered I-beam will be decomposed into three parts, the web, the top flange, and the bottom flange. Then the rotation transformation equation is applied to each part, then displacements of an arbitrary point on either the web or the flanges are determined.

It should be noted that, when rotation transformation equation is applied, it remains the same expression for the web and the flanges except that the ranges of x and y values

are changed, which are discussed in this section. Then, by employing the finite normal strain, the section properties are derived for five different cases.

4.1.1 Rotation Transformation Equation in the Web

Consider point P with displacements u_p, v_p, and w_p being an arbitrary point on the web; and point O with displacements u_o, v_o, and w_o is the centroid of the cross section.

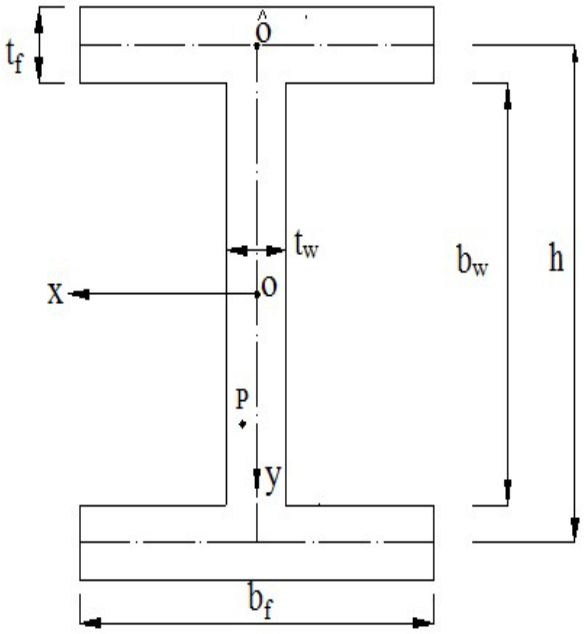

Figure 4.3(a) Cross section View With An Arbitrary Point P

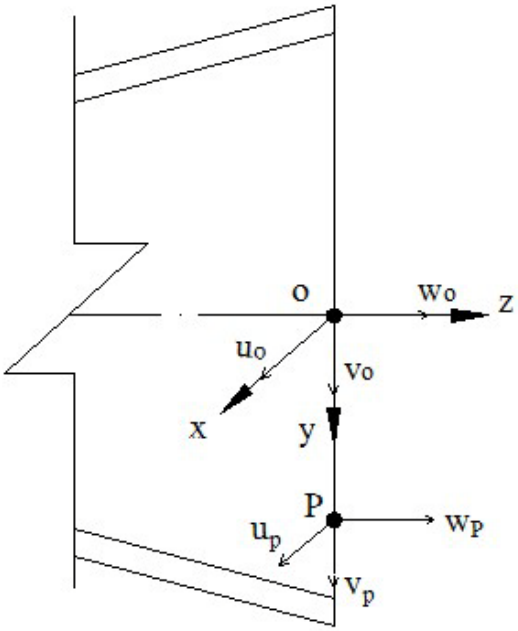

Figure 4.3(b) Displacements of the Point P

As discussed in Section 3.1.2, displacements of point P can be written as:

$$\begin{Bmatrix} u_p \\ v_p \\ w_p \end{Bmatrix} = \begin{Bmatrix} u \\ v \\ w \end{Bmatrix} + [T_R] \begin{Bmatrix} x \\ y \\ -\omega k_z \end{Bmatrix} - \begin{Bmatrix} x \\ y \\ 0 \end{Bmatrix} \tag{4-6}$$

where the values of x and y are bounded as given below:

$$-\frac{t_w}{2} \le x \le \frac{t_w}{2} \tag{4-7}$$

$$\frac{b_w}{2} \le y \le -\frac{b_w}{2} \tag{4-8}$$

4.1.2 Rotation Transformation Equation In The Flange

Consider point Q being an arbitrary point on the flange with displacements u_q, v_q, and w_q in the x-, n-, and s- directions, respectively. To evaluate these displacements, a set of auxiliary displacements $\hat{u}_q$, v_q, and $\hat{w}_q$ for point Q in the x-, y-, and z- directions are introduced.

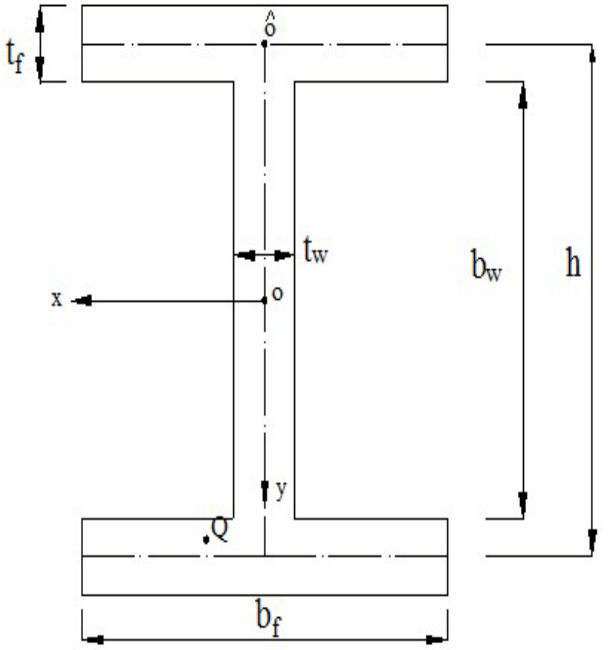

Figure 4.4(a) Cross-section View with An Arbitrary Point Q

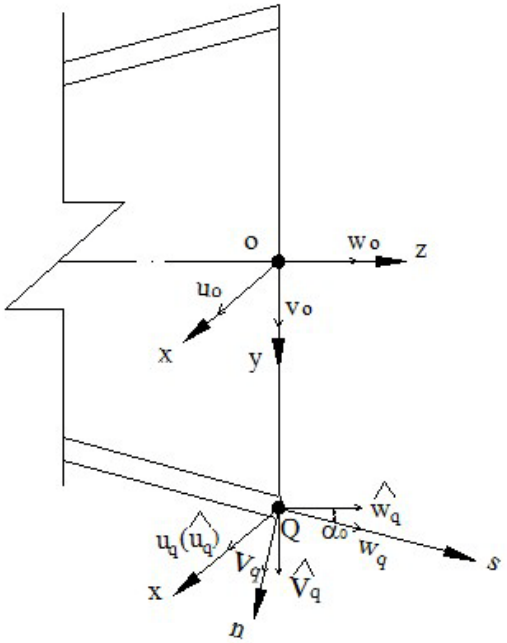

Figure 4.4(b) Displacements of An Arbitrary Point Q

The displacement functions for $\hat{\hat{u}}_q$, v_q, and $\hat{w}_q$ can be written as:

$$\begin{Bmatrix} \hat{u}_q \\ \hat{v}_q \\ \hat{w}_q \end{Bmatrix} = \begin{Bmatrix} u \\ v \\ w \end{Bmatrix} + [T_R] \begin{Bmatrix} x \\ y \\ -\omega k_z \end{Bmatrix} - \begin{Bmatrix} x \\ y \\ 0 \end{Bmatrix} \tag{4-9}$$

Displacements u_q, v_q, and w_q are calculated in terms of displacements $\hat{\hat{u}}_q$, v_q, $\hat{w}_q$, and angle α_0 considering geometry of the cross section (See Figure 4.4b). For both the top and the bottom flange, one may have:

$$u_q = \hat{\hat{u}}_q \tag{4-10}$$

$$v_q = \hat{v}_q \cos\alpha_0 + \hat{w}_q \sin\alpha_0 \tag{4-11}$$

$$w_q = \hat{w}_q \cos\alpha_0 - \hat{v}_q \sin\alpha_0 \tag{4-12}$$

Eqs. (4-10) to (4-12) may be expressed in matrix form:

$$\begin{Bmatrix} u_q \\ v_q \\ w_q \end{Bmatrix} = \begin{bmatrix} 1 & 0 & 0 \\ 0 & \cos\alpha_0 & \sin\alpha_0 \\ 0 & -\sin\alpha_0 & \cos\alpha_0 \end{bmatrix} \begin{Bmatrix} \hat{\hat{u}}_q \\ \hat{v}_q \\ \hat{w}_q \end{Bmatrix} = [T] \begin{Bmatrix} u_q \\ v_q \\ w_q \end{Bmatrix} \tag{4-13}$$

Where

$$[T] = \begin{bmatrix} 1 & 0 & 0 \\ 0 & \cos\alpha_0 & \sin\alpha_0 \\ 0 & -\sin\alpha_0 & \cos\alpha_0 \end{bmatrix} \tag{4-14}$$

Substituting Eq. (4-9) into the right-hand side of Eq. (4-13), one has displacements of an arbitrary point Q on the flange:

$$\begin{Bmatrix} u_q \\ v_q \\ w_q \end{Bmatrix} = [T] \begin{Bmatrix} \hat{u}_q \\ \hat{v}_q \\ \hat{w}_q \end{Bmatrix} = [T] \left(\begin{Bmatrix} u \\ v \\ w \end{Bmatrix} + [T_R] \begin{Bmatrix} x \\ y \\ -\omega k_z \end{Bmatrix} - \begin{Bmatrix} x \\ y \\ 0 \end{Bmatrix} \right) \tag{4-15}$$

where the values of x and y are bounded and are given by the equations below.

For the top flange:

$$-\frac{b_f}{2} \le x \le \frac{b_f}{2} \tag{4-16}$$

$$-\frac{h}{2} - \frac{t_f}{2} \le y \le -\frac{h}{2} + \frac{t_f}{2} \tag{4-17}$$

For the bottom flange:

$$-\frac{b_f}{2} \le x \le \frac{b_f}{2} \tag{4-18}$$

$$\frac{h}{2} - \frac{t_f}{2} \le y \le \frac{h}{2} + \frac{t_f}{2} \tag{4-19}$$

4.2 FINITE NORMAL STRAIN

Finite normal strain is a well defined concept, only the longitudinal finite normal strain is used in this work. After the displacements have been obtained for an arbitrary point on both the web and the flanges, the longitudinal finite normal strain can be employed to define the strains.

For point P on the web, the longitudinal normal finite strain is:

$$\varepsilon_{\mathrm{p}} = \frac{dw_p}{dz} + \frac{1}{2}\left[\left(\frac{du_p}{dz}\right)^2 + \left(\frac{dv_p}{dz}\right)^2 + \left(\frac{dw_p}{dz}\right)^2\right] \tag{4-20}$$

For point Q on the flanges, the longitudinal normal finite strain is:

$$\varepsilon_{\mathrm{q}} = \frac{dw_q}{ds} + \frac{1}{2}[(\frac{du_q}{ds})^2 + (\frac{dv_q}{ds})^2 + (\frac{dw_q}{ds})^2] \tag{4-21}$$

where

$$\frac{dz}{ds} = \cos\alpha_0 \tag{4-22}$$

4.3 DERIVATION OF SECTION PROPERTIES

In this section, several well defined deformation patterns are investigated, and the corresponding section properties of a doubly-symmetric web-tapered I-beam are derived. This is done based on the formulations presented in the previous sections.

4.3.1 Axial Deformation

When displacement in $z-$direction is the only displacement, one has no rotation, thus $\theta = 0$, then $\theta_x = \theta_y = \theta_z = 0$; from Eq.(3-16), $k_z = \frac{d\phi}{dz} = \frac{d(\theta\cos\gamma)}{dz} = 0$; the displacements of the centroid are $u = v = 0$, and $w \neq 0$. From Eq. (3-13), one has

$$[T_R] = \begin{bmatrix} 1 & 0 & 0 \\ 0 & 1 & 0 \\ 0 & 0 & 1 \end{bmatrix} \tag{4-23}$$

4.3.1.1 Axis deformation of the web

The displacements of point P on the web in terms of centroidal displacement are given by Eq. (4-6),

$$\begin{Bmatrix} u_p \\ v_p \\ w_p \end{Bmatrix} = \begin{Bmatrix} u \\ v \\ w \end{Bmatrix} + [T_R] \begin{Bmatrix} x \\ y \\ 0 \end{Bmatrix} - \begin{Bmatrix} x \\ y \\ 0 \end{Bmatrix} = \begin{Bmatrix} 0 \\ 0 \\ w \end{Bmatrix} \tag{4-24}$$

From Eq. (4-20), we can express the strain of point P as

$$\varepsilon_{\mathrm{p}} = \frac{dw_p}{dz} + \frac{1}{2}\left[0 + 0 + (w_p{}')^2\right] = w' + \frac{1}{2}w'^2 \tag{4-25}$$

If the higher order term is disregarded, the linear term is:

$$\varepsilon_{\mathrm{p}}{}^{L} = w' \tag{4-26}$$

The corresponding axial force on the web is

$$N_w = \int \sigma_w t_w dy = \int E\varepsilon_P{}^{L} t_w dy = Ew' A_w \tag{4-27}$$

4.3.1.2 Axial deformation of the flange

First, we need to find $\hat{u_q}$, v_q, and $\hat{w}_q$ using Eq. (4-9),

$$\begin{Bmatrix} \hat{u}_q \\ \hat{v}_q \\ \hat{w}_q \end{Bmatrix} = \begin{Bmatrix} u \\ v \\ w \end{Bmatrix} + [T_R] \begin{Bmatrix} x \\ y \\ 0 \end{Bmatrix} - \begin{Bmatrix} x \\ y \\ 0 \end{Bmatrix} = \begin{Bmatrix} 0 \\ 0 \\ w \end{Bmatrix} \tag{4-28}$$

Then u_q, v_q, and w_q are calculated using Eq. (4-13)

$$\begin{Bmatrix} u_q \\ v_q \\ w_q \end{Bmatrix} = \begin{bmatrix} 1 & 0 & 0 \\ 0 & \cos\alpha_0 & \sin\alpha_0 \\ 0 & -\sin\alpha_0 & \cos\alpha_0 \end{bmatrix} \begin{Bmatrix} \hat{u}_q \\ \hat{v}_q \\ \hat{w}_q \end{Bmatrix} = \begin{Bmatrix} 0 \\ w\sin\alpha_0 \\ w\cos\alpha_0 \end{Bmatrix} \tag{4-29}$$

The normal strain is calculated using Eq. (4-21):

$$\varepsilon_{\mathrm{q}} = \frac{dw_q}{ds} + \frac{1}{2}\left[0^2 + (\frac{dv_q}{ds})^2 + (\frac{dw_q}{ds})^2 \right]$$

$$= w^{'}\cos^2\alpha_0 + \frac{1}{2}[(w\sin\alpha_0\cos\alpha_0)^2 + (w^{'}\cos^2\alpha_0)^2] \tag{4-30}$$

The nonlinear terms in Eq. (4-30) show that the deformation in the flange is a curve due to the axial deformation in the web. For simplicity, only the linear terms are kept:

$$\varepsilon_{\mathrm{q}}^{\ L} = w^{'}\cos^2\alpha_0 . \tag{4-31}$$

The corresponding axial force in the s-direction on the flange is

$$N_{f,s} = EA_f\varepsilon_q^{\ L} = EA_f w^{'}\cos^2\alpha_0 . \tag{4-32}$$

The component of $N_{f,s}$ in the z-direction is

$$N_{f,z} = N_{f,s}\cos\alpha_0 = EA_f w^{'}\cos^3\alpha_0 . \tag{4-33}$$

4.3.1.3 Derivation of the cross section area

If one sums up the forces in z-direction using Eqs. (4-27) and (4-33), the axial force of the whole cross section in the z-direction can be determined:

$$N = 2N_{f,z} + N_w$$

$$= Ew'(2A_f \cos^3 \alpha_0 + A_w) \tag{4-34}$$

Thus, the effective cross-section area is

$$A = 2A_f \cos^3 \alpha_0 + A_w . \tag{4-35}$$

4.3.2 Bending about x-axis

When rotation about x-axis is the only displacement, one has

$$\theta = v', \ \alpha = 0, \ \beta = \gamma = 90^o;$$

$$\theta_x = \theta \cos\alpha = v', \ \ \theta_y = \theta \cos\beta = 0, \ \ \theta_z = \phi = \theta \cos\gamma = 0;$$

$$k_z = d\phi / dz = 0;$$

$$u = v = w = 0. \tag{4-36}$$

Substituting Eq. (4-36) into Eq. (3-13), we have

$$[T_R] = \begin{bmatrix} 1 & 0 & 0 \\ 0 & 1 - \dfrac{v'^2}{2} & -v' \\ 0 & v' & 1 - \dfrac{v'^2}{2} \end{bmatrix} \tag{4-37}$$

4.3.2.1 Bending about x–axis of the web

Using Eq. (3-12), we have:

$$\begin{Bmatrix} u_p \\ v_p \\ w_p \end{Bmatrix} = \begin{Bmatrix} u + x - x \\ v + (1 - v'^2/2)y - y \\ v'y + w \end{Bmatrix} = \begin{Bmatrix} 0 \\ -v'^2 y/2 \\ v'y \end{Bmatrix}. \tag{4-38}$$

Then from Eq. (4-20):

$$\varepsilon_{\mathrm{p}} = \frac{dw_p}{dz} + \frac{1}{2}\left[0^2 + (\frac{dv_p}{dz})^2 + (\frac{dw_p}{dz})^2\right]$$

$$= v''y + \frac{1}{2}\left[(v''v'y)^2 + (v''y)^2\right] \tag{4-39}$$

When linear terms are kept:

$$\varepsilon_P{}^L = v''y\,. \tag{4-40}$$

Thus, the moment about x-axis considering only the web may be calculated

$$M_w = \int \sigma_w y t_w dy = \int E\varepsilon_p{}^L y t_w dy = Ev''t_w \frac{h^3}{12} \tag{4-41}$$

4.3.2.2 Bending about x–axis of the flanges

First, we need to find $\hat{u_q}$, v_q, and $\hat{w}_q$ using Eq. (3-12)

$$\begin{Bmatrix} \hat{u}_q \\ \hat{v}_q \\ \hat{w}_q \end{Bmatrix} = \begin{Bmatrix} u \\ v \\ w \end{Bmatrix} + \begin{bmatrix} 1 & 0 & 0 \\ 0 & 1 - \frac{v'^2}{2} & -v' \\ 0 & v' & 1 - \frac{v'^2}{2} \end{bmatrix} \begin{Bmatrix} x \\ y \\ 0 \end{Bmatrix} - \begin{Bmatrix} x \\ y \\ 0 \end{Bmatrix} = \begin{Bmatrix} 0 \\ -v'^2 y/2 \\ yv' \end{Bmatrix} \tag{4-42}$$

Then from Eq. (4-13), we get:

$$\begin{Bmatrix} u_q \\ v_q \\ w_q \end{Bmatrix} = \begin{bmatrix} 1 & 0 & 0 \\ 0 & \cos\alpha_0 & \sin\alpha_0 \\ 0 & -\sin\alpha_0 & \cos\alpha_0 \end{bmatrix} \begin{Bmatrix} \hat{u}_q \\ \hat{v}_q \\ \hat{w}_q \end{Bmatrix} = \begin{Bmatrix} 0 \\ yv' \sin\alpha_0 - v'^2 y\cos\alpha_0 / 2 \\ yv' \cos\alpha_0 + v'^2 y\sin\alpha_0 / 2 \end{Bmatrix} \tag{4-43}$$

Using Eq. (4-21) to determine the normal strain:

$$\varepsilon_{q,s} = \frac{dw_q}{ds} + \frac{1}{2}\left[(\frac{du_q}{ds})^2 + (\frac{dv_q}{ds})^2 + (\frac{dw_q}{ds})^2 \right]$$

$$= yv'' \cos^2\alpha_0 + v'v'' y\sin\alpha_0\cos\alpha_0 + \frac{1}{2}(yv'' \sin\alpha_0 \cos\alpha_0 - v'v'' y\cos^2\alpha_0)^2$$

$$+ \frac{1}{2}(yv'' \cos^2\alpha_0 + v'v'' y\sin\alpha_0\cos\alpha_0)^2 \tag{4-44}$$

When linear terms are kept:

$$\varepsilon_{q,s}{}^L = yv'' \cos^2\alpha_0 . \tag{4-45}$$

Then, the axial forces in the top and the bottom flange are obtained based on Eqs. (4-16) to (4-19):

For the top flange:

$$N_{f,s1} = EA_f \varepsilon_{f,s1}{}^L = E\int_{-\frac{h}{2}-\frac{t_f}{2}}^{-\frac{h}{2}+\frac{t_f}{2}} \varepsilon_{f,s1}{}^L b_f dy .$$

$$= -\frac{1}{2} Ev'' \cos^2\alpha_0 A_f \tag{4-46}$$

Likewise, for the bottom flange:

$$N_{f,s2} = EA_f \varepsilon_{f,s2}{}^L = E\int_{\frac{h}{2}-\frac{t_f}{2}}^{\frac{h}{2}+\frac{t_f}{2}} \varepsilon_{f,s2}{}^L b_f dy$$

$$= \frac{1}{2} E v'' \cos^2 \alpha_0 A_f \,. \tag{4-47}$$

4.3.2.3 Derivation of the moment of inertia about the x-axis

The moment of the whole cross-section about x-axis can be derived using Eqs. (4-41), (4-46) and (4-47):

$$M_x = N_{f,s2} \frac{h}{2} \cos \alpha_0 - N_{f,s1} \frac{h}{2} \cos \alpha_0 + M_w$$

$$= E v'' \left(\frac{A_f h^2}{2} \cos^3 \alpha_0 + \frac{1}{12} t_w h^3 \right). \tag{4-48}$$

From standard moment-curvature relations

$$I_x = \left(\frac{A_f h^2}{2} \cos^3 \alpha_0 + \frac{1}{12} t_w h^3 \right). \tag{4-49}$$

4.3.3 Bending about y-axis

When rotation about y-axis is the only displacement, one has,

$$\theta = u', \alpha = \gamma = 90^0, \beta = 0^0;$$

$$\theta_x = \theta \cos \alpha = 0, \quad \theta_y = \theta \cos \beta = u', \quad \theta_z = \theta \cos \gamma = 0;$$

$$k_z = d\phi / dz = d\theta_z / dz = 0;$$

$$u = v = w = 0. \tag{4-50}$$

4.3.3.1 Bending about the y –axis of the web

The moment about the weak axis in the web is relatively small compared to the moment in the flanges, thus, it is neglected here.

4.3.3.2 Bending about the y –axis of the flanges

Substituting Eq. (4-50) into Eq. (3-13), we get

$$\left[T_R\right]=\begin{bmatrix} 1-\dfrac{u'^2}{2} & 0 & u' \\ 0 & 1 & 0 \\ -u' & 0 & 1-\dfrac{u'^2}{2} \end{bmatrix} \tag{4-51}$$

We need to find $\hat{u}_q$, v_q, and $\hat{w}_q$ first using Eq. (3-12):

$$\begin{Bmatrix} \hat{u}_q \\ \hat{v}_q \\ \hat{w}_q \end{Bmatrix}=\begin{Bmatrix} u \\ v \\ w \end{Bmatrix}+\begin{bmatrix} 1-\dfrac{u'^2}{2} & 0 & u' \\ 0 & 1 & 0 \\ -u' & 0 & 1-\dfrac{u'^2}{2} \end{bmatrix}\begin{Bmatrix} x \\ y \\ 0 \end{Bmatrix}-\begin{Bmatrix} x \\ y \\ 0 \end{Bmatrix} =\begin{Bmatrix} \dfrac{u'^2 x}{2} \\ 0 \\ -u' x \end{Bmatrix} \tag{4-52}$$

Using Eq. (4-13), we get:

$$\begin{Bmatrix} u_q \\ v_q \\ w_q \end{Bmatrix}=\begin{bmatrix} 1 & 0 & 0 \\ 0 & \cos\alpha_0 & \sin\alpha_0 \\ 0 & -\sin\alpha_0 & \cos\alpha_0 \end{bmatrix}\begin{Bmatrix} \hat{u}_q \\ \hat{v}_q \\ \hat{w}_q \end{Bmatrix}=\begin{Bmatrix} -u'^2 x/2 \\ -u' x\sin\alpha_0 \\ -u' x\cos\alpha_0 \end{Bmatrix} \tag{4-53}$$

From Eq. (4-21), we can have:

$$\varepsilon_{\mathrm{q,s}} = \frac{dw_q}{ds} + \frac{1}{2}\left[(\frac{du_q}{ds})^2 + (\frac{dv_q}{ds})^2 + (\frac{dw_q}{ds})^2 \right]$$

$$= -u^{"} x\cos\alpha_0 + \frac{1}{2}\left[(u^{'}u^{"} x\cos\alpha_0)^2 + (u^{"} x\cos^2\alpha_0)^2 \right] \tag{4-54}$$

When only the linear terms are kept:

$$\varepsilon_{\mathrm{q,s}}{}^{L} = -u^{"} x\cos\alpha_0 . \tag{4-55}$$

Thus, the moment of the bottom flange about the n-axis can be determined:

$$M_{f,n2} = \int_{-b_f/2}^{b_f/2} E\varepsilon_{q,s}{}^{L} x t_f dx$$

$$= Eu^{"}\cos^2\alpha_0 \frac{1}{12} b_f{}^3 t_f . \tag{4-56}$$

Likewise, for the top flange, we have:

$$M_{f,n1} = Eu^{"}\cos^2\alpha_0 \frac{1}{12} b_f{}^3 t_f . \tag{4-57}$$

4.3.3.3 Derivation of the moment of inertia about the y-axis

Finally, the bending moment of the whole cross section about the y-axis can be determined by combining Eqs. (4-56) and (4-57):

$$M_y = M_{f,n1}\cos\alpha_0 + M_{f,n2}\cos\alpha_0$$

$$= Eu^{"}\cos^3\alpha_0 \frac{1}{6} b_f{}^3 t_f = Eu^{"} I_y \tag{4-58}$$

Where $I_y = \cos^3\alpha_0 \frac{1}{6} b_f{}^3 t_f$ (4-59)

4.3.4 Free Torsional Deformation

In this case, there is a pure twist about the z-axis in the cross section, the twisting angle is θ_z.

$$\theta = \theta, \alpha = \beta = 90^0, \gamma = 0^0;$$

$$\theta_x = \theta\cos\alpha = 0, \quad \theta_y = \theta\cos\beta = 0, \quad \theta_z = \theta\cos\gamma = \theta;$$

$$k_z = d\phi/dz = d\theta_z/dz = \theta';$$

$$u = v = w = 0. \tag{4-60}$$

Substituting Eq. (4-60) into Eq. (3-13), we get

$$[T_R] = \begin{bmatrix} 1-\theta^2/2 & -\theta & 0 \\ \theta & 1-\theta^2/2 & 0 \\ 0 & 0 & 1 \end{bmatrix} \tag{4-61}$$

4.3.4.1 Torsional deformation of the web

The twist of the web about the z-axis is $\theta_z = \theta$, from the classical thin-walled theory developed by Vlasov (1961), the resultant free torsional torque is given by

$$T_w = GJ_w \frac{d\theta}{dz} \tag{4-62}$$

Where

$$J_w = b_w t^3{}_w / 3 \tag{4-63}$$

4.3.4.2 Torsional deformation of the flanges

The twisting angle of the top flange about the s_1-direction is

$$\theta_{s1} = \theta \cos\alpha \tag{4-64}$$

Then the corresponding twist is obtained

$$\frac{d\theta_{s1}}{ds_1} = \theta' \cos^2\alpha \tag{4-65}$$

The resultant free torsional torque of the top flange with respect to the s_1-direction is given by

$$T_{f_1,s_1} = GJ_f \frac{d\theta_{s_1}}{ds_1} \cos = GJ_f \theta' \quad {}^2\alpha \tag{4-66}$$

where $J_f \neq 3^3 b_f$ (4-67)

Likewise, one may have the expression for the bottom flange.

$$T_{f_2,s_2} = GJ_f \frac{d\theta_{s_2}}{ds_2} \cos = GJ_f \theta' \quad {}^2\alpha \tag{4-68}$$

4.3.4.2 Derivation of torsional constant

Finally, using Eqs. (4-66) and (4-68), one may express the torque of the whole cross section about the z-axis

$$T = T_{f_1,z} + T_{f_2,z} + T_w = (T_{f_1,s1} + T_{f_2,s2}) \cos\alpha_0 + T_w$$

$$= 2GJ_f \theta' \cos^3\alpha_0 + GJ_w \theta' = G\theta'(2J_f \cos^3\alpha_0 + J_w) \tag{4-69}$$

Where we find the equivalent free torsional constant of the cross-section

$$J = 2J_f \cos^3 \alpha_0 + J_w = \frac{2b_f t_f^{\ 3}}{3} \cos^3 \alpha_0 + \frac{b_w t_w^{\ 3}}{3} \tag{4-70}$$

4.3.5 Warping Strain of the Flanges Due to Free Torsional Deformation

4.3.5.1 Warping strain of the top flange in s_1-direction

Due to the assumption of zero linear shear strain on the middle surface of the top flange:

$$\gamma_{sx} = \frac{\partial w_{s_1}}{\partial x} + \frac{\partial \bar{u}}{\partial s_1} = 0 \tag{4-71}$$

w_{s_1} and $\bar{u}$ are the displacements of an arbitrary point on the middle surface of the top flange along the s_1- and x-axis, respectively.

To get $\bar{u}$, set $y = -\frac{h}{2}$ in Eq. (3-13) using Eqs. (4-60) and (4-61), and make the differentiation with respect to the s_1-axis, we will obtain

$$\bar{u} = \frac{h\theta}{2} - \theta^2 x / 2 \tag{4-72}$$

$$\frac{\partial \bar{u}}{\partial s_1} = \bar{u} \cos \alpha_0 = \cos \alpha_0 (\theta \tan \alpha_0 + \theta' \frac{h}{2}) - \theta \theta' x \cos \alpha_0 \tag{4-73}$$

Then we can write the expression for w_{s1} from Eq. (4-71)

$$w_{s1} = -\left[\theta \tan\alpha_0 \cos\alpha_0 x + \frac{h\theta'}{2} \cos\alpha_0 x - \theta\theta' x^2 \cos\alpha_0 / 2 \right]$$

$$= -\left[\theta x \sin\alpha_0 + \frac{h\theta'}{2} x \cos\alpha_0 - \frac{\theta\theta'}{2} x^2 \cos\alpha_0 \right] \tag{4-74}$$

Neglecting the nonlinear terms in Eq. (4-21), the linear term of the strain can be determined

$$\varepsilon_{f,s1}{}^{L} = \frac{dw_{s1}}{ds_1} = w'_{s1} \cos\alpha_0$$

$$= -x(\frac{h\theta''}{2} + 2\theta' \tan\alpha_0) \cos^2\alpha_0 \tag{4-75}$$

The bending moment of the top flange about the n_1-axis is given by:

$$M_{f,n1} = \int_{-b_f/2}^{b_f/2} E\varepsilon_{f,s}{}^{L} x t_f dx$$

$$= -E\cos^2\alpha_0 (\frac{h\theta''}{2} + 2\theta' \tan\alpha_0) \int_{-b_f/2}^{b_f/2} x^2 dx$$

$$= -EI_{yf} \cos^2\alpha_0 (\frac{h\theta''}{2} + 2\theta' \tan\alpha_0) . \tag{4-76}$$

The shear force along the x-axis due to the warping is thus determined:

$$Q_{f,n1} = \frac{dM_{n,f1}}{ds_1} = M'_{n1,f1} \cos\alpha_0$$

$$= -EI_{yf} \cos^3\alpha_0 (\frac{h\theta'''}{2} + 3\theta'' \tan\alpha_0) \tag{4-77}$$

4.3.5.2 Warping strain of the top flange in s_2-direction

Likewise, the shear force along the bottom flange can also be analyzed using the same procedure, which is listed with the other parameters as below:

$$w_{s2} = x(\frac{h\theta^{'}}{2} + \theta \tan\alpha_0)\cos\alpha_0 \tag{4-78}$$

$$\varepsilon_{f,s2}{}^{L} = x(\frac{h\theta^{''}}{2} + 2\theta^{'} \tan\alpha_0)\cos^2\alpha_0 \tag{4-79}$$

$$M_{f2,n1} = EI_{yf} \cos^2\alpha_0(\frac{h\theta^{''}}{2} + 2\theta^{'} \tan\alpha_0) \tag{4-80}$$

$$Q_{f2,n1} = EI_{yf} \cos^3\alpha_0(\frac{h\theta^{'''}}{2} + 3\theta^{''} \tan\alpha_0)\,. \tag{4-81}$$

4.3.5.3 Derivation of the warping constant

Finally, the bi-moment of the cross-section can be evaluated using Eqs. (4-76) and (4-80)

$$B_w = \frac{h}{2}\cos\alpha_0(M_{n_1,f_1} - M_{n_2,f_2})$$

$$= -hEI_{yf} \cos^3\alpha_0(h\theta^{''}/2 + 2\theta^{'} \tan\alpha_0) = -E(I_w\theta^{'})^{'} \tag{4-82}$$

where $I_w = 2I_{yf} \cos^3\alpha_0(\frac{h}{2})^2$ (4-83)

4.4 CONCLUSION

By investigating five deformation cases, the rotation transformation equation is used to derive the displacements and strains for an arbitrary point in the cross section of a doubly-symmetric web-tapered I-beam. It has been shown that the results of the section properties have a good agreement with Tong and Zhang (2003a), which demonstrates the efficiency as well as the accuracy of the rotation transformation equation in analyzing a web-tapered I-beam problem. The normal finite strain is truncated in this derivation process, depending upon desire accuracy, some of the nonlinear terms may be considered in calculations if required.

5.0 FINITE ELEMENT METHOD

The finite element analysis is a powerful numerical method to solve problems in many engineering fields and mathematical physics. Since the analytical solutions to many cases are difficult to obtain due to complicated geometries, loadings and material properties, the finite element method, which requires the solution of a system of simultaneous equations rather than complicated differential equations, provides a much easier way to generate results within acceptable errors.

The general steps to formulate the finite element solution begin with discretizing the structure into smaller elements. After this, the type for each element must be selected, and it should be chosen to closely model the actual behavior of the real body. Next, a displacement function is assumed for each element. The most common displacement function is a polynomial function expressed in terms of the nodal unknowns. The total number of polynomial functions needed to describe the displacement of an element depends on the number of degrees of freedom of the element. The strain-displacement relationship and stress-strain relationship are then defined for each element. These relationships are necessary to derive equations describing each element's behavior.

Equivalent loads at each node of the element need to be defined. Then the element stiffness matrices may be derived using one of several methods including energy methods as used in this Chapter. It should be noted that, unlike other energy methods such as the principle of virtual work, the principle of minimum total potential energy is applicable only for elastic materials. In this paper, the element stiffness matrices for flexural-torsional buckling of a beam element, including the elastic stiffness matrix and the geometric stiffness matrix, will be produced using principle of minimum total potential energy.

After the element stiffness matrices are derived, the element matrices will be converted from the local to global coordinate system for the entire structure using transformation matrix. Then through the assembly process, the governing equation for the whole structure can be obtained. The global stiffness matrix will be singular when there are no boundary conditions applied to the structure. In order to remove the singularity, the boundary conditions are applied to the matrix so that the structure does not move as a rigid body. This process involves partitioning the global matrix into the free and restrained degrees of freedom. The section of the global stiffness matrix corresponding to the free degrees of freedom of the structure is used for solving the problem. For the flexural-torsional buckling problem, the partitioned global elastic and geometric stiffness matrices are used to solve for the buckling loads.

In this paper, the objective is to apply the finite element method to a doubly-symmetric web-tapered I-beam to calculate the flexural-torsional buckling load of the structure.

At each node of an element, there are seven degrees of freedom, the lateral displacement u, the transverse displacement v, the longitudinal displacement w, the rotation about the longitudinal axis ϕ, the in-plane bending rotation v', the lateral bending rotation u', and the out of plane torsional curvature ϕ'. If the in-plane of loading displacements are disregarded, there are four degrees of freedom at each node, u, u', ϕ, and ϕ', therefore, there are a total of eight degrees of freedom for each element.,

Figure 5.1 shows the element degrees of freedom (axial deformation is not considered). The coordinate system is chosen so that *x*-axis is the major principal axis and *y*-axis is the minor principal axis of the cross-section prior to buckling, that is $I_x > I_y$. The *z* axis is the centroidal axis of the element.

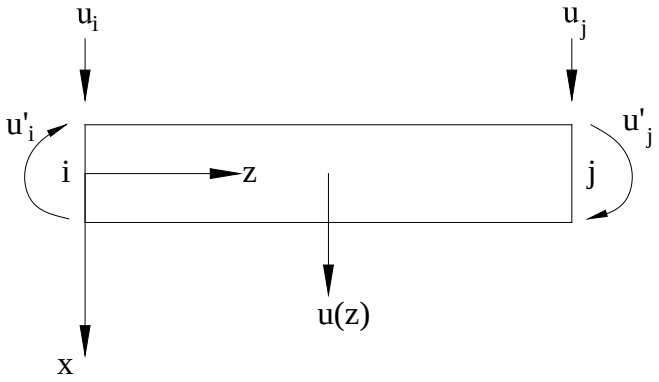

(a.)

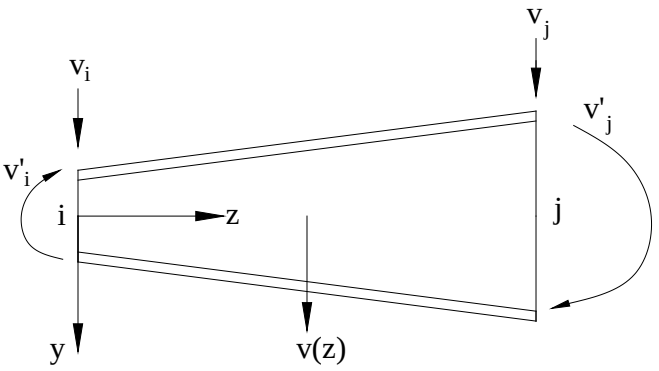

(b.)

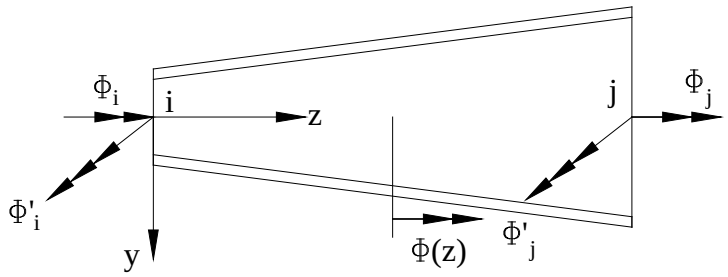

(c.)

Figure 5.1 Element Degrees of Freedom

Because the cross-section of the flexural-torsional beam element has two principal planes, and small displacements theory are assumed, the generalized displacements, $u(z)$, $v(z)$, and $\phi(z)$ are decoupled. Since there are four nodal displacements for each generic displacement, a complete cubic displacement function may be assumed for each of them. The displacement functions for $u(z)$, $v(z)$, and $\phi(z)$ expressed in terms of their shape functions are

$$u(z)=[N]\{u\},\ \ v(z)=[N]\{v\},\ \ \phi(z)=[N]\{\phi\} \tag{5-1}$$

where

$$[N]=\left[\frac{1}{L^3}(2z^3-3z^2L+L^3)\quad \frac{1}{L^3}(Lz^3-2z^2L^2+zL^3)\quad \frac{1}{L^3}(-2z^3+3z^2L)\quad \frac{1}{L^3}(Lz^3-z^2L^2)\right] \tag{5-2}$$

$$\{u\}=\{u_i,u_i',u_j,u_j'\}^T,\{v\}=\{v_i,v_i',v_j,v_j'\}^T,\{\phi\}=\{\phi_i,\phi_i',\phi_j,\phi_j'\}^T \tag{5-3}$$

The matrix [N] is the shape function matrix for the element. Each term of the shape function matrix expresses the shape of the assumed displacement function over the domain of the element when the element degree of freedom corresponding to the shape function has unit value and all other degrees of freedom are zero. The first variation of Eq. (5-1) is

$$\delta u(z) = [N]\{\delta u\}, \quad \delta v(z) = [N]\{\delta v\}, \quad \delta\phi(z) = [N]\{\delta\phi\} \tag{5-4}$$

In this study, it is assumed that a beam element is linearly tapered, the origin of the coordinate system is the near node, then $h(z)$ is a linear function of z.

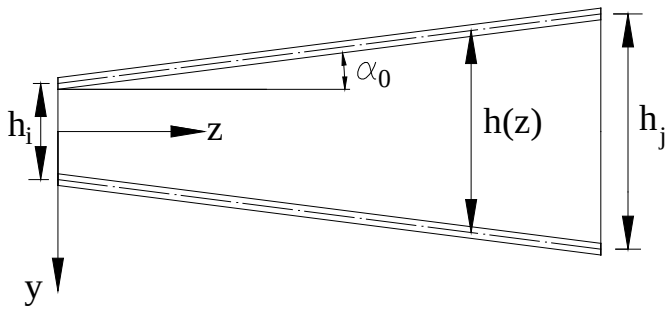

Figure 5.2 The Depth of the I-Beam

Figure 5.2 shows the relation between the depth $h(z)$ at an arbitrary location and the depth at two nodes, node i and node j, then one may have:

$$h(z) = [1 - \frac{z}{L} \quad \frac{z}{L}]\{h_i \quad h_j\}^T = (\frac{L-z}{L})h_i + \frac{z}{L}h_j \tag{5-5}$$

where h_i and h_j are the depths of the cross section at node i and node j, respectively, and L is the element length.

One also finds that

$$\frac{dh(z)}{dz} = \frac{h_j - h_i}{L} = 2\tan\alpha_0 \tag{5-6}$$

The stiffness matrices are calculated next, including the elastic and the geometric stiffness matrices, based on the energy equation given by Eq. (3-83). The energy equation is derived using the rotation transformation equation in terms of the displacements at the centroid of a cross section. However, as mentioned in Chapter 4, the web and the flanges in a doubly-symmetric web-tapered I-beam are using different coordinate systems due to the tapered effects. Therefore, the cross section is decomposed into three parts, the web, the top flange and the bottom flange. The energy equations for the web element and the flange element are formulated separately, from which the elastic stiffness matrix and the geometric stiffness matrix for each part are derived. Then, the stiffness matrices for a web-tapered I-beam element, including both the flange elements and the web element, are obtained based on the transformation matrix that can transform the displacements of the centroid of the flange in *xns* coordinate to the displacements of the centroid of the web in *xyz* coordinate.

Before the energy equations for each part are formulated, the transformation matrices are derived next.

5.1 DERIVATION OF TRANSFORMATION MATRIX $\hat{T}$ AND T_e

To transform the displacements of the centroid of the flanges in *xns* coordinate to the displacements of the centroid of the web in *xyz* coordinate, as shown in Figure 5.3, there are two steps involved.

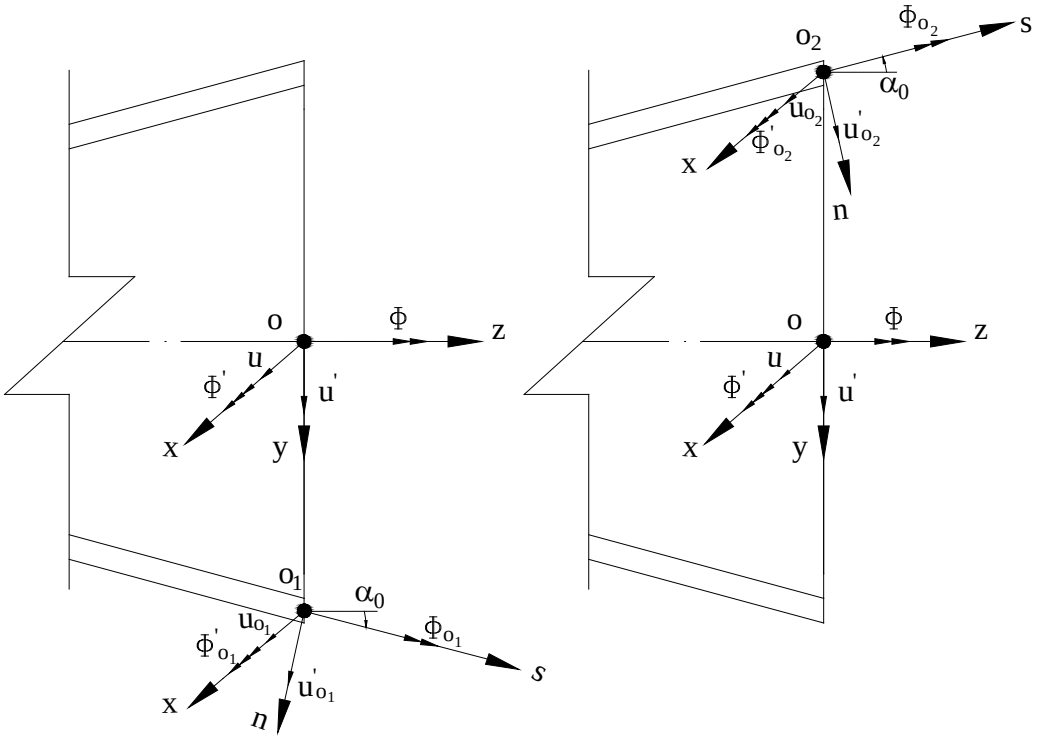

Figure 5.3 Displacements of the Centroid of the Web and the Flanges

The first step is to transform the direction of displacements at centroid of the flanges from *xns* directions to their equivalent displacements in *xyz* directions. Then, the second step is to translate the displacements at centroid of the flange from O_1, and O_2 in *xyz* directions to the displacement at centroid of the web in *xyz* directions. The first and the second step process will produce the transformation matrices $\hat{T}$, and T_e, respectively.

5.1.1 Derivation of Transformation Matrix $\hat{T}$

The transformation matrix that changes the direction of displacements at the centroid of the flanges from *xns* directions to the displacements at the centroid of the flanges in *xyz* directions may be developed based on Figure 5.4.

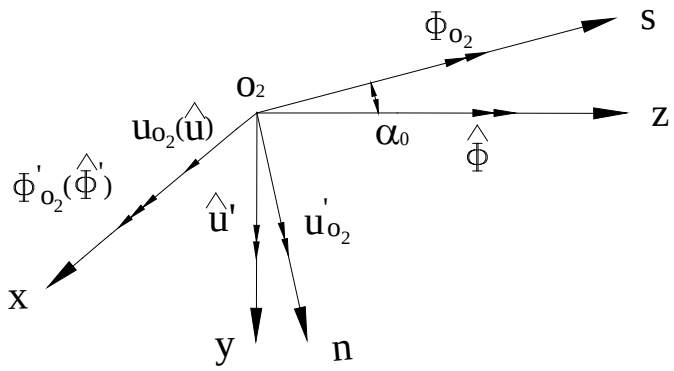

(a) Top flange

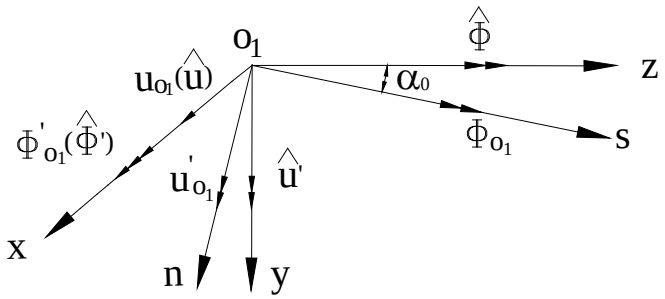

(b) Bottom flange

Figure 5.4 Displacements at the Centroid of the Flanges in *xns* and *xyz* Directions

From the Figure 5.4, one may have:

For the top flange:

$$u_{o_2} = \hat{u} \tag{5-7}$$

$$u'_{o_2} = \hat{u}'\cos\alpha_0 + \hat{\phi}\sin\alpha_0 \tag{5-8}$$

$$\phi_{o_2} = -\hat{u}'\sin\alpha_0 + \hat{\phi}\cos\alpha_0 \tag{5-9}$$

$$\phi'_{o_2} = \hat{\phi}' \tag{5-10}$$

One may rewrite Eqs.(5-7) to (5-10) in the matrix form

$$\begin{Bmatrix} u_{o_2} \\ u'_{o_2} \\ \phi_{o_2} \\ \phi'_{o_2} \end{Bmatrix} = \begin{bmatrix} 1 & 0 & 0 & 0 \\ 0 & \cos\alpha_0 & \sin\alpha_0 & 0 \\ 0 & -\sin\alpha_0 & \cos\alpha_0 & 0 \\ 0 & 0 & 0 & 1 \end{bmatrix} \begin{Bmatrix} \hat{u} \\ \hat{u}' \\ \hat{\phi} \\ \hat{\phi}' \end{Bmatrix} \tag{5-11}$$

For the bottom flange:

$$u_{o_1} = \hat{u} \tag{5-12}$$

$$u'_{o_1} = \hat{u}'\cos\alpha_0 - \hat{\phi}\sin\alpha_0 \tag{5-13}$$

$$\phi_{o_1} = \hat{u}'\sin\alpha_0 + \hat{\phi}\cos\alpha_0 \tag{5-14}$$

$$\phi'_{o_1} = \hat{\phi}' \tag{5-15}$$

One may rewrite Eqs.(5-12) to (5-15) in the matrix form

$$\begin{Bmatrix} u_{o_1} \\ u'_{o_1} \\ \phi_{o_1} \\ \phi'_{o_1} \end{Bmatrix} = \begin{bmatrix} 1 & 0 & 0 & 0 \\ 0 & \cos\alpha_0 & -\sin\alpha_0 & 0 \\ 0 & \sin\alpha_0 & \cos\alpha_0 & 0 \\ 0 & 0 & 0 & 1 \end{bmatrix} \begin{Bmatrix} \hat{u} \\ \hat{u}' \\ \hat{\phi} \\ \hat{\phi}' \end{Bmatrix} \tag{5-16}$$

Eqs. (5-11) and (5-16) applies to the transformation of displacements at the top and bottom flanges at node i. If we expand the matrices to an element including both nodes i and j, the transformation matrix $\hat{T}$ for the top and bottom flanges are obtained.

For the top flange, based on Eq. (5-11), one has:

$$(\hat{T})_{top} = \begin{bmatrix} 1 & 0 & 0 & 0 & 0 & 0 & 0 & 0 \\ 0 & \cos\alpha_0 & \sin\alpha_0 & 0 & 0 & 0 & 0 & 0 \\ 0 & -\sin\alpha_0 & \cos\alpha_0 & 0 & 0 & 0 & 0 & 0 \\ 0 & 0 & 0 & 1 & 0 & 0 & 0 & 0 \\ 0 & 0 & 0 & 0 & 1 & 0 & 0 & 0 \\ 0 & 0 & 0 & 0 & 0 & \cos\alpha_0 & \sin\alpha_0 & 0 \\ 0 & 0 & 0 & 0 & 0 & -\sin\alpha_0 & \cos\alpha_0 & 0 \\ 0 & 0 & 0 & 0 & 0 & 0 & 0 & 1 \end{bmatrix} \tag{5-17a}$$

For the bottom flange, based on Eq. (5-16), one may have:

$$(\hat{T})_{bottom} = \begin{bmatrix} 1 & 0 & 0 & 0 & 0 & 0 & 0 & 0 \\ 0 & \cos\alpha_0 & -\sin\alpha_0 & 0 & 0 & 0 & 0 & 0 \\ 0 & \sin\alpha_0 & \cos\alpha_0 & 0 & 0 & 0 & 0 & 0 \\ 0 & 0 & 0 & 1 & 0 & 0 & 0 & 0 \\ 0 & 0 & 0 & 0 & 1 & 0 & 0 & 0 \\ 0 & 0 & 0 & 0 & 0 & \cos\alpha_0 & -\sin\alpha_0 & 0 \\ 0 & 0 & 0 & 0 & 0 & \sin\alpha_0 & \cos\alpha_0 & 0 \\ 0 & 0 & 0 & 0 & 0 & 0 & 0 & 1 \end{bmatrix} \tag{5-17b}$$

5.1.2 Derivation of Transformation Matrix T_e

Based on geometry (Figure 5.5), one may calculate the relation between the displacements at centroid of the flanges in *xyz* directions and the displacements at centroid of the web in *xyz* directions:

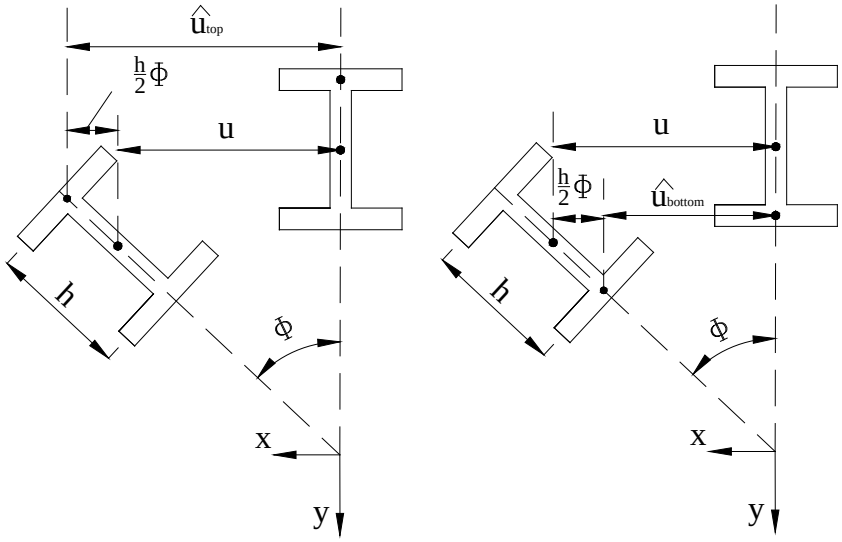

Figure 5.5 Relation between Displacements of the Web and the Flanges

For the top flange, one has:

$$\hat{u}_{top} = u + \frac{h}{2}\phi \tag{5-18a}$$

For the bottom flange:

$$\hat{u}_{bottom} = u - \frac{h}{2}\phi \tag{5-18b}$$

Based on Eq. (5-18), one may calculate

$$\hat{u}'_{top} = u' + \frac{h'}{2}\phi + \frac{h}{2}\phi' \tag{5-19a}$$

$$\hat{u}'_{bottom} = u' - \frac{h'}{2}\phi - \frac{h}{2}\phi' \tag{5-19b}$$

where $h' = 2\tan\alpha_0$.

Eqs. (5-18) and (5-19) may be implemented for node i to derive a transformation matrix relating displacements of the centroid of the flanges in xyz directions to the displacements of the centroid of the web in xyz directions:

For the top flange:

$$\begin{Bmatrix} \hat{u}_i \\ \hat{u}_i' \\ \hat{\phi}_i \\ \hat{\phi}_i' \end{Bmatrix}_{Top} = \begin{bmatrix} 1 & 0 & \frac{h_i}{2} & 0 \\ 0 & 1 & \tan\alpha_o & \frac{h_i}{2} \\ 0 & 0 & 1 & 0 \\ 0 & 0 & 0 & 1 \end{bmatrix} \begin{Bmatrix} u_i \\ u_i' \\ \phi_i \\ \phi_i' \end{Bmatrix} \tag{5-20a}$$

For the bottom flange:

$$\begin{Bmatrix} \hat{u}_i \\ \hat{u}_i' \\ \hat{\phi}_i \\ \hat{\phi}_i' \end{Bmatrix}_{Bottom} = \begin{bmatrix} 1 & 0 & -\frac{h_i}{2} & 0 \\ 0 & 1 & -\tan\alpha_o & -\frac{h_i}{2} \\ 0 & 0 & 1 & 0 \\ 0 & 0 & 0 & 1 \end{bmatrix} \begin{Bmatrix} u_i \\ u_i' \\ \phi_i \\ \phi_i' \end{Bmatrix} \tag{5-20b}$$

One may expand the matrices, Eq.(5-20), to an element including both nodes i and j, the transformation matrix $\hat{T}_e$ for both the top and bottom flanges are obtained.

For the top flange:

$$(T_e)_{top} = \begin{bmatrix} 1 & 0 & \frac{h_i}{2} & 0 & 0 & 0 & 0 & 0 \\ 0 & 1 & \tan\alpha_0 & \frac{h_i}{2} & 0 & 0 & 0 & 0 \\ 0 & 0 & 1 & 0 & 0 & 0 & 0 & 0 \\ 0 & 0 & 0 & 1 & 0 & 0 & 0 & 0 \\ 0 & 0 & 0 & 0 & 1 & 0 & \frac{h_j}{2} & 0 \\ 0 & 0 & 0 & 0 & 0 & 1 & \tan\alpha_0 & \frac{h_j}{2} \\ 0 & 0 & 0 & 0 & 0 & 0 & 1 & 0 \\ 0 & 0 & 0 & 0 & 0 & 0 & 0 & 1 \end{bmatrix} \tag{5-21a}$$

For the bottom flange:

$$(T_e)_{bottom} = \begin{bmatrix} 1 & 0 & -\frac{h_i}{2} & 0 & 0 & 0 & 0 & 0 \\ 0 & 1 & -\tan\alpha_0 & -\frac{h_i}{2} & 0 & 0 & 0 & 0 \\ 0 & 0 & 1 & 0 & 0 & 0 & 0 & 0 \\ 0 & 0 & 0 & 1 & 0 & 0 & 0 & 0 \\ 0 & 0 & 0 & 0 & 1 & 0 & -\frac{h_j}{2} & 0 \\ 0 & 0 & 0 & 0 & 0 & 1 & -\tan\alpha_0 & -\frac{h_j}{2} \\ 0 & 0 & 0 & 0 & 0 & 0 & 1 & 0 \\ 0 & 0 & 0 & 0 & 0 & 0 & 0 & 1 \end{bmatrix} \tag{5-21b}$$

Finally, using Eqs. (5-17) and (5-21), one may express the displacements of the centroid of the flanges as

$$\{d_e\}_{topflange} = [\hat{T}]_{top}[T_e]_{top}\{d_e\}_{web} \tag{5-22a}$$

$$\{d_e\}_{bottomflange} = [\hat{T}]_{bottom}[T_e]_{bottom}\{d_e\}_{web} \tag{5-22b}$$

where

$$\{d_e\}_{web} = \begin{Bmatrix} u_i \\ u_i' \\ \phi_i \\ \phi_i' \\ u_j \\ u_j' \\ \phi_j \\ \phi_j' \end{Bmatrix} = \text{the local nodal displacement vector of an element} \tag{5-23}$$

The elastic and geometric stiffness matrices of an element in local coordinates both are 8 by 8 because there are eight local displacements for each element that correspond to the displacements at buckling. The arrangement of the elements for the stiffness and the geometric stiffness matrices is shown by Eqs. (5-24) and (5-25). Both matrices are symmetric about the main diagonal.

$$\begin{array}{c} \\ u_i \\ u_i' \\ \phi_i \\ \phi_i' \\ u_j \\ u_j' \\ \phi_j \\ \phi_j' \end{array} \begin{array}{c} \begin{array}{cccccccc} u_i & u_i' & \phi_i & \phi_i' & u_j & u_j' & \phi_j & \phi_j' \end{array} \\ \begin{bmatrix} k11 & k12 & k13 & k14 & k15 & k16 & k17 & k18 \\ & k22 & k23 & k24 & k25 & k26 & k27 & k28 \\ & & k33 & k34 & k35 & k36 & k37 & k38 \\ & & & k44 & k45 & k46 & k47 & k48 \\ & & & & k55 & k56 & k57 & k58 \\ & & & & & k66 & k67 & k68 \\ & & & & & & k77 & k78 \\ & & & & & & & k88 \end{bmatrix} \end{array} \tag{5-24}$$

$$
\begin{array}{c}
 \\ u_i \\ u'_i \\ \phi_i \\ \phi'_i \\ u_j \\ u'_j \\ \phi_j \\ \phi'_j
\end{array}
\begin{array}{c}
\begin{array}{cccccccc} u_i & u'_i & \phi_i & \phi'_i & u_j & u'_j & \phi_j & \phi'_j \end{array} \\
\left[\begin{array}{cccccccc}
g11 & g12 & g13 & g14 & g15 & g16 & g17 & g18 \\
 & g22 & g23 & g24 & g25 & g26 & g27 & g28 \\
 & & g33 & g34 & g35 & g36 & g37 & g38 \\
 & & & g44 & g45 & g46 & g47 & g48 \\
 & & & & g55 & g56 & g57 & g58 \\
 & & & & & g66 & g67 & g68 \\
 & & & & & & g77 & g78 \\
 & & & & & & & g88
\end{array}\right]
\end{array}
\tag{5-25}
$$

These stiffness matrices are derived based on the energy Eq. (3-83) that have been developed in Chapter 3. The first three terms of Eq. (3-83) contribute to the generation of the elastic stiffness matrix and the last four terms contribute to the generation of the geometric stiffness matrix.

5.2 DERIVATION OF ELASTIC STIFFNESS MATRIX K_e

5.2.1 Elastic Stiffness Matrix of the Web

The equation that contributes to the elastic stiffness matrix of the web is given by

$$
\frac{1}{2}\int_L \left[EI_{y_w}\left(\frac{d^2(\delta u)}{dz^2}\right)^2 + GJ_w\left(\frac{d(\delta\phi)}{dz}\right)^2 + EI_{\omega_w}\left(\frac{d^2(\delta\phi)}{dz^2}\right)^2 \right] dz\,, \tag{5-26}
$$

Eq.(5-26) may be expressed in a matrix formulation:

$$
\frac{1}{2}\int_L \{\delta\varepsilon\}^T [D]\{\delta\varepsilon\}\, dz\,, \tag{5-27}
$$

where

$$\{\delta\varepsilon\} = \left\{ \frac{d^2(\delta u)}{dz^2} \quad \frac{d(\delta\phi)}{dz} \quad \frac{d^2(\delta\phi)}{dz^2} \right\}^T \tag{5-28}$$

and

$$[D] = \begin{bmatrix} EI_{y_w} & & \\ & GJ_w & \\ & & EI_{\omega_w} \end{bmatrix} \tag{5-29}$$

Thus, based on Eq. (5-4), Eq. (5-26) is expanded as

$$\frac{1}{2}\int_L \begin{Bmatrix} \{\delta u\} \\ \{\delta\phi\} \end{Bmatrix}^T \begin{bmatrix} [N_{,zz}] & 0 \\ 0 & [N_{,z}] \\ 0 & [N_{,zz}] \end{bmatrix}^T \begin{bmatrix} EI_{y_w} & & \\ & GJ_w & \\ & & EI_{\omega_w} \end{bmatrix} \begin{bmatrix} [N_{,zz}] & 0 \\ 0 & [N_{,z}] \\ 0 & [N_{,zz}] \end{bmatrix} \begin{Bmatrix} \{\delta u\} \\ \{\delta\phi\} \end{Bmatrix} dz \tag{5-30}$$

where

$$[N] = \left[\frac{1}{L^3}(2z^3 - 3z^2L + L^3) \quad \frac{1}{L^3}(Lz^3 - 2z^2L^2 + zL^3) \quad \frac{1}{L^3}(-2z^3 + 3z^2L) \quad \frac{1}{L^3}(Lz^3 - z^2L^2) \right] \tag{5-31}$$

$$[N_{,z}] = \left[\frac{1}{L^3}(6z^2 - 6zL) \quad \frac{1}{L^3}(3Lz^2 - 4zL^2 + L^3) \quad \frac{1}{L^3}(-6z^2 + 6zL) \quad \frac{1}{L^3}(3Lz^2 - 2zL^2) \right] \tag{5-32}$$

$$[N_{,zz}] = \left[\frac{1}{L^3}(1 \quad z - 6zL) \quad \frac{1}{L^3}(6Lz - 4L^2) \quad \frac{1}{L^3}(-1 \quad z + 6zL) \quad \frac{1}{L^3}(6Lz - 2L^2) \right] \tag{5-33}$$

and

$$I_{y_w} = \int_{A_w} x^2 dA_w = h_w(z) \int_{-t_w/2}^{t_w/2} x^2 dx = [\frac{L-z}{L} h_i + \frac{z}{L} h_j] t_w{}^3 / 12 \tag{5-34}$$

$$J_w = \int_{A_w} 4t_P{}^2 dA_w = h_w(z) \int_{-t_w/2}^{t_w/2} 4x^2 dx = h_w(z) t_w{}^3 / 3 = (\frac{L-z}{L} h_i + \frac{z}{L} h_j) t_w{}^3 / 3 \tag{5-35}$$

$$I_{\omega_w} = \int_{A_w} \omega^2 dA_w = \int_{-h_w(z)/2}^{h_w(z)/2} \int_{-t_w/2}^{t_w/2} \left(\int_{-t_w/2}^{t_w/2} -y dx + \int_{-h_w(z)/2}^{h_w(z)/2} x dy \right)^2 dx dy$$

$$= \frac{1}{6} \frac{t_w{}^3}{L^3} (L^3 h_i{}^3 - 3L^2 h_i{}^3 z + 3L^2 h_i{}^2 z h_j + 3L h_i{}^3 z^2 - 6L h_i{}^2 z^2 h_j$$

$$+3L h_i z^2 h_j{}^2 - h_i{}^3 z^3 + 3h_i{}^2 z^3 h_j - 3h_i z^3 h_j{}^2 + z^3 h_j{}^3) \tag{5-36}$$

The elastic stiffness matrix for the web is thus determined:

$$[K_e]_{web} = \int_L \begin{bmatrix} [N_{,zz}] & 0 \\ 0 & [N_{,z}] \\ 0 & [N_{,zz}] \end{bmatrix}^T \begin{bmatrix} EI_{y_w} & 0 & 0 \\ 0 & GJ_w & 0 \\ 0 & 0 & EI_{\omega_w} \end{bmatrix} \begin{bmatrix} [N_{,zz}] & 0 \\ 0 & [N_{,z}] \\ 0 & [N_{,zz}] \end{bmatrix} dz \tag{5-37}$$

5.2.2 Elastic Stiffness Matrix of the Flange

The equation that contributes to the elastic stiffness matrix is given by

$$\frac{1}{2} \int_{L_f} \left[EI_n \left(\frac{d^2(\delta u)}{ds^2} \right)^2 + GJ_f \left(\frac{d(\delta \phi_s)}{ds} \right)^2 + EI_{\omega f} \left(\frac{d^2(\delta \phi_s)}{ds^2} \right)^2 \right] ds\,, \tag{5-38}$$

It can be expressed in a matrix form:

$$\frac{1}{2}\int_{L_f}\{\delta\varepsilon\}^T[D_f]\{\delta\varepsilon\}\,ds \tag{5-39}$$

where

$$\{\delta\varepsilon\}=\left\{\frac{d^2(\delta u)}{ds^2}\quad\frac{d(\delta\phi_s)}{ds}\quad\frac{d^2(\delta\phi_s)}{ds^2}\right\}^T \tag{5-40}$$

and

$$\left[D_f\right]=\begin{bmatrix}EI_n & & \\ & GJ_f & \\ & & EI_{\omega f}\end{bmatrix} \tag{5-41}$$

$$I_n=\int_{A_f}x^2dA_f\ ,\quad J_f=\int_{A_f}t_p{}^2dA_f\ ,\quad I_{\omega f}=\int_{A_f}\omega^2dA_f \tag{5-42}$$

Eq. (5-38) is rewritten as

$$\frac{1}{2}\int_{L_f}\begin{Bmatrix}\{\delta u\}\\ \{\delta\phi_s\}\end{Bmatrix}^T\begin{bmatrix}\left[N_{,ss}\right] & 0\\ 0 & \left[N_{,s}\right]\\ 0 & \left[N_{,ss}\right]\end{bmatrix}^T\begin{bmatrix}EI_n & & \\ & GJ_f & \\ & & EI_{\omega_f}\end{bmatrix}\begin{bmatrix}\left[N_{,ss}\right] & 0\\ 0 & \left[N_{,s}\right]\\ 0 & \left[N_{,ss}\right]\end{bmatrix}\begin{Bmatrix}\{\delta u\}\\ \{\delta\phi_s\}\end{Bmatrix}ds \tag{5-43}$$

where N is the shape function for displacements and is given by:

$$[N]=\left[\frac{1}{L_f{}^3}(2s^3-3s^2L_f+L_f{}^3)\quad\frac{1}{L_f{}^3}(L_fs^3-2s^2L_f{}^2+sL_f{}^3)\quad\frac{1}{L_f{}^3}(-2s^3+3s^2L_f)\quad\frac{1}{L_f{}^3}(L_fs^3-s^2L_f{}^2)\right]$$

(5-44)

$$[N_{,s}]=\left[\frac{1}{L_f{}^3}(6s^2-6sL_f)\quad\frac{1}{L_f{}^3}(3L_fs^2-4sL_f{}^2+L_f{}^3)\quad\frac{1}{L_f{}^3}(-6s^2+6sL_f)\quad\frac{1}{L_f{}^3}(3L_fs^2-2sL_f{}^2)\right]$$

(5-45)

$$[N_{,ss}] = \left[\frac{1}{L_f^3}(1 \;\; s - 6L_f) \quad \frac{1}{L_f^3}(6L_f s - 4L_f^2) \quad \frac{1}{L_f^3}(-1 \;\; s + 6L_f) \quad \frac{1}{L_f^3}(6L_f s - 2L_f^2) \right]$$

(5-46)

where L_f is the length of the flange in an element, and $L_f = L / \cos\alpha_0$.

The elastic stiffness matrix for the flange is thus determined:

$$[K_e]_{flange} = \int_{L_f} \begin{bmatrix} [N_{,ss}] & 0 \\ 0 & [N_{,s}] \\ 0 & -[N_{,ss}] \end{bmatrix}^T \begin{bmatrix} EI_n & 0 & 0 \\ 0 & GJ_f & 0 \\ 0 & 0 & EI_{\omega_f} \end{bmatrix} \begin{bmatrix} [N_{,ss}] & 0 \\ 0 & [N_{,s}] \\ 0 & -[N_{,ss}] \end{bmatrix} ds \qquad (5\text{-}47)$$

The elastic stiffness matrix for a beam element, in the local coordinates xyz, is the sum of the elastic stiffness matrix of the web and the flanges, and it is given by Eq. (5-48):

$$[K_e] = [K_e]_{web} + [(T_e)_{top}]^T \left[(\hat{\hat{T}})_{top} \right]^T [K_e]_{flange} \left[(T)_{top} \right] [(T_e)_{top}]$$
$$+ [(T_e)_{bottom}]^T \left[(\hat{\hat{T}})_{bottom} \right]^T [K_e]_{flange} \left[(T)_{bottom} \right] [(T_e)_{bottom}] \qquad (5\text{-}48)$$

5.3 DERIVATION OF GEOMETRIC STIFFNESS MATRIX G_e

Since the geometric stiffness is not related to the cross section properties of the structure, it is developed based on a complete web-tapered I-beam element. The equation that contributes to the geometric stiffness matrix is given by

$$\frac{1}{2}\lambda \int_L [(2M_x)(\frac{d^2(\delta u)}{dz^2})\delta\phi + F(\frac{d\delta u}{dz})^2]dz + \frac{1}{2}\lambda \int_L q a_z (\delta\phi)^2 dz + \frac{1}{2}\lambda \Sigma P e_z (\delta\phi)^2$$

(5-49)

$$F = EA_w(\frac{dw}{dz}) \tag{5-50}$$

$$M_x = -EI_{x_w}(\frac{d^2v}{dz^2}) \tag{5-51}$$

Eq.(5-49) can be expressed in a finite formulation:

$$\frac{1}{2}\lambda\int_L \{\delta\varepsilon\}^T [D]\{\delta\varepsilon\}\, dz + \frac{1}{2}\lambda \sum Pe_z(\delta\phi)^2 \tag{5-52}$$

where

$$\{\delta\varepsilon\} = \left\{\frac{d(\delta u)}{dz} \quad \frac{d^2(\delta u)}{dz^2} \quad \delta\phi\right\}^T \tag{5-53}$$

and

$$[D] = \begin{bmatrix} F & 0 & 0 \\ 0 & 0 & M_x \\ 0 & M_x & qa_z \end{bmatrix} \tag{5-54}$$

where

$$M_x = M_i + V_i z \quad \text{for} \quad 0 < z < z_p \tag{5-55a}$$

$$M_x = M_i + V_i z - P(z - z_P) \quad \text{for} \quad z_p < z < L \tag{5-55b}$$

z_p =the distance along the beam to the point of the applied concentrated load

$$F = F_i \tag{5-56}$$

Based on Eq. (5-4), Eq. (5-52) can be expanded as

$$\frac{1}{2}\lambda\int_L \begin{Bmatrix}\{\delta u\}\\ \{\delta\phi\}\end{Bmatrix}^T \begin{bmatrix}[N_{,z}] & 0\\ [N_{,zz}] & 0\\ 0 & [N]\end{bmatrix}^T [D] \begin{bmatrix}[N_{,z}] & 0\\ [N_{,zz}] & 0\\ 0 & [N]\end{bmatrix} \begin{Bmatrix}\{\delta u\}\\ \{\delta\phi\}\end{Bmatrix} dz$$

$$+\frac{1}{2}\lambda\left\{\begin{Bmatrix}\delta u\\ \delta\phi\end{Bmatrix}^T [[0] \quad [N]]^T (Pe) [[0] \quad [N]] \begin{Bmatrix}\{\delta u\}\\ \{\delta\phi\}\end{Bmatrix}\right\}\Bigg|_{z=z_p} \tag{5-57}$$

The geometric stiffness matrix is thus determined:

$$[K_g] = \int_L \begin{bmatrix}[N_{,z}] & 0\\ [N_{,zz}] & 0\\ 0 & [N]\end{bmatrix}^T [D] \begin{bmatrix}[N_{,z}] & 0\\ [N_{,zz}] & 0\\ 0 & [N]\end{bmatrix} dz + [[0] \quad [N]]^T (Pe) [[0] \quad [N]]\Big|_{z=z_p} \tag{5-58}$$

Eq. (5-58) produces an 8 by 8 matrix, whose deformation vectors are not ordered the same as the vectors in Eq. (5-25). Therefore, the terms in the matrix derived by Eq. (5-58) must be moved to the appropriate positions to fill the stiffness matrix shown in Eq. (5-25). The terms of the geometric stiffness matrix are calculated and positioned in the proper locations in Appendix B.

For each individual element, the stain energy together with the work done by external forces are expressed in terms of the buckling nodal deformations and the element stiffness in the finite element formulation

$$\frac{1}{2}\{\delta d_e\}^T \left([K_e] + \lambda [K_g]\right)\{\delta d_e\} \tag{5-59}$$

where $[K_e]$ and $[K_g]$ are given by Eqs.(5-48) and (5-58).

6.0 FLEXURAL-TORSIONAL BUCKLING EIGENVALUE PROBLEM SOLUTION

A finite element analysis of the structured systems requires that the structure be divided into several elements. The number and type of the elements depends on the geometry, material, and loading condition of the structure. In this section, it is assumed that one is interested in calculation of the flexural-torsional buckling load of a single tapered beam subjected to arbitrary loading and stable support condition. Therefore, the beam is divided into *n* elements. For each element, as it was shown in Chapter 5, the second variation of the total potential energy in the global coordinate system may be expressed

$$\frac{1}{2}\delta^2 \prod_e = \frac{1}{2}\{\delta D_e\}^T \left([K_e] + \lambda [G_e]\right)\{\delta D_e\} \tag{6-1}$$

Where

$[K_e]$ is the element elastic stiffness matrix in global coordinates

$[G_e]$ is the element geometric stiffness matrix in global coordinates

$$\{\delta D_e\}^T = \{\delta U_i, \quad \delta U_i', \quad \delta\Phi_i, \quad \delta\Phi_i', \quad \delta U_j, \quad \delta U_j', \quad \delta\Phi_j, \quad \delta\Phi_j'\}^T \tag{6-2}$$

To predict the buckling loads of the structure, the element matrices must be combined together by the superposition process with respect to the degrees of freedom. Therefore, the second variation of the total potential energy equation of the structure becomes:

$$\{\delta D\}^T \left(\sum[K_e] + \lambda \sum[G_e]\right)\{\delta D\} = 0 \tag{6-3}$$

where

$\sum[K_e]$ is the structure global elastic stiffness matrix

$\sum[G_e]$ is the structure global geometric stiffness matrix

Since the variation of the displacement does not equal zero, Eq. (6-3) becomes

$$\left(\sum[K_e] + \lambda \sum[G_e]\right)\{\delta D\} = 0 \tag{6-4}$$

Eq. (6-4) is in the form of a generalized linear eigenvalue problem, and it can be solved to determine the flexural-torsional buckling loads. A symmetric positive definite matrix of order n has n eigenvalues λ_n and n non-zero eigenvectors $\{\delta D\}_n$. The lowest eigenvalue defines the load set at which the structure first buckles, and the corresponding eigenvector defines the buckling mode of the structure.

In order to calculate the eigenvalues and eigenvectors of a generalized eigenvalue problem, the problem should be converted to a standard eigenvalue problem (Griffiths and Smith 1991). In other words, a generalized eigenvalue problem of the form

$$\left([A] + \lambda [B]\right)\{X\} = 0 \tag{6-5}$$

should be converted to the standard form of

$$\left([A] + \lambda [I]\right)\{X\} = 0 \tag{6-6}$$

where

$[I]$ is the identity matrix.

To do so, one should first apply the Cholesky decomposition (Griffiths and Smith 1991) to the stiffness matrix $[K]$. The Cholesky decomposition is the numerical method to

decompose a square and symmetric matrix to the product of an upper triangular and the transpose of the upper triangular matrix. This process can be written as

$$[K]=[C][C]^T \tag{6-7}$$

The next step is to substitute for the stiffness matrix in the generalized eigenvalue equation (6-3) using Eq. (6-7)

$$\left([C][C]^T\right)\cdot\{\delta D\}=-\lambda[G]\cdot\{\delta D\} \tag{6-8}$$

Using premultiplication in Eq. (6-8), one may have

$$[C]^T\cdot\{\delta D\}=-\lambda[C]^{-1}[G]\cdot\{\delta D\} \tag{6-9}$$

Introduce

$$\{\delta\overline{D}\}=[C]^T\cdot\{\delta D\}\text{, or }\ \{\delta D\}=\left([C]^T\right)^{-1}\{\delta\overline{D}\} \tag{6-10}$$

Substitute Eq. (6-10) in Eq. (6-9), one may have

$$\{\delta\overline{D}\}=-\lambda\left([C]^{-1}[G]\left([C]^T\right)^{-1}\right)\cdot\{\delta\overline{D}\} \tag{6-11}$$

Moving all the terms on the right side in Eq. (6-11) to the left, one may rewrite Eq. (6-12)

$$\left([C]^{-1}[G]\left([C]^T\right)^{-1}+\frac{1}{\lambda}[I]\right)\cdot\{\delta D\}=0 \tag{6-12}$$

Eq. (6-12) is in the form of a standard eigenvalue problem. It can be expressed more closely to Eq. (6-5) if it is rewritten as

$$\left([S]+\gamma[I]\right)\{D\}=0 \tag{6-13}$$

where

$$[S]=[C]^{-1}[G]\left([C]^T\right)^{-1} \tag{6-14}$$

$$\gamma=\frac{1}{\lambda} \tag{6-15}$$

The last step is to solve the standard eigenvalue problem. There are many numerical methods to solve a standard eigenvalue problem, the selection of the methods depends on the size of the matrix. Since the matrices in a flexural-torsional buckling problem can become very large, the matrices may be converted to a simpler form using Householder's method before solving for the eigenvalues (Griffiths and Smith 1991). Householder's method converts a symmetric matrix into a tridiagonal matrix, a tridiagonal matrix has non-zero elements only on the diagonal plus or minus one column (Press 1992). The eigenvalues of a tridiagonal matrix may be then solved using QL iteration (Press 1992). The buckling loads are the trial applied loads multiplied by the smallest eigenvalue, λ, which may be described by the relationship

$$\{F\}_{cr} = \lambda \{F\} \tag{6-16}$$

where $\{F\}_{cr}$ is the vector of the buckling loads, $\{F\}$ is the vector of the trial loads, and λ is a buckling parameter.

7.0 SOFTWARE DEVELOPMENT

There are many software packages that can be used to solve eigenvalues and eigenvectors of a standard eigenvalue problem. However, the solution of a generalized eigenvalue problem in our research is a complex and time consuming process for large matrices. Therefore, our aim is to develop a software package of special purpose to determine the flexural-torsional buckling load of a doubly-symmetric web-tapered I-beam.

Object-oriented technology can be defined as a method of analysis, design and implementation of software that considers a problem as a real world situation. This technology was selected for the program design and implementation over other software development technologies because of the numerous advantages it offers in software organization and that it can support a finite element application. Unlike traditional procedural programming languages, object-oriented programming languages focus on breaking the software into modular units, and each unit is modeled based upon a real-world concept, not a computer concept. Since the models are close to a real problem, a more precise and concise software can be developed. This programming approach was developed to provide a more organized methodology to software development in comparison to the older disorganized approaches.

There are many languages that support object-oriented design, including Smalltalk, Eiffel, C++, and etc. There is no particular object-oriented language superior to the others; rather, it is best to select a programming language based on its ability to provide sufficient support of the desired programming style (Stroustrup 1991). The object-oriented language used in this program design is C/C++.

C/C++ is a structured language convenient for software development or revision, and it is also a mid-level language that can be used as a high-level language, and can directly access the hardware like a low-level language. Among many programming languages, C/C++ was selected because it has become one of the most popular ones that support object-oriented design.

7.1 OBJECT-ORIENTED MODELING AND PROGRAMMING CONCEPTS

The fundamental idea behind object-oriented languages is to combine into a single unit both data and the functions that operate on that data. Such a unit is called an object; it is the smallest unit of a system. This concept of combining data and functions into one entity is known as encapsulation. An object's functions, called member functions in C++, typically provide a secure way to access the data. An object may call on another object's member functions in order to perform an operation or to retrieve some data. However, objects have the ability to limit the access of their data and member functions from other objects so that the information cannot be accessed directly. The data is hidden, so it is safe from accidental

alteration. Data encapsulation and data hiding are key terms in the description of object-oriented languages.

A C++ program typically consists of a number of objects, which communicates with each other by calling one another's member functions (Robert 2004). This communication between objects in an object-oriented program is similar to the way real world objects communicate with each other. The organization of a typical C++ program is shown in Figure 7.1.

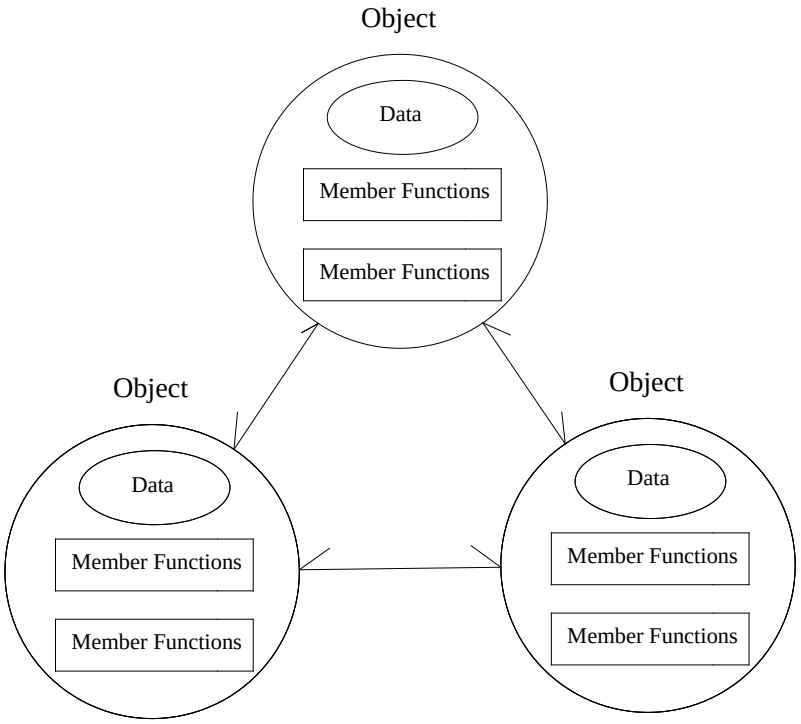

Figure 7.1 The object-oriented paradigm

Every object provides an interface to other objects through its accessible functions, and objects may only use the interface of another object in order to communicate with it. The internal structure of the object is hidden so that any changes that occur to the internal

structure will only affect the object's implementation. When an instance of either class is created, other objects may only access the object properties that are declared public within the code. Private and protected data and member functions have restricted access by other objects. Therefore, the public features of a class make up the interface of an object of that class, and the private and protected features of an object are used to aid in the object's implementation.

An object must have four characteristics (Rumbaugh et al. 1991): identity, classification, polymorphism, and inheritance.

Each object has an identity. Even if all the properties of two different objects are identical, their identities are not the same; each has a unique identifier or handle. Often, object-oriented programming systems assign invisible arbitrary numbers to serve as handles.

A group of objects cannot combine into a new object, but they may form a class if they share common properties, characteristics, or legal operations. A class is the outline, or template, of an object; it describes all of the attributes and operations that an object of its type contains, as shown by Figure 7.2 below. A class is only an abstraction, while an object represents an actual real world item. Once a class is defined, many objects of that class may be created with each object being unique yet possessing all of the same features as the other objects. Each object is created at run-time according to the class specification and is said to be an instance of a class.

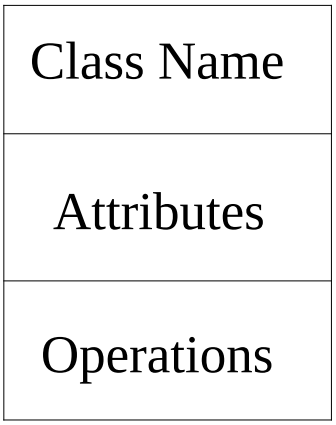

Figure 7.2 Class Illustration

The third characteristic of an object is polymorphism. Polymorphism is the ability for the same operation to behave differently on different classes (Rumbaugh et al. 1991). A function or operator may have the same name in two classes; however, it can act differently depending on which class it is operating on. One object can indicate its own class, and each class can choose its own method of operation.

The last characteristic is inheritance. It is a concept of object-oriented programming that allows a class to be expanded by creating a new class based on the original class or classes. The new class is called the derived class and the original class is called the base class. The derived class inherits all of the features of the base class and adds its own new features as well. Only the features new to the inherited class must be added to the class definition. Inheritance is a categorical relationship between objects. For example, in Figure 7.3, there are two classes called Class A and Class B. Class B is derived from Class A, thus Class B is a specific type of Class A. Both classes have their attributes and

operations encapsulated in a single entity. The diagram shows a base class and a derived class with all of the base classes' features along with new attributes and new operations. Only the two new features of the derived class, as shown in the bold print, need to be added to the class definition because the derived class will automatically inherit all of the features of the base class. Inheritance saves a lot of time in programming by allowing for reusability of existing code without having to modify the existing code, and it improves software development by allowing for separations of specific variations of a class. In addition, the derived class has the ability to overwrite the base class implementation of the operation and use its own implementation. Therefore, the same function may act differently on each of the classes, which actually demonstrates the object-oriented concept of polymorphism.

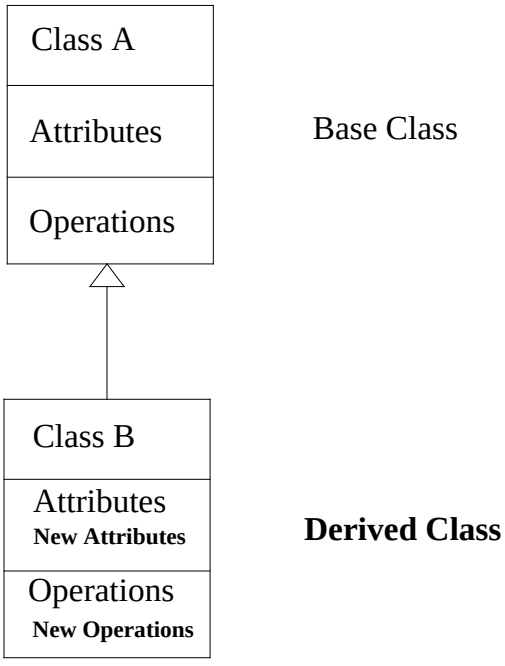

Figure 7.3 Inheritance Illustration

Objects, classes, polymorphism, and inheritance are only a few of the many object-oriented concepts. These are just the beginning to all of the advantages that object-oriented programming has to offer. More specific concepts will be discussed throughout the program development in the following sections. One technical advancement that has brought object-oriented concepts to the point that they are at today is abstraction. Abstraction allows a programmer to focus on the overall entity under consideration without getting mired in the details. This means focusing on defining an object rather than on the implementation of an object. When an object user needs information from the object, the user needs to know what the object is and does, rather than how the object is implemented. The goal of abstraction is "to isolate those aspects that are important for some purpose and suppress those aspects that are unimportant" (Rumbaugh et al. 1991).

7.2 PROGRAM DESIGN

The development of the executable program required for this project necessitated a software package designed by Phusit Dontree (1994). The LBuck program developed by Dontree was written in C++; however, many of the features of the programming were outdated and only applicable to uniform I-beams. The goal is to rework the original LBuck program to make it applicable to doubly-symmetric web-tapered I-beams. In object-oriented terminology, this process is known as refactoring.

The term refactoring is used to describe a technique of changing the internal structure of a program in order to make it easier to understand and cheaper to modify, without changing its observable behavior (Fowler 1999). The decision to refactor the existing program rather than start from scratch owes to many features that work well in original LBuck program. By refactoring the program, the design of the software can be improved and utilized for any researcher's purpose. Kent Beck (as quoted in Fowler, 1999), who was one of the first people to recognize the importance of refactoring, stated four main things that make a program hard to work with: 1) programs that are hard to read are hard to modify, 2) programs that have duplicate logic are hard to modify, 3) programs that require additional behavior that requires you to change running code are hard to modify, and 4) programs with complex conditional logic are hard to modify. These four main issues will be seriously considered while refactoring the program.

Object-oriented software development must follow a specific design process. This process must outline every single step during the design of the program from the abstract concepts to the detailed codes. The Rational Unified Process developed by Grady Booch, James Rumbaugh, and Ivar Jacobson (Jacobson et al. 1999) provides a modern approach to software development which can be tailored to model real world situations. This approach consists of four main phases: inception, elaboration, construction, and transition, which is shown in Figure 7.4.

The inception phase is where the scope of the project is determined. Also the core architecture will be established, and the critical risk while assuring feasibility is identified and

reduced (Jacobson 2000). The elaboration phase is the stage where all of the details are collected to create a plan for the construction. The construction phase is where the system is built, which involves many iterations. The transition phase is the stage where any work left until the end must be completed, such as specific forms of testing.

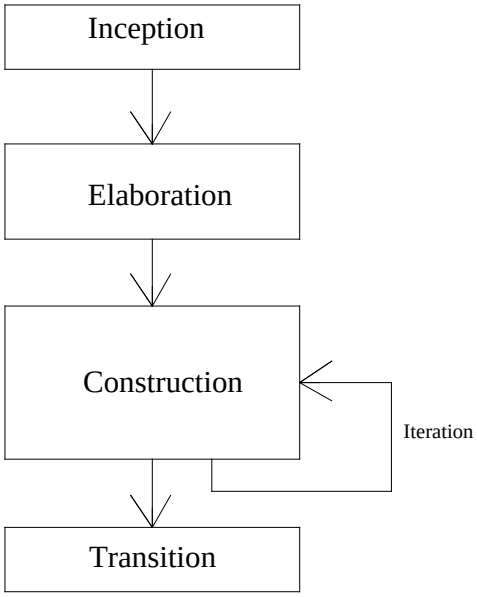

Figure 7.4 Rational Unified Process

The design process is going to focus on the LBuck programs. And the details of each phase will be discussed in the following sections.

7.3 OBJECT-ORIENTED MODELING AND PROGRAMMING FLEXURAL-TORSIONAL BUCKLING PROBLEMS

This section explains the details of each phase of the software development of the flexural-torsional buckling problem of doubly symmetric web-tapered I-beams: inception, elaboration, construction and the transition.

7.3.1 Inception

For the inception phase of the project, the scope may be summarized as: refactor an existing program that calculates the flexural-torsional buckling loads of a beam.

7.3.2 Elaboration

This phase begins with a technique called use case modeling. Use case modeling intends to communicate with the user how the system and its environment are related, it is one of the most important parts in software development. This process will ensure that the client and other program developers of the design will understand the users' needs. Use cases have two important roles: (1) they capture a system's functional requirements and (2) they structure each object model into a manageable view (Jacobson 2000).

The first step in developing the use cases is to determine the actors. An actor is something or someone that will use the system. Actors do not need to be human, and it can

be other systems that require information from the current system. For this particular program, the actor is the Project program, which is the user interface. The user interface is the system that calls on the LBuck to execute, and it requires the flexural-torsional buckling loads of the structure from the program.

The next step is to consider all scenarios that need to deal with. A scenario is a sequence of steps describing an interaction between an actor and a system (Fowler 2000). A group of related scenarios is a use case. For this particular program, the scenario is the flexural-torsional buckling analysis of a doubly symmetric web-tapered I-beam. The user interaction for this scenario makes up the use case model, and it is essentially inputting background information to calculate the flexural-torsional buckling loads of the structure.

It is important to provide detailed descriptions of the use case along with the diagram. The description of the use case for the program is: the user enters into the program the structure properties, dimensions, loads, and restraints. The program uses the data to calculate the flexural-torsional buckling load of the structure.

In this stage, it is also necessary to understand the operations of the LBuck program, and to collect all of the details needed for the refactoring process in the construction phase of the program. Figure 7.5 shows the refactoring process of the construction phase (Robert 2004). The goal is to modify the original code and rebuild new models based on current research needs.

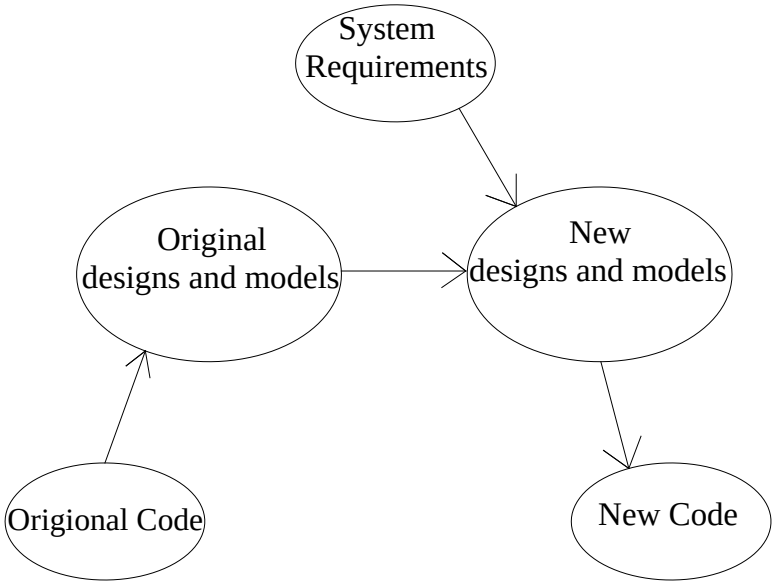

Figure 7.5 Refactoring Process

7.3.3 Construction

The construction phase is the main focus of the project that the program will be analyzed, constructed, and tested. This process also requires the most amount of time compared to the other phases.

The first step in the construction phase is to take the use cases and develop the classes. Figure 7.6 (Robert 2004) below shows the possible classes for the LBuck program. The next step is to consider the class relationships. The proposed classes should be checked before the classes are finally determined to see if they work for the program. And due to that the construction phase allows for many iterations, the classes and their relations may change several times before the program is completed.

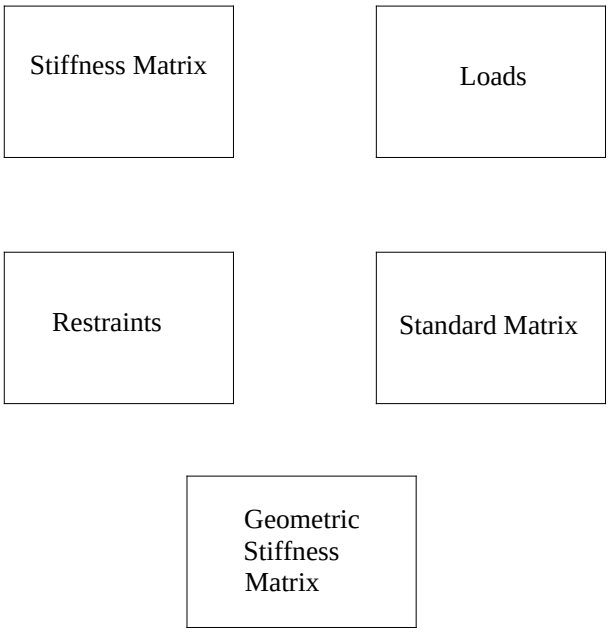

Figure 7.6 Possible LBuck Program Classes

7.3.3.1 Modeling

It is necessary to communicate the design at a high level to make sure other program developers understand the program. The only way to accomplish this is to communicate the system models with an effective modeling language. This type of modeling language must allow more complex modeling than the use case modeling because it must communicate with the internal structure of the system. The Unified Modeling Language (UML) developed by Rumbaugh, Jacobson, and Booch (1999), which supports object-oriented design and may be used along with the Rational Unified Process, serves such functions. It is applied throughout the whole design process for a full range of systems.

Before refactoring the codes, models of the system must be created first to plan out the structure of the program, which is shown in Figure 7.7 (Robert 2004). The UML provides

several general categories in which the program models may fall into. The model categories for this project are structural classification views and dynamic behavior views. The use case modeling discussed in Section 7.3.2 is also a part of the UML.

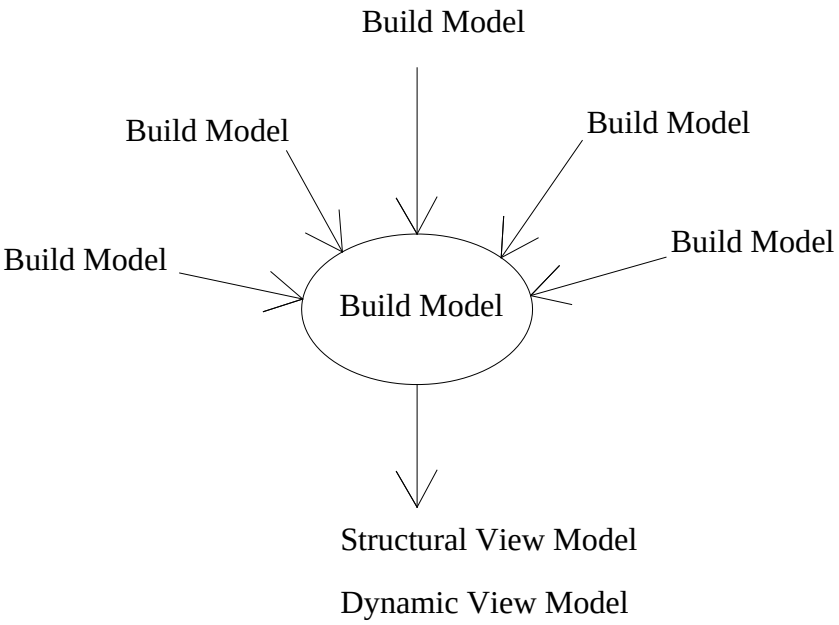

Figure 7.7 Modeling Procedure

7.3.3.1.1 Structural classification view

The structural classification view shows the relations among the elements within the program. One main type of structural views is the static view that shows the relations among the classes, which is illustrated by a class diagram. And object-oriented programming supports four important modeling tools to form class diagrams: classification/instantiation, aggregation/ decomposition, association/individualization, and generalization/specialization (Mezini 1998).

Classification/instantiation is the modeling mechanism for designer to show the class. Classification is the process where instances are created from classes, and instantiation is the process where instances are extended to form the classes. The class diagram combines the data and operations of a class into a single element shown as a rectangle in Figure 7.9 (Robert 2004). Figure 7.8 shows an example of a class diagram representing the class *Stiffness*. The data for the class is the global stiffness matrix, and the operation is to fill the stiffness matrix. The + and – signs indicate the visibility of the information: the + sign indicates the public data, the – sign indicates the private data. The entire set of classes for the LBuck program is shown in Figure 7.9 (Robert 2004).

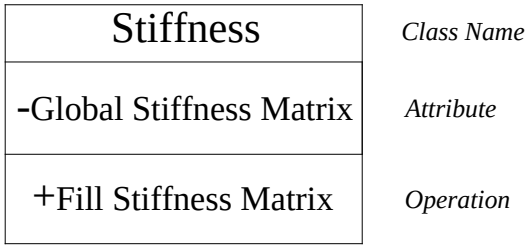

Figure 7.8 Example Class Diagram

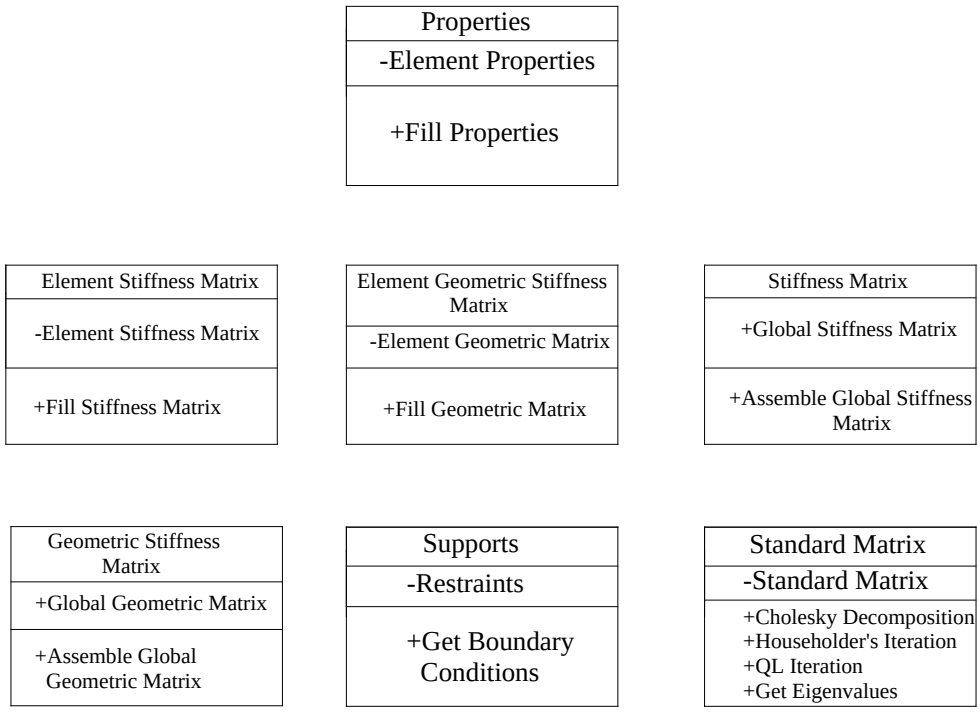

Figure 7.9 LBuck Program Classes

The other three tools, aggregation/decomposition, association/individualization, and generalization/specialization are to show the relations among the classes. Aggregation/decomposition describes the relation between abstractions as parts and wholes. Association/individualization shows the relation between abstractions by connecting items that share some sort of semantic connection in an association, or by separating items through individualization. And generalization/ specialization expresses the relation between a generalized abstraction and a specialized abstraction. This modeling mechanism is supported by the object-oriented concept of inheritance.

The LBuck program's class diagram is analyzed and shown in Figure 7.10 (Robert 2004).

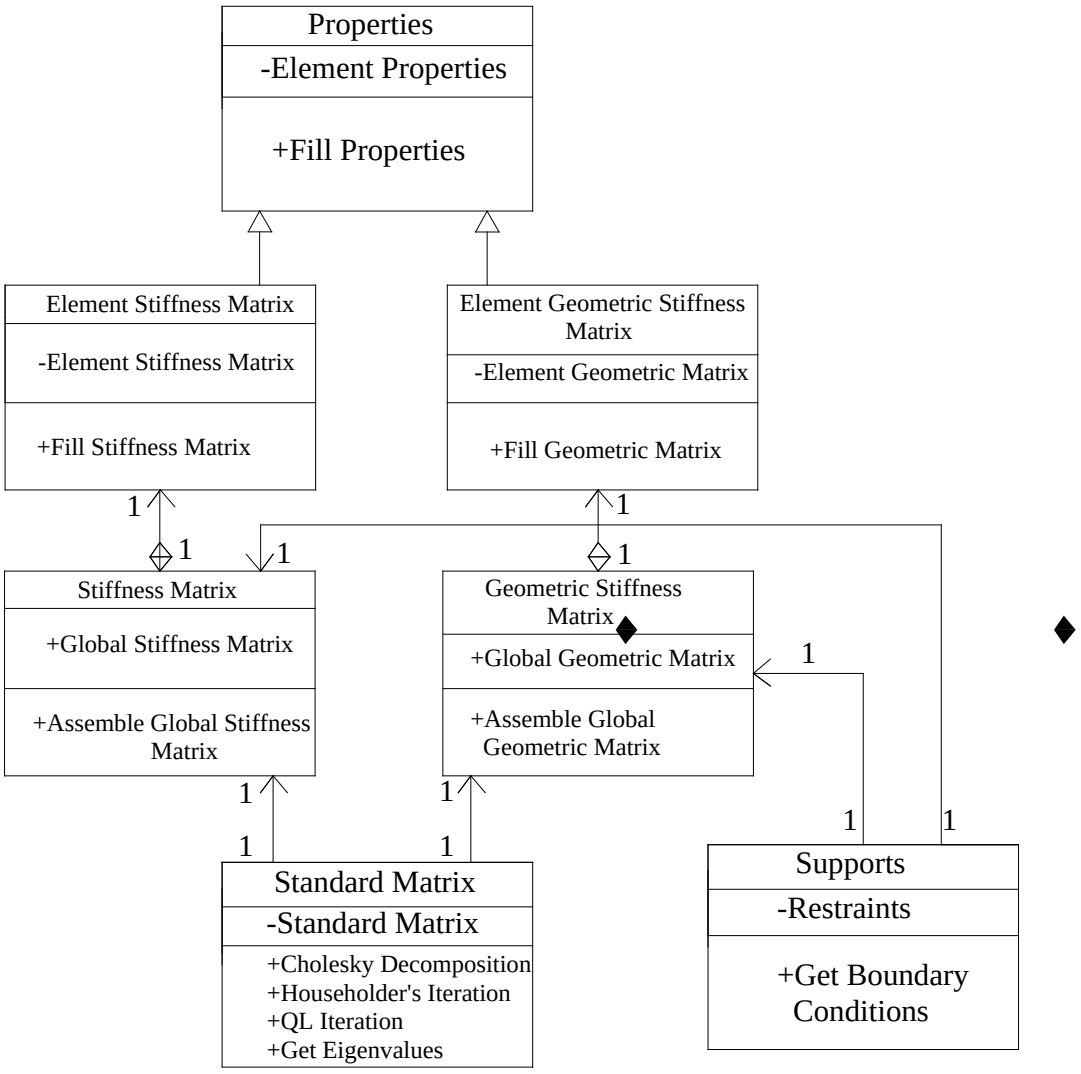

Figure 7.10 LBuck Program Class Diagram

The Element Stiffness Matrix and Element Geometric Stiffness Matrix classes are derived from the Properties base class as indicated by the inheritance open arrowheads. The other class associations are shown with the solid arrows. The solid arrows show the navigability between the classes, and in all of these cases it is unidirectional.

One of the new features shown on the diagram is the black diamond which is used to indicate composition. Composition is another one of the basic concepts of object-oriented programming. Composition is a specific form of aggregation. This shows the conceptual relationship of an element stiffness matrix being a part of a global stiffness matrix. Composition is a stronger form of aggregation where the part may belong to only one whole and the life of the part is the life of the whole. The Stiffness Matrix and the Geometric Stiffness Matrix classes are the "whole" and the Element Stiffness Matrix and Element Geometric Stiffness Matrix classes are the "parts". The Standard Matrix class must be associated with the Stiffness Matrix and the Geometric Stiffness Matrix classes in order to calculate the standard matrix. The Restraints are applied to both the stiffness matrix and the geometric stiffness matrix; therefore, associations between these classes are indicated. At the ends of the arrows are numbers indicating the multiplicity of the instances of the classes with (*) denoting infinity. For example, a Stiffness matrix object may be associated with anywhere from one to an infinite number of element stiffness matrices at a conceptual level; however, each element stiffness matrix may be associated with only one stiffness matrix. The ordered keyword is a constraint implying there is an ordering of the objects that it is associated with and that a particular object can appear on the total list of objects only once.

7.3.3.1.2 Dynamic behavior view

The dynamic behavior view provides a visual model of the system over a period of time, and it helps developers to understand which objects are instantiated and how the objects interact

with each other during the program execution. A sequence diagram is a specific type of dynamic behavior view that displays the interaction as a two-dimensional chart. The sequence diagram of LBuck program is shown in Figure 7.11 (Robert 2004). It is important to notice that all of the same behaviors are being implemented in this model, only now the behaviors are redistributed among the objects to enhance the object-oriented features of the program design.

The assemble Stiffness process creates a new element stiffness matrix object for each element in the discretized structure. Each element object reads the properties for the element and fills the matrix in the Fill_Element_Matrix process. Each matrix is sent back to the Stiffness Matrix object and assembled into the appropriate position in the global stiffness matrix. The exact same process occurs for the Geometric Matrix object. The assemble Geometric process creates a new Element Geometric Matrix object for each element in the discretized structure. Each element object reads the properties for the element and fills the element geometric stiffness matrix in the Fill_Element_Matrix process. Each element matrix is sent back to the Geometric Matrix object and assembled into the appropriate position in the global stiffness matrix.

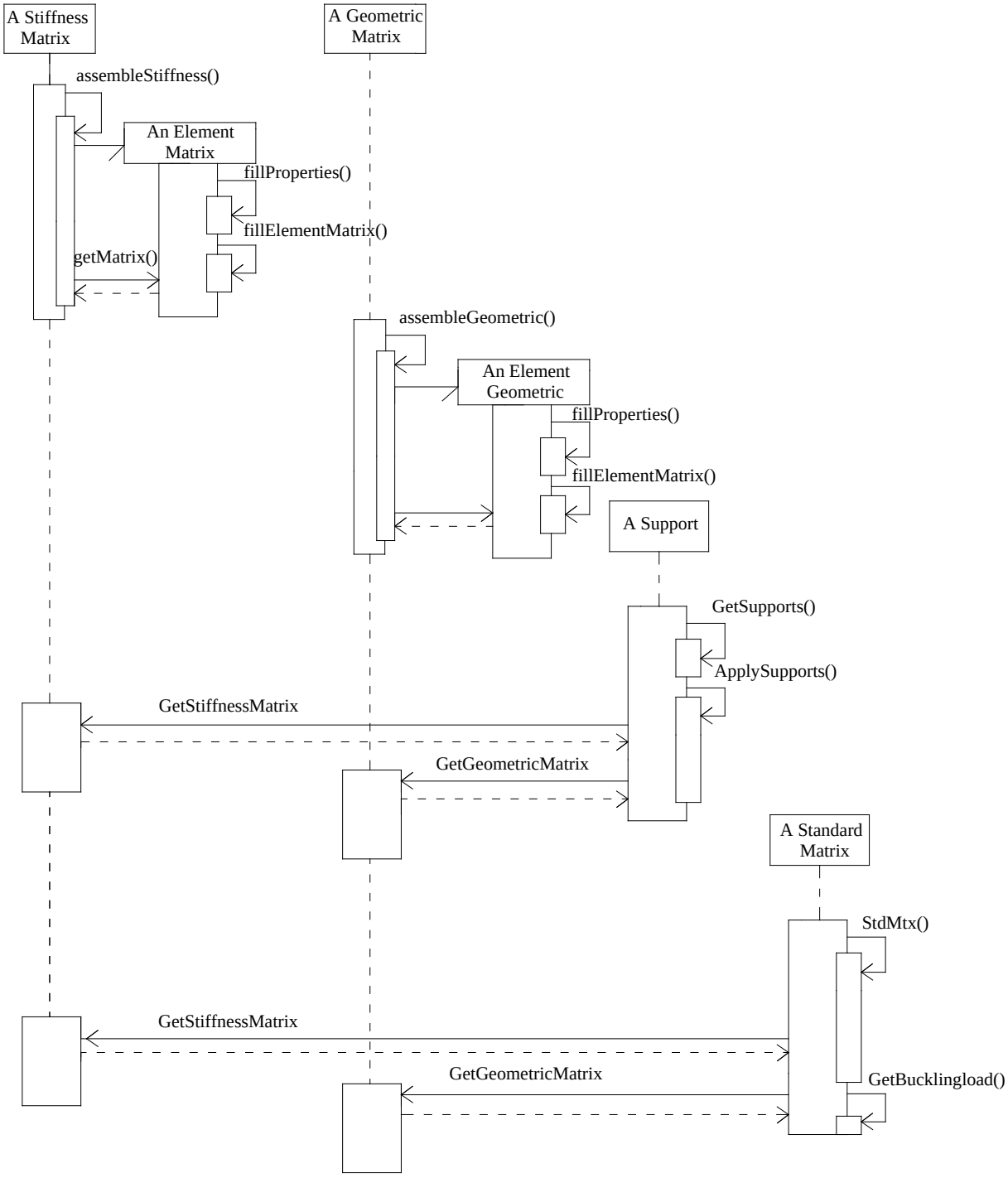

Figure 7.11 LBuck Program Sequence Diagram

The support object reads in the supports in the getSupports process. It applies the boundary conditions to the structure in the applySupports process. The Standard Matrix object changes the generalized eigenvalue problem to the standard eigenvalue problem. Consequently, the global stiffness matrix and global geometric stiffness matrix are combined to the standard matrix. The standard matrix is then solved for the eigenvalues. The final step is the print process. This process is different depending on the type of analysis. For the buckling analysis, the buckling parameter, or eigenvalue, is printed as the result of the anlaysis. The buckling load is the multiplication of the eigenvalue and the trial loads. For the prebuckling anlaysis, the eigenvalue is checked within the print process before the results are printed. If the eigenvalue is not equal to one, the eigenvalue is returned to the beginning of the program as a multiplication factor. The trial loads are multiplied by the multiplication factor and the entire process starts again. The program continues until the eigenvalue is close to one, and the trial loads for that iteration are the buckling loads.

It is often difficult to understand the flow of behaviors within a program, and dynamic behavior views help to model the flow control so that the sequence of behaviors become apparent. The sequence diagrams for both the Frame and LBuck programs help to increase the clarity of how the objects collaborate within the program during its implementation.

An activity diagram is another type of dynamic behavior view. “An activity graph shows the computational activities involved in performing a calculation” (Rumbaugh et al. 1991). It describes a sequence of activities and helps when trying to understand the flow of work in a calculation. Activity diagrams are much like flowcharts except that they allow

for parallel behavior. Since they are so much like flowcharts, many people believe that activity diagrams are not object-oriented; however, they are included as part of the UML and are useful in describing complicated behavior.

An activity diagram is shown in Figure 7.12 (Robert 2004) to describe the standard matrix procedure. The standard matrix function is called as shown in the sequence diagram of Figure 7.11; however, the order of the calculations for the standard matrix function is not shown on the diagram. These details are left out of the diagram to maintain clarity, yet they are important in understanding the operations of the program. The activity diagram in Figure 7.12 is used to illustrate these details.

The diagram shows two swim lanes: restraints and standard matrix. Swim lanes are used to try to link the actions to the objects in order to enhance the object-oriented features of the diagram. The name of the class associated with the action is shown at the top of the diagram, and the descriptions of the action are shown in the ovals below. The order of the functions is related by the arrows.

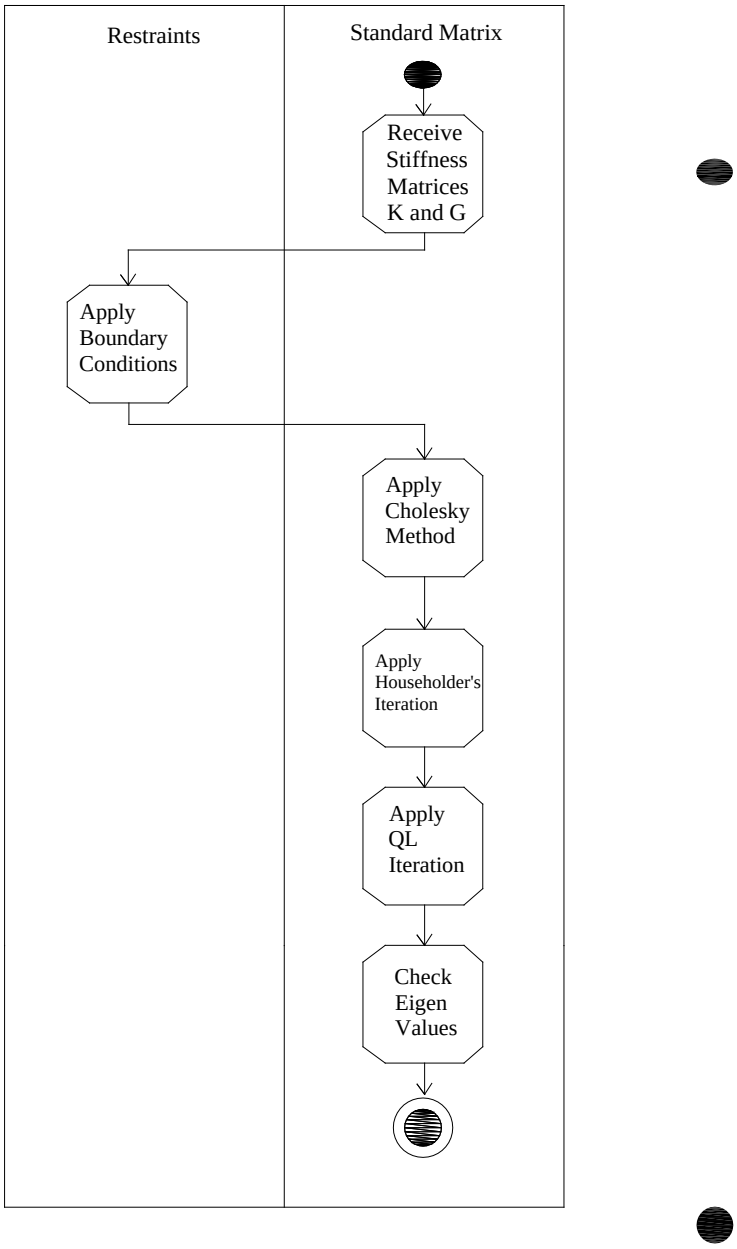

Figure 7.12 Activity Diagram

7.3.3.2 Coding

Once the abstract models are completed, the design can move back to the coding process. Two-dimensional arrays are used in the classes to store the matrices. Passing an array as an

argument between two functions is different from passing other types of variables. The name of an array is its address, and arrays must be passed by their names, or addresses. Normally, there are two ways for an object to access the array of another object: (1) make the array public data, (2) make the two objects friends to each other.

The coding for LBuck program begins with defining the classes:

```
class Properties
{
    protected:
        int j1,j2,joint_num;
        float E,G,Jf,Iwf,L,Lf,In,tw,d,zi,zj,hi,hj,tanA0,A0,element_num,length;
        float Fi,Vi,Vj,Mi;
        float z[MSize];
        float h[MSize];
        float v[MSize];
        float mi[MSize];
    public:
        virtual void Fill_Properties(int, int, float)=0;
};
```

The Properties class stores the properties of the structure. The Fill_Properties () function stores the properties in matrix form.

```
class Element_Stiffness:public Properties
{
private:
    float KE[MSize][MSize];
    float EW[MSize][MSize];
    float EF[MSize][MSize];
    float P[MSize][MSize];
    float Q[MSize][MSize];
    float PT[MSize][MSize];
    float QT[MSize][MSize];
    float C[MSize][MSize];
    float CT[MSize][MSize];
    float DT[MSize][MSize];
    float D[MSize][MSize];
    float X1[MSize][MSize];
    float X2[MSize][MSize];
    float X3[MSize][MSize];
    float X4[MSize][MSize];
    float Y1[MSize][MSize];
    float Y2[MSize][MSize];
    float Y3[MSize][MSize];
```

```
    float Y4[MSize][MSize];
public:
    friend int main();
    friend class Stiffness;
    void Fill_Element_Stiffness(float, int, float);
    void Fill_Properties(int, int, float);
};
```

The Element_Stiffness class is derived from the Properties class. The Fill_Element_Stiffness1 () function fills the buckling stiffness matrix. And the stiffness matrix will be stored in the KE two-dimensional array.

```
class Element_Geometric:public Properties
{
    private:
        float KG[MSize][MSize];
        float GW[MSize][MSize];
        float GF[MSize][MSize];
        float P[MSize][MSize];
        float Q[MSize][MSize];
        float PT[MSize][MSize];
        float QT[MSize][MSize];
        float C[MSize][MSize];
```

```
        float CT[MSize][MSize];
        float DT[MSize][MSize];
        float D[MSize][MSize];
        float X1[MSize][MSize];
        float X2[MSize][MSize];
        float X3[MSize][MSize];
        float X4[MSize][MSize];
        float Y1[MSize][MSize];
        float Y2[MSize][MSize];
        float Y3[MSize][MSize];
        float Y4[MSize][MSize];
    public:
        friend class Geometric;
        void Fill_Element_Geometric(float,int,float);
        void Fill_Properties(int, int, float);
};
```

The Element_Geometric class is also derived from the Properties class. The Fill_Element_Geometric () function fills the buckling geometric stiffness matrix. The geometric stiffness matrix is stored in the GE two a dimensional array.

```
class Stiffness
{
private:
    Element_Stiffness stiff;    //Element Stiffness matrix
    int element_num;//number of elements
    float length;
public:
    float A[MSize][MSize];
    Stiffness(int);
    void Assembling_Stiffness_Matrix(float,int,float);
};
```

The Stiffness class contains an Element_Stiffness matrix object. Each element stiffness matrix will be assembled into the global stiffness matrix, A, using the Assembling_Stiffness_Matrix () function, and then deleted in order to save memory space.

```
class Geometric
{
    private:
        Element_Geometric geom;    //element geometric matrix
        int element_num; //number of elements
        float length;
    public:
```

```
        float B[MSize][MSize];
        Geometric(int);
        void Assembling_Geometric_Matrix(float,int,float);
};
```

Similarly, there is an Element_Geometric matrix object. And each element geometric stiffness matrix will be assembled into global geometric stiffness matrix, B, using the Assembling_Stiffness_Matrix () function.

```
class Standard_Matrix
{
    private:
        int size;
        float dia[MSize];
        float C[MSize][MSize];
        float off[MSize];
        float buckling_load;
    public:
        Standard_Matrix();
        void standard_matrix(float[MSize][MSize],float[MSize][MSize],int);
        float pythag(float,float);
        void choldc(float[MSize][MSize]);
        void tred2(float[MSize][MSize]);
```

```
        void tqli(float[MSize][MSize]);
        float getBucklingLoad();
};
```

The Standard_Matrix class creates the standard eigen-value problem from the elastic stiffness matrix and the geometric stiffness matrix. The Standard_Matrix () function calls upon the functions choldc (), tred2 (), and tqli (), in addition, it is the function used to store the standard matrix. The pythag () function is the Pythagorean function. The choldc () function is the Cholesky method which changes the stiffness matrix to the upper triangular matrix (Press 1992). The tred2 () function displays the Householder's iteration which changes the standard matrix to a tridiagonal matrix. And the eigenvlaue of the tridiagonal matrix will be calculated in tqli () function through QL iteration (Press 1992).

```
class Supports
{
private:
    int restrain[MSize];
    int rest;
    int size;           //Total degrees of freedom
    int free_size;      //Free degrees of freedom
public:
    Supports(int);
    void Get_boundary_conditions();
```

```
    int Boundary_Condition(float[MSize][MSize],float[MSize][MSize]);
};
```

The Supports class is used to store the restraint information. The Get_boundary_conditions () function is used to input the boundary conditions. The Boundary_Condition () function is used to apply the restraints to the global stiffness and geometric stiffness matrices.

The source files now should be implemented to the classes. The original program provided the data that are only applicable to doubly symmetric uniform I-beams, therefore, those codes have to be modified and reorganized.

7.3.4 Transition

The transition phase is the last stage in the design process, which focuses on testing and fixing bugs. The goal of this phase is to ensure that the product is applicable to practical use. In this stage, the testing will be conducted to compare the results of the program with those of the existing solutions. Once the transition phase is completed, the program is ready to use.

The complete program code for the LBuck programs is in Appendix C.

8.0 FLEXURAL-TORSIONAL BUCKLING OF BEAMS: EXAMPLES

The buckling load is an important criterion for the structural steel design. In this chapter, three example cases, the cantilever with a tip concentrated load, the beam subjected to free end moments with different boundaries, and the simply supported tapered beam with two equal end moments, are analyzed using the LBUCK program developed in this research.

The second variation of the total potential energy presented in Chapter 3, in which the prebuckling behavior is disregarded, is used in conjunction with finite element methods to develop the computer program. The LBUCK program will be verified by comparing the lateral buckling loads of beams with results from typical theories in existing literatures.

8.1 BUCKLING ANALYSIS: EXAMPLE 1

Since the lateral buckling loads of prismatic uniform thin-walled beams have been extensively investigated and widely accepted, a cantilever of uniform I-section is analyzed to help verify the program developed in this paper.

A cantilevered beam with a concentrated load at the free end is analyzed first (See Figure 8.1). The load is applied at the shear center. The properties of the cantilever are E = 210 GPa (30458 ksi), ν = 0.3, h = 600 mm (23.62 in), t_f = 10 mm (0.394 in), t_w = 8 mm

(0.315 in), and b = 180 mm (7.09 in), while the length of the cantilever L varies from 2.0 to 10.0 m (78.75 to 393.7 in).

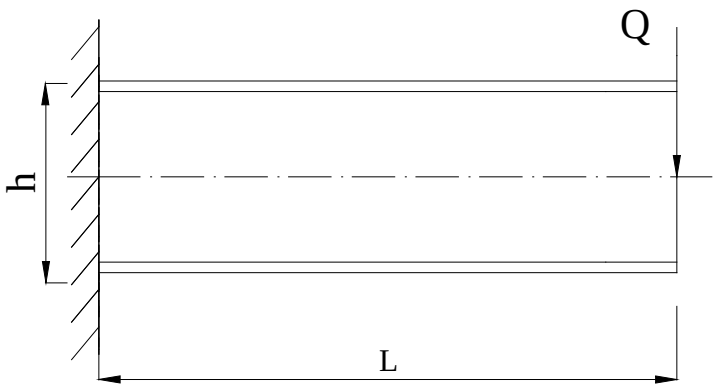

Figure 8.1 Lateral Buckling of Uniform I-beam

A cantilevered beam is fixed at the built-in support so that it is restrained against the deflection as well as the rotation both in-plane and out-of-plane direction, while it is free at the other end so that it can deflect and rotate both in-plane and out-of-plane of loading. The solution obtained by the finite element buckling analysis from the LBUCK program, Q_{LBUCK}, is compared to the results of Trahair (1993, p. 175), which is graphed in Figure 8.2.

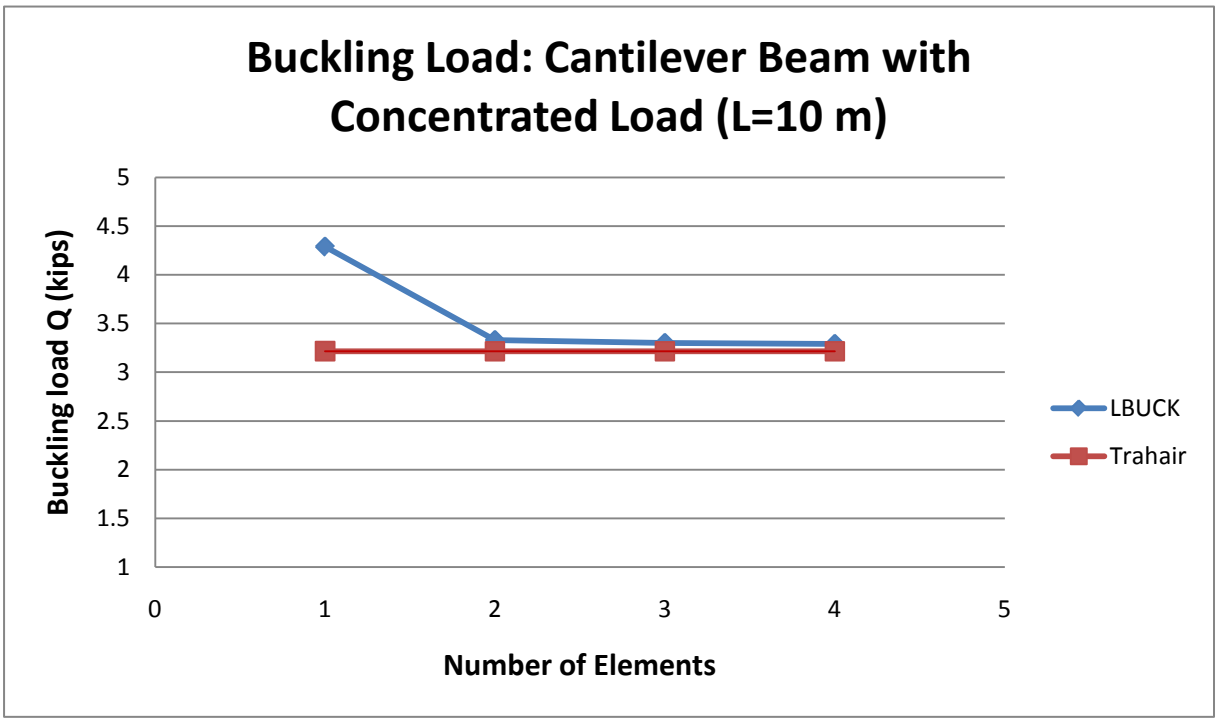

Figure 8.2 Buckling Load: Cantilever Beam with Concentrated Load (L=10 m)

From Figure 8.2, it can be seen that the finite element solution obtained from the LBUCK program converges to Trahair's solution with little variation in buckling load when two or more elements are used to model the beam, which suggests that, in this type of problem, at least two elements needed to model the beam. To investigate the effects of the beam lengths on the efficiency of the LBUCK program on predicting flexural buckling load, a non-dimensional analysis on the beam under various beam lengths is conducted, and the results are compared to Trahair' solution and are graphed in Figure 8.3.

Trahair (1993) provides a linear equation that describes the relationship between the beam properties and the buckling load:

$$QL^2 / \sqrt{EI_y GJ} = 3.95 + 3.52\sqrt{\pi^2 EI_\omega / GJL^2} \qquad (8\text{-}1)$$

This relationship is graphed as a solid line in Figure 8.3. By inputting different lengths of the beam, from 2 m to 10 m, into the LBUCK program, nine corresponding buckling loads are obtained and shown as square symbols in Figure 8.3. Comparison with Trahair (1993) shows that for smaller values of K parameter, which indicates a larger value of the length, the results from LBUCK program are closer to Trahair's data.

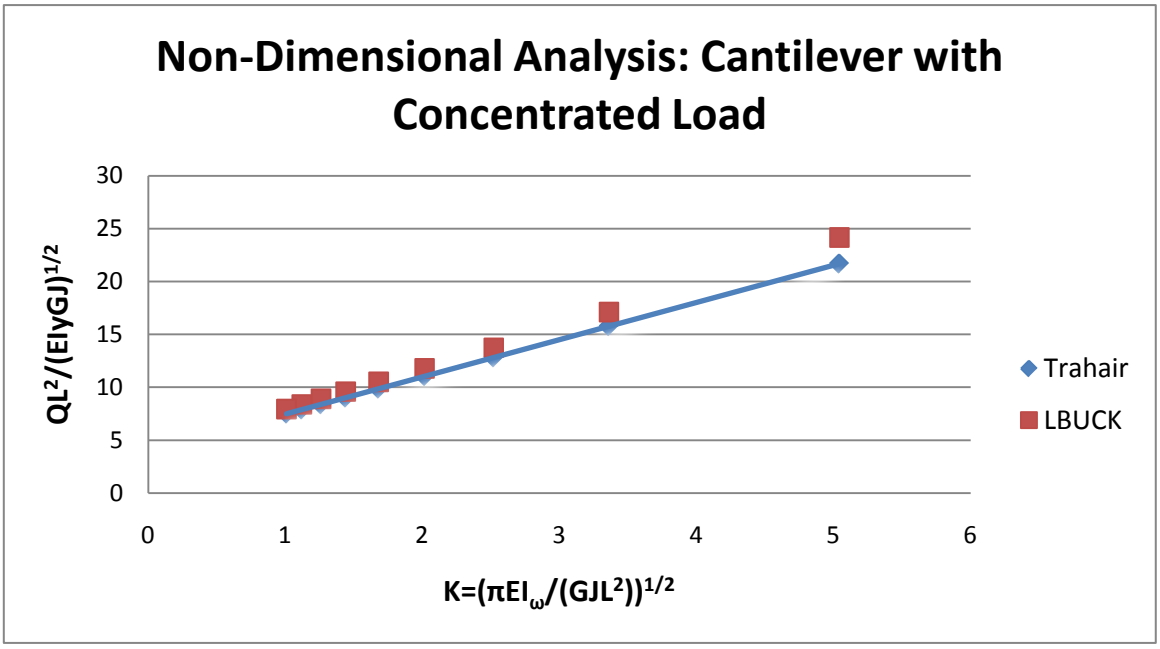

Figure 8.3 Non-Dimensional Analysis: Cantilever with Concentrated Load

To assess a better idea of the accuracy of the LBUCK program in this example, an error analysis of the buckling loads is conducted and the results are presented in Figure 8.4.

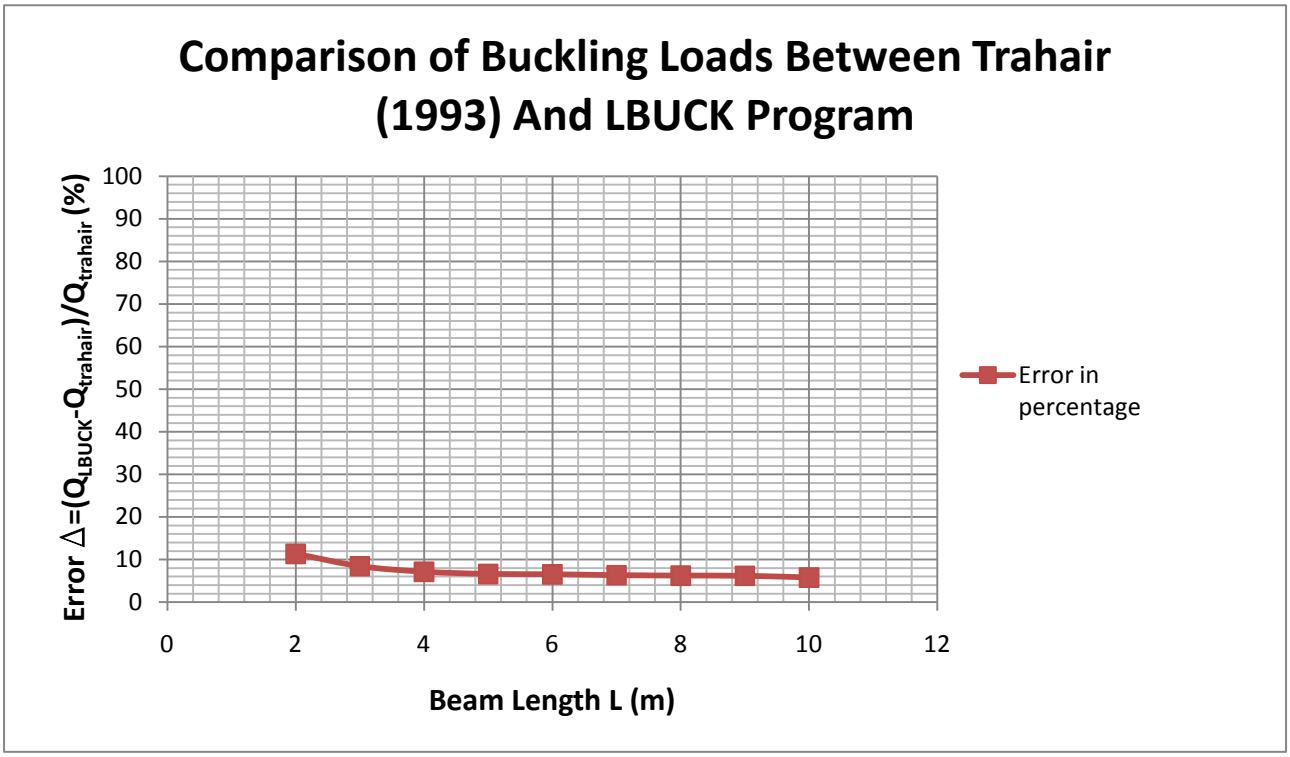

Figure 8.4 Comparison of Buckling Loads

It can be seen from Figure 8.4 that the lateral buckling load obtained using the LBUCK program developed in this research shows an acceptable agreement with Trahair's solution. This error analysis also indicates that, when the length of the beam is increased, the LBUCK program gives better predictions with the error less than 5%.

8.2 BUCKLING ANALYSIS: EXAMPLE 2

In this section, a beam subjected to free end moments with three different boundary conditions is analyzed.

A cantilevered beam in uniform bending is first analyzed in this section, as shown in Figure 8.5. The elastic buckling moments predicted for a uniform beam with a doubly-symmetric I-section of such conditions is given by Trahair (1983), and it is an approximate solution:

$$ML / \sqrt{EI_y GJ} = 1.6 + 0.8K \tag{8-2}$$

where

$$K = \sqrt{(\pi^2 EI_w / GJL^2)} \tag{8-3}$$

The beam is a W12x120 section, and the properties for the beam are b_f =312.9 mm (12.32 in), t_f = 28.07 mm (1.105 in), E = 206.84 GPa (30000 ksi), G = 82.74 GPa (12000 ksi), h_0 = 333.25 mm (13.12 in), t_w = 18.034 mm (0.71 in), and the length of the cantilever L varies from 2 m (78.75 in) to 10 m (393.70 in) (See Figure 8.5)

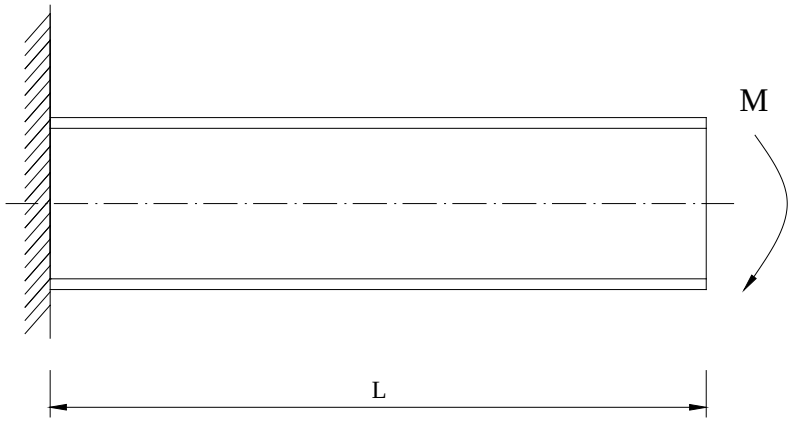

Figure 8.5 lateral Buckling of A Cantilevered Doubly-symmetric I-beam Under End Moments

A non-dimensional analysis is conducted on this model (Figure 8.6). By comparing the results from the LBUCK program to those from the approximate solution, it is found that the LBUCK program can give a good prediction of the critical moment; the error between these two methods of analysis is less than 5%.

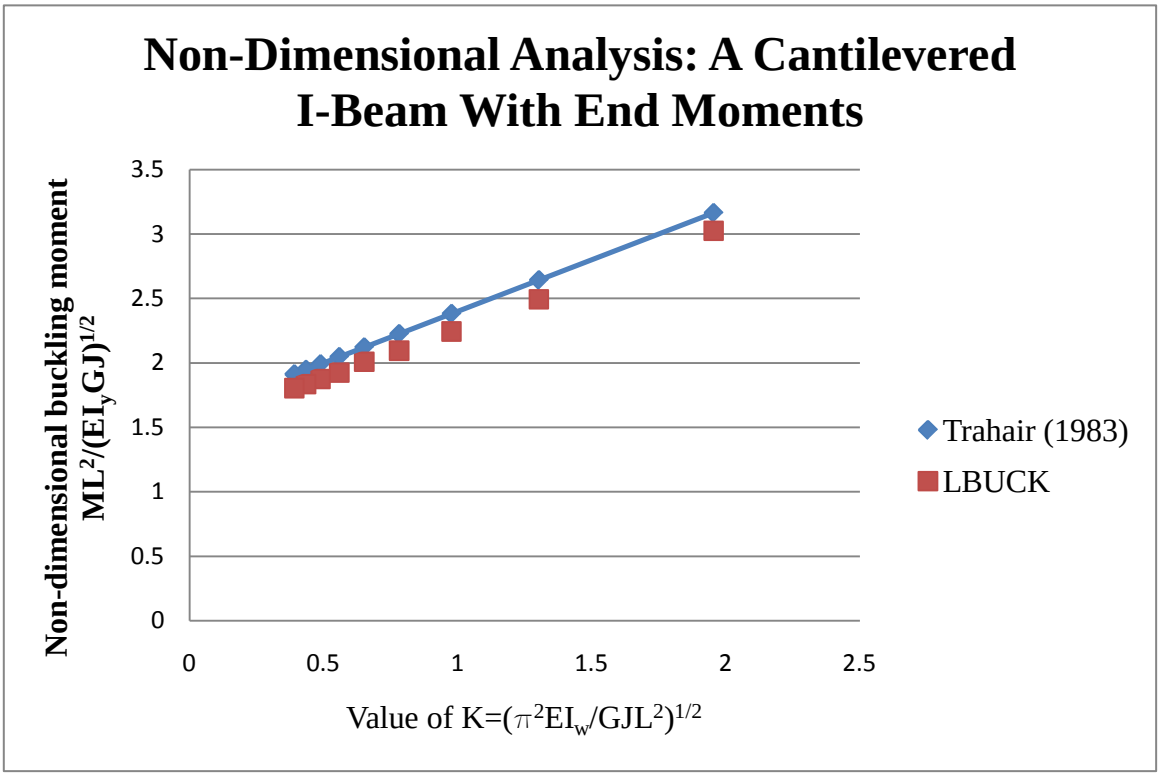

Figure 8.6 Non-Dimensional Analysis: A Cantilevered I-Beam with End Moments

A simply-supported I-beam in uniform bending is also analyzed here, as shown in Figure 8.7. Bleich (1952) provides an exact solution:

$$ML / \sqrt{EI_y GJ} = \pi \sqrt{(1+K^2)} \tag{8-4}$$

where K is given by Eq. (8-3).

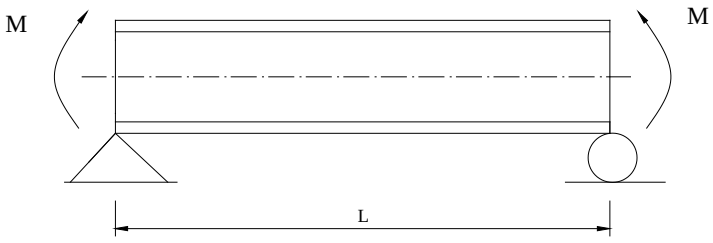

Figure 8.7 Lateral Buckling of Simply Supported I-beams

A similar non-dimensional analysis is conducted and the results are presented below:

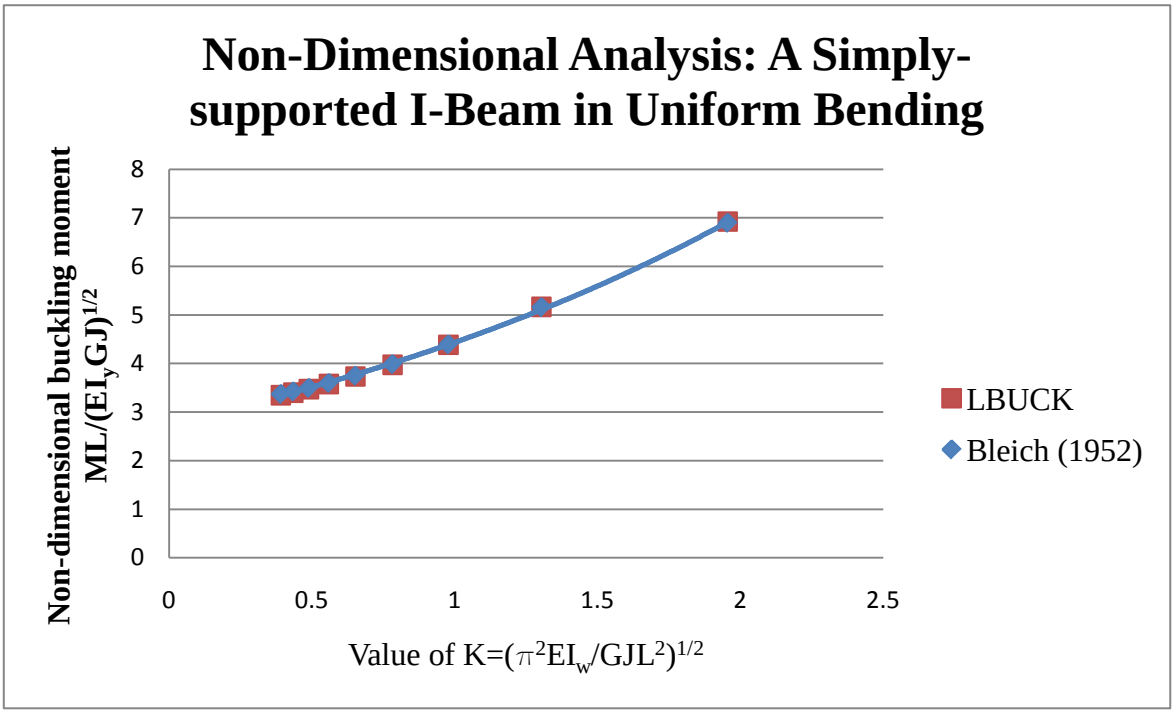

Figure 8.8 Non-Dimensional Analysis: A Simply-supported I-Beam in Uniform Bending

It can be seen from Figure 8.8 that the LBUCK program shows a close agreement with the results from Bleich (1952), with the error less than 1% when four elements are used.

The elastic buckling of an overhanging segment free to warp in uniform bending is analyzed here (Figure 8.10). An overhanging beam is continuous over an end support and cantilevered beyond it (Figure 8.9). The elastic resistance to lateral buckling of the overhanging segment is frequently taken as that of a cantilever built-in at its support, as shown in Figure 8.5. However, it will be shown in this paper that the built-in support condition overestimates the buckling load of an overhanging segment. For a built-in cantilever, the support conditions are specified as being prevented from deflecting, twisting ($u = \phi = 0$), rotating about the minor axis ($u' = 0$), and from warping ($\phi' = 0$) at the support. However, these two latter conditions should be modified in the case of an overhanging segment, since continuity at the support will generally result in $u' \neq 0$ and $\phi' \neq 0$.

Trahair (1983) provides an approximate solution to the buckling analysis of an overhanging segment in such boundary conditions:

$$ML / \sqrt{EI_y GJ} = 1.6 + 0.05K \tag{8-5}$$

where K is given by Eq. (8-3).

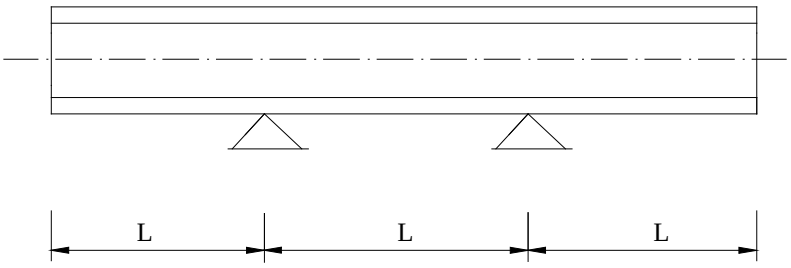

Figure 8.9 Side-view of An Overhanging Beam

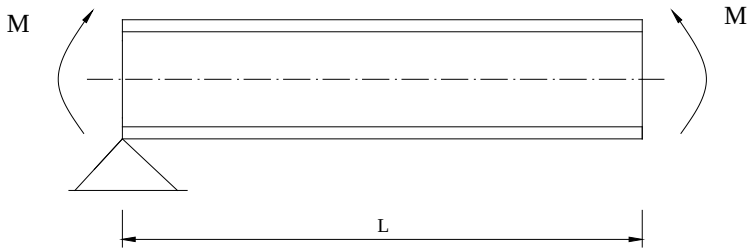

Figure 8.10 Lateral Buckling of An Overhanging Segment in Uniform Bending

A non-dimensional analysis is conducted and the results are presented below:

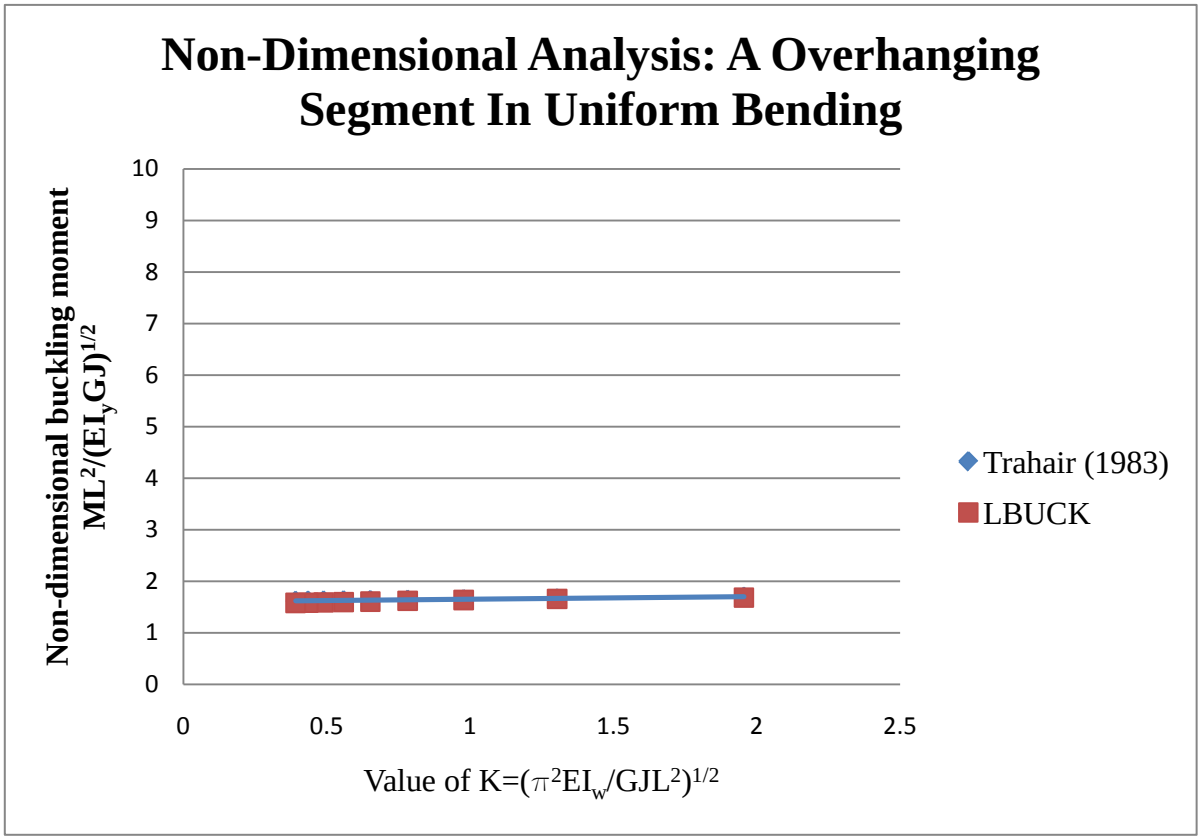

Figure 8.11 Non-Dimensional Analysis: An Overhanging Segment in Uniform Bending

It can be seen from Figure 8.11 that the LBUCK program shows a close agreement with the results from Trahair (1983), with the error less than 3%.

To provide more insight on the difference of the buckling load among an overhanging segment, a built-in cantilever, and a simply-supported beam, a non-dimensional graph (Figure 8.12) of the buckling analysis of all three conditions in this section is plotted. Figure 8.12 that the built-in support condition will overestimate the buckling load of an overhanging

segment, and it can be seen that LBUCK program gives a good prediction of the buckling moments of such type of beams.

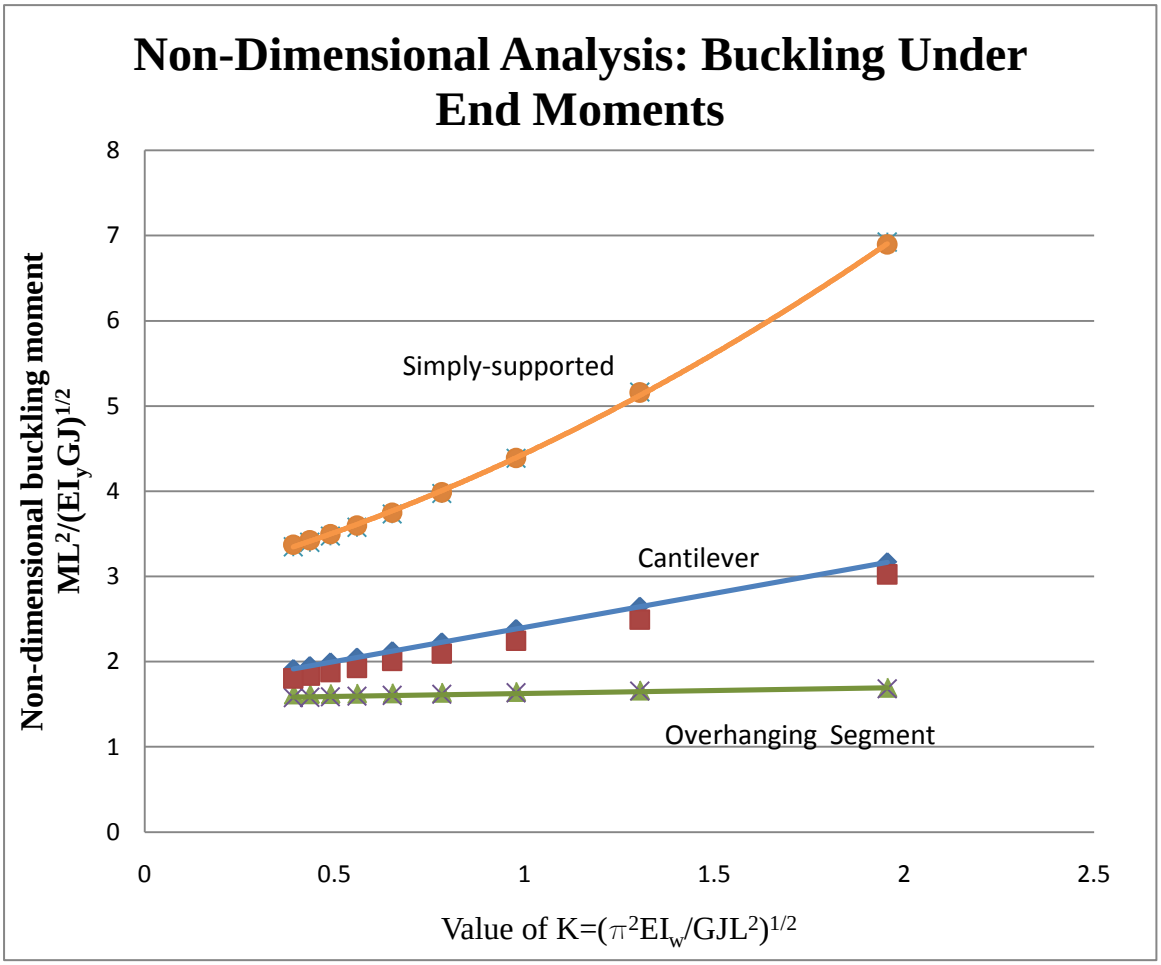

Figure 8.12 Non-Dimensional Analysis: Buckling Under End Moments

8.3 BUCKLING ANALYSIS EXAMPLE 3

A simply supported web-tapered beam with rectangular cross-section subjected to two end moments is analyzed in this example. A simply-supported beam is restrained against in-plane of loading vertical deflections, but it is unrestrained against in-plane of loading

rotations; also the beam is restrained against out-of-plane of loading deflections and twist rotations, but it is unrestrained against minor axis rotations and against warping displacements.

The results from the LBUCK program will be compared to an existing closed form solution developed by Lee (1959).

The properties of the cross section are b_f =0 in, t_f =0 in, E = 206.84 GPa (30000 ksi), G = 82.74 GPa (12000 ksi), h_0 =0.5 m (19.685 in), t_w =0.01 m (0.394 in), and the length of the beam L varies from 4 m (157.48 in) to 10 m (393.70 in) (See Figure 8.13).

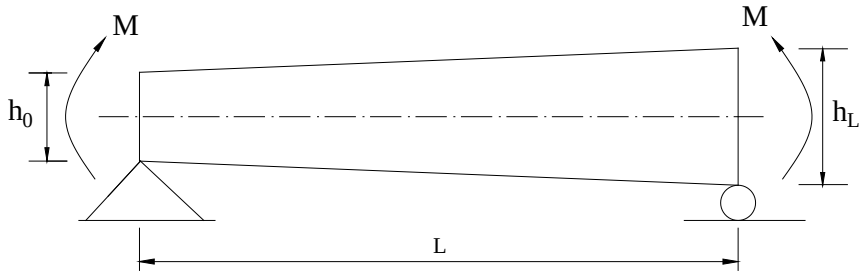

Figure 8.13 Lateral Buckling of Web-tapered Simply Supported Beams

The closed form solution of the critical moment for a beam of length L with simply supported ends is given by (Lee 1959)

$$M_{cr} = \frac{\delta}{\ln(1+\delta)} \frac{\pi\sqrt{EI_0 GJ_0}}{L} \tag{8-6}$$

where δ is the taper ratio and can be expressed in form of taper angle α:

$$\delta = 2L\alpha / h_0 \tag{8-7}$$

The results of a buckling analysis of the structure conducted with the program along with the closed form solution of the critical moment are graphed in Figure 8.14. In this example, the finite element solution converges to the closed form solution as the number of the elements is increased. The finite element representation with a single element gives an error of 12.6%. The finite element representation with two or more elements gives an error of less than 2%. Therefore, the finite element method gives the most accurate results when two or more elements are used to model the structure.

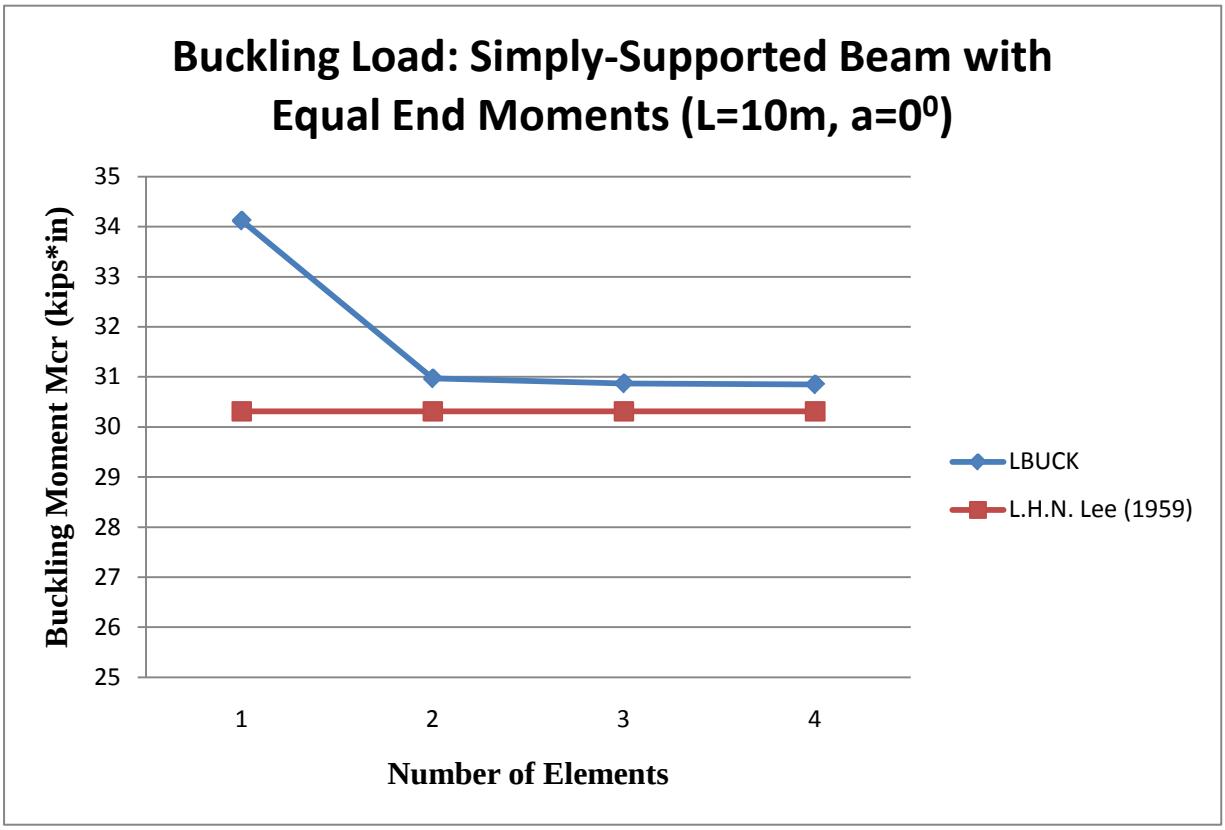

Figure 8.14 Buckling Load: Simply-Supported Beam with Equal End Moments

To investigate the effects of the taper ratio on the structure, a beam of 10 m length under different taper angles is analyzed. By comparing the results from the LBUCK program to Lee's solution, which is graphed in Figure 8.15, it can be seen that the buckling load of the beam is becoming larger as the taper angle is increased; and both the LBUCK program and Lee's solution show a linear trend of the buckling loads as the beam taper ratio is increased, these two methods of solution give close results.

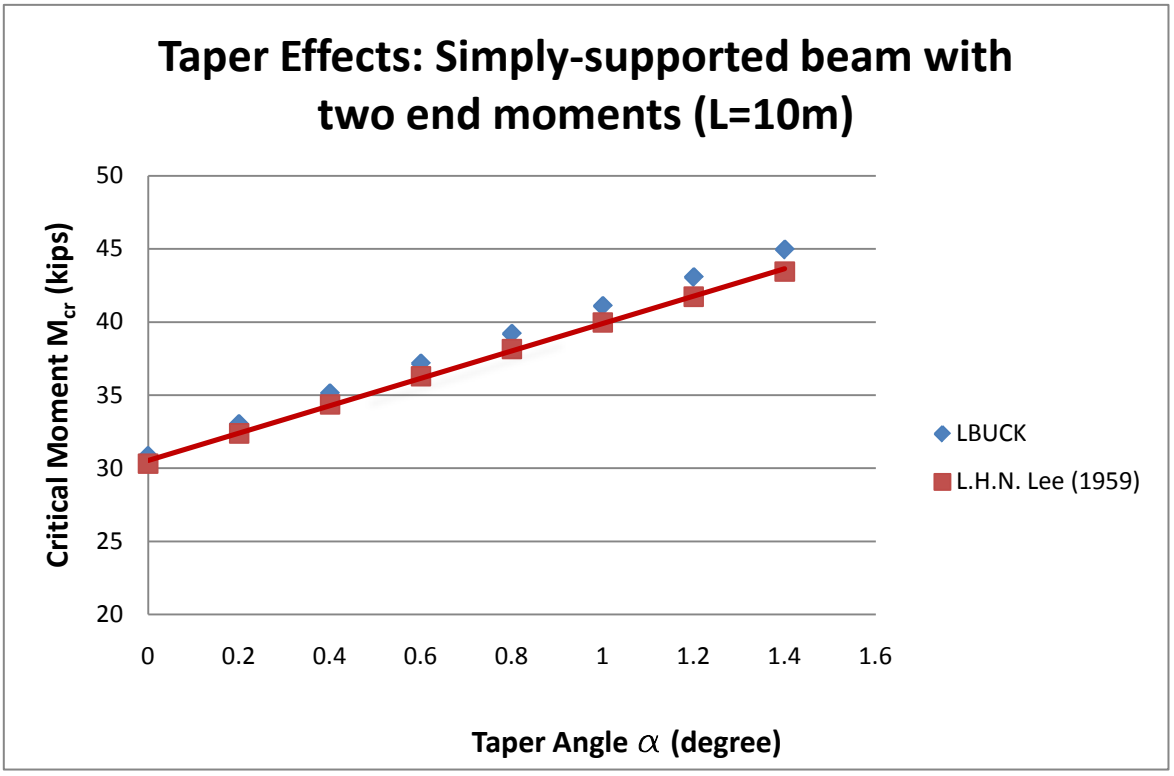

Figure 8.15 Taper Effects: Simply-Supported Beam with Two Equal End Moments

To provide more insight of the difference between the buckling loads under these two methods, an error analysis between these two solutions is conducted and the results are

graphed in Figure 8.16. The data from Figure 8.15 are used for this error analysis. It can be seen that as the taper angle increases, the error of the results will be larger, but it is still within an acceptable range (5%).

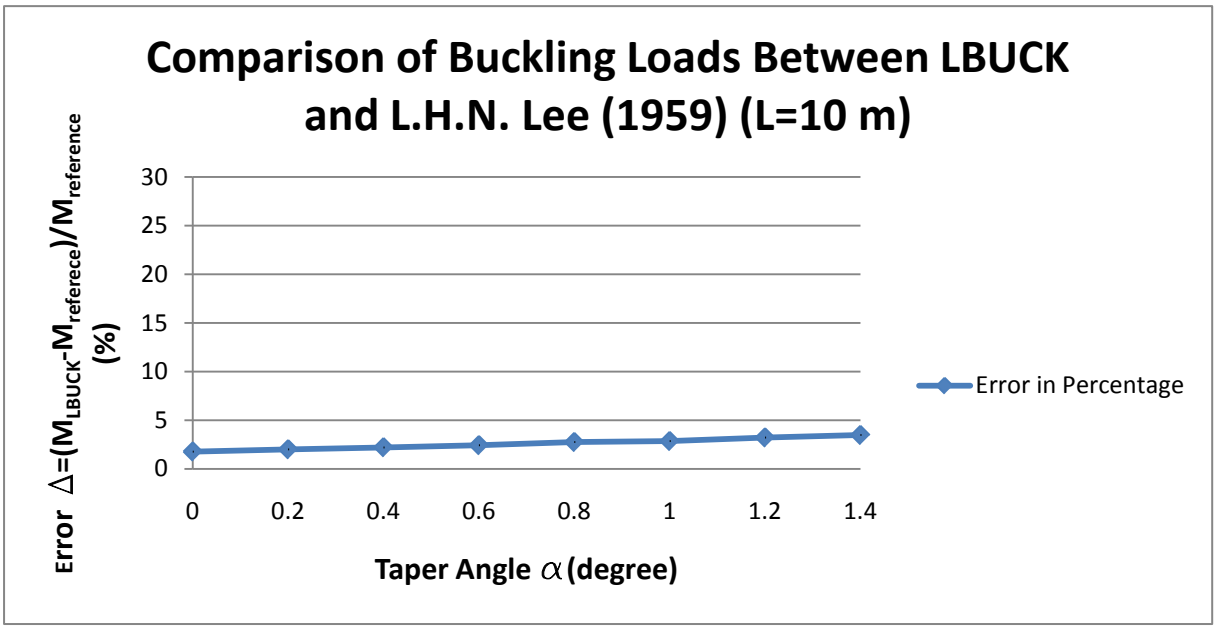

Figure 8.16 Comparison of Buckling Loads

However, this is only the case for the beam length of 10 m. The next investigation concerns error analysis with different taper angles and beam lengths.

Figure 8.17 shows the error analysis of the beam with three different taper angles of different beam lengths. In the figure, the three curves represent the errors under three different taper angles, 0 degree, 0.8 degree, and 1.4 degree. The figure shows that the LBUCK program can give better results either when the length of the beam is increased or the taper angle is decreased.

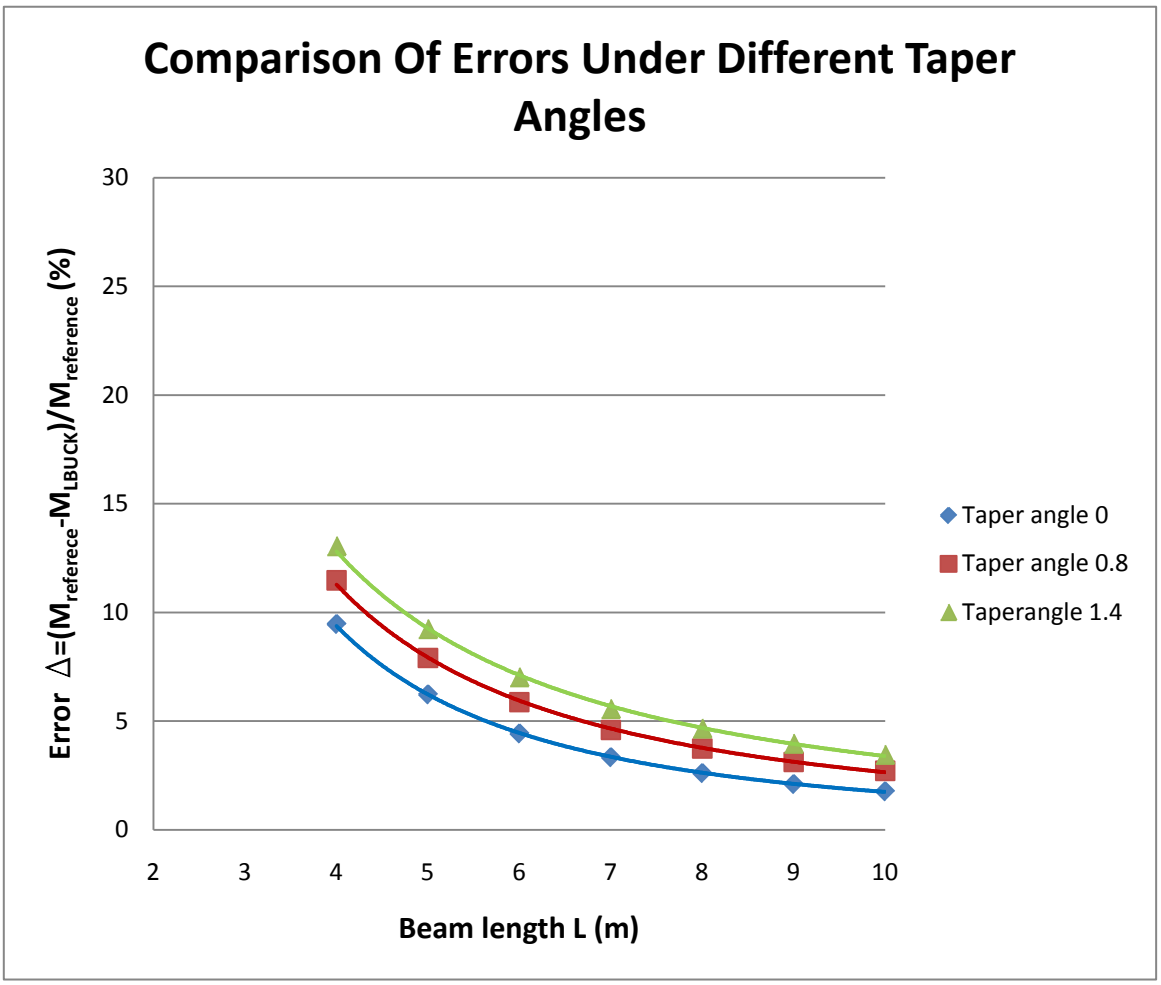

Figure 8.17 Comparison of Errors Under Different Taper Angles

8.4 CONCLUSION

Buckling analysis of three example cases is conducted in this chapter, comparisons and discussions show that the program developed based on the total potential energy presented in this paper can give good predictions of the lateral-buckling loads of doubly-symmetric tapered beams of some certain type of loading conditions as well as the boundary conditions, such as the simply-supported beam with rectangular cross-section subjected to end moments. However, it is of interest that the theory presented in this paper should be extended and

applied to more general cases, such as tapered beams of I-sections subjected to distributed loading or more complex boundary conditions, and the effects of the loadings on the buckling loads of the beams remains to be investigated in the future research.

9.0 SUMMARY

Theoretical analysis of flexural-torsional buckling of doubly-symmetric web-tapered I-beams using finite element method is mainly investigated in this study. The first two chapters present an introduction to the topic and a review of existing literatures. Chapter 3 presents the derivation of the total potential energy equations. Chapter 4 verifies the validity of the transformation equation to derive the cross section properties compared to those from the reference. Chapter 5 implements the finite element method into the total potential energy equation, and Chapter 6 explains the eigenvalue solution procedure to a generalized matrix problem. Chapter 7 introduces the concept of object-oriented technology and software development. Three example cases are analyzed in Chapter 8. And the following paragraph is a summary and findings of this research.

To calculate the flexural-torsional buckling load of a doubly-symmetric web-tapered I-beam, the study began with the derivation of the energy equations. The total potential energy equation was derived for the flexural-torsional buckling of a beam element by summing up the strain energy and the potential energy of the external loads. The first variation of the total potential energy equals to zero is the statement of the minimum total potential energy. The second variation of the total potential energy equals to zero indicates the transition from a stable to an unstable configuration. The development of the theory in

this research is based on the second variation of the total potential energy. The finite element method is then implemented into the energy equations to derive the element elastic stiffness and geometric stiffness matrices of a doubly-symmetric web-tapered beam element. Cubic polynomials were assumed for the displacement functions. Due to the tapered effects, the web-tapered I-beam element is synthesized into three parts, the top flange, the web, and the bottom flange. Some transformation matrices were developed based on geometry to convert the energy equations of the flanges in their own coordinate systems to the web coordinate system. The stiffness matrices then can be formulated for an individual web-tapered I-beam element. Stiffness matrices of individual elements in global coordinates were then summed up to provide the stiffness and geometric stiffness matrices of a beam consisting of several elements.

The final equation for calculating the flexural-torsional buckling loads is in the form of a generalized eigenvalue problem. It is converted to a standard eigenvalue equation using the Cholesky method. Householder's method is then used to change the standard matrix into a tridiagonal matrix. The eigenvalue of the tridiagonal matrix was calculated using QL iteration. The buckling parameter is the inverse of the smallest eigenvalue.

Computer technology was utilized due to the compatibility of finite element method with software. An existing software that has used the finite element equations of a beam-column element to calculate the flexural-torsional buckling loads of a plane frame structure is refactored. The contents of the program are modified to meet current needs.

The original program was not object-oriented and not user friendly. Object-oriented technology was applied to the existing flexural-torsional buckling program by refactoring the existing program. First, the basic system requirements were determined. Next, models were created considering object-oriented concepts to communicate with the new software structure. The models considered included the user case diagram, the class diagram, the sequence diagram, and the activity diagram. Then, the program code was changed from an older procedural structure to an object-oriented structure reflecting the object-oriented models. Object-oriented software development is a useful tool in engineering applications to increase the flexibility of the software applications. An object-oriented design of an existing flexural-torsional buckling analysis program was presented in this study.

In Chapter 8, three example cases were analyzed to compare the results from the software package to the existing theoretical solutions. The finite element method always predicts a buckling factor that is larger than the actual value from an existing closed form solution. To increase the accuracy of the finite element solution, more elements are needed to model the beam. The examples show that the program can provide reasonable results when at least two elements are used, and they also show that the program developed based upon the theory proposed provides good results when analyzing the beams as presented in Chapter 8, which encourages the further research on more complex situations.

Further research remains to be the development of the program based on the theory that can investigate the flexural-torsional buckling of doubly-symmetric web-tapered I-beam. The research of interest should be: the effects of loading position on the buckling load, the

flexural-torsional buckling load of web-tapered I-beam subjected to more complex loading conditions, e.g., distributed loading, combination of distributed load with concentrated loads, as well as more complex boundary conditions, e.g., continuous beams, frame structures.

APPENDIX A.

DERIVATION OF THE ROTATION TRANSFORMATION MATRIX

Point P stands for the point with the coordinates of (x, y, z) with respect to a fixed, right-handed coordinate system. When point P moves to point Q, the motion can be described into two stages: (1) point P translates to point R where the distance is described by the translation vector $\vec{d}$, and (2) point R rotates to point Q through the angel θ about the axis AB of rotation which is parallel to the translation vector $\vec{d}$. The final position is point Q with coordinates of (x, y, z) with respect to the coordinate system $oxyz$.

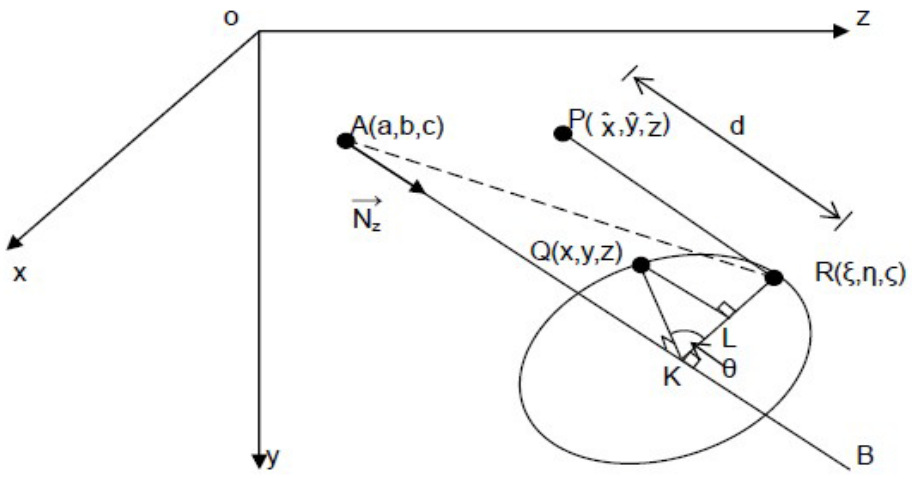

Figure A. 1 Rigid Body Movement

The objective of this Appendix is to show that the coordinates of the point Q can be calculated from the coordinate of the point P, the component of a translation vector $\vec{d}$ and direction cosines of the axis of rotation AB.

The axis of rotation AB passes through the point C, which has coordinates (a,b,c) and has direction-angles of α, β, and γ with respect to the $oxyz$ coordinate system. Points Q and R are located in a plane perpendicular to the line AB. A unit vector $\vec{N}$ on the axis of rotation AB has the same directional cosines as the rotation angle $\vec{\theta}$ and is given by

$$\vec{N} = \cos\alpha\vec{i} + \cos\beta\vec{j} + \cos\gamma\vec{k} \qquad \text{(A-1)}$$

The vector $\overrightarrow{oQ}$ can be broken into its vector components expressed by

$$\overrightarrow{oQ} = \overrightarrow{oR} + \overrightarrow{RL} + \overrightarrow{LQ} \qquad \text{(A-2)}$$

Therefore, the vector $\overrightarrow{oQ}$ may be found by determining each of its components, $\overrightarrow{oR}$, $\overrightarrow{RL}$, and $\overrightarrow{LQ}$ in terms of the coordinates of point P, the components of a translation vector $\vec{d}$, direction cosines of the axis of rotation AB, and rotational angle θ.

A. 1 VECTOR *oR*

The point P translates to the point R with coordinates (ε,η,ζ) with respect to the $oxyz$ coordinate system. The coordinate of point R may be expressed in terms of the coordinates of point P and the translation vector $\vec{d}$ as

$$\xi = \hat{x} + \vec{d}\cos\alpha \tag{A-3}$$

$$\eta = \hat{y} + \vec{d}\cos\beta \tag{A-4}$$

$$\zeta = \hat{z} + \vec{d}\cos\gamma \tag{A-5}$$

A. 2 VECTOR *RL*

The point K shown in Figure A.1 is the projection of points R and Q on the axis AB. The vectors KR and KQ are equal in magnitude and are radii of the rotation about AB, where the rotation angle, θ, is the angle $R\hat{K}Q$. The point L shown in Figure A.1 is the projection of the point Q on the line KR. The vector $\overrightarrow{KR}$ may be defined as

$$\overrightarrow{KR} = \overrightarrow{AR} - \overrightarrow{AK} \tag{A-6}$$

And it can be expanded as

$$\overrightarrow{KR} = [(\xi - a)\vec{i} + (\eta - b)\vec{j} + (\zeta - c)\vec{k}] - \overrightarrow{AK} \tag{A-7}$$

Vector $\overrightarrow{AK}$ is the projection of $\overrightarrow{AR}$ on line AB. Therefore,

$$\overrightarrow{AK} = (\overrightarrow{AR} \cdot \vec{N})\vec{N} \tag{A-8}$$

By considering the components of vectors $\overrightarrow{AR}$ and $\vec{N}$, Eq. (A-8) may be expressed as

$$\overrightarrow{AK} = [(\xi - a)\cos\alpha + (\eta - b)\cos\beta + (\zeta - c)\cos\gamma](\cos\alpha\vec{i} + \cos\beta\vec{j} + \cos\gamma\vec{k}) \tag{A-9}$$

Substituting Eq. (A-9) into (A-7) gives

$$\overrightarrow{KR} = [(\xi - a) - \cos\alpha((\xi - a)\cos\alpha + (\eta - b)\cos\beta + (\zeta - c)\cos\gamma)]\vec{i}$$

$$+[(\eta - b) - \cos\beta((\xi - a)\cos\alpha + (\eta - b)\cos\beta + (\zeta - c)\cos\gamma)]\vec{j}$$

$$+[(\zeta - c) - \cos\gamma((\xi - a)\cos\alpha + (\eta - b)\cos\beta + (\zeta - c)\cos\gamma)]\vec{k} \qquad \text{(A-10)}$$

The vector $\overrightarrow{RL}$ may be written as

$$\overrightarrow{RL} = \overrightarrow{RK} - \overrightarrow{LK} \qquad \text{(A-11)}$$

$$\overrightarrow{RL} = -\overrightarrow{KR} + \overrightarrow{KR}\cos\theta \qquad \text{(A-12)}$$

$$\overrightarrow{RL} = -(1 - \cos\theta)\overrightarrow{KR} \qquad \text{(A-13)}$$

Substituting Eq. (A-10) into Eq. (A-13) gives

$$\overrightarrow{RL} = -(1 - \cos\theta)[(\xi - a) - \cos\alpha((\xi - a)\cos\alpha + (\eta - b)\cos\beta + (\zeta - c)\cos\gamma)]\vec{i}$$

$$-(1 - \cos\theta)[(\eta - b) - \cos\beta((\xi - a)\cos\alpha + (\eta - b)\cos\beta + (\zeta - c)\cos\gamma)]\vec{j}$$

$$-(1 - \cos\theta)[(\zeta - c) - \cos\gamma((\xi - a)\cos\alpha + (\eta - b)\cos\beta + (\zeta - c)\cos\gamma)]\vec{k} \qquad \text{(A-14)}$$

A. 3 VECTOR *LQ*

By definition of vector cross-product

$$\overrightarrow{N} \times \overrightarrow{AR} = [(\zeta - c)\cos\beta - (\eta - b)\cos\gamma]\vec{i} + [(\xi - a)\cos\gamma - (\zeta - c)\cos\alpha]\vec{j}$$

$$+[(\eta - b)\cos\alpha - (\xi - a)\cos\beta]\vec{k} \qquad \text{(A-15)}$$

And

$$|\vec{N}\times\overrightarrow{AR}|=AR\sin K\hat{A}R \tag{A-16}$$

From triangle ARK,

$$AR\sin K\hat{A}R=KR \tag{A-17}$$

Therefore,

$$|\vec{N}\times\overrightarrow{AR}|=KR \tag{A-18}$$

A unit vector, $\overrightarrow{N_{LQ}}$, in the direction LQ is defined as

$$\overrightarrow{N_{LQ}}=\frac{\vec{N}\times\overrightarrow{AR}}{|\vec{N}\times\overrightarrow{AR}|} \tag{A-19}$$

Substituting Eq. (A-18) into (A-19) gives

$$\overrightarrow{N_{LQ}}=\frac{\vec{N}\times\overrightarrow{AR}}{KR} \tag{A-20}$$

Substituting Eq. (A-15) into Eq. (A-20) gives

$$\vec{N}_{LQ}=\frac{1}{KR}\{[(\zeta-c)\cos\beta-(\eta-b)\cos\gamma]\vec{i}+[(\xi-a)\cos\gamma-(\zeta-c)\cos\alpha]\vec{j}$$

$$+[(\eta-b)\cos\alpha-(\xi-a)\cos\beta]\vec{k}\} \tag{A-21}$$

Since

$$LQ=KQ\sin\theta=KR\sin\theta \tag{A-22}$$

The vector $\overrightarrow{LQ}$ may be expressed as

$$\overrightarrow{LQ}=KR\sin\theta\vec{N}_{LQ} \tag{A-23}$$

From Eq. (A-21) and (A-23), the vector $\overrightarrow{LQ}$ may be written as

$$\overrightarrow{LQ} = \sin\theta\{[(\zeta - c)\cos\beta - (\eta - b)\cos\gamma]\vec{i} + [(\xi - a)\cos\gamma - (\zeta - c)\cos\alpha]\vec{j}$$

$$+[(\eta - b)\cos\alpha - (\xi - a)\cos\beta]\vec{k}\} \qquad \text{(A-24)}$$

A. 4 FINITE DISPLACEMENTS TRANSFORMATION

To define the finite displacements transformation matrix, consider the x y and z components of Eq. (A-2) in the form of

$$x = \xi + RL_x + LQ_x \qquad \text{(A-25a)}$$

$$y = \eta + RL_y + LQ_y \qquad \text{(A-25b)}$$

$$z = \zeta + RL_z + LQ_z \qquad \text{(A-25c)}$$

Substituting in for vectors $\overrightarrow{RL}$ from Eq. (A-14) and $\overrightarrow{LQ}$ from Eq. (A-24) into (A-25a) to (A-25c) gives

$$x = \xi - (1-\cos\theta)[(\xi - a) - (\xi - a)\cos^2\alpha - (\eta - b)\cos a\cos\beta - (\zeta - c)\cos\alpha\cos\gamma]$$

$$+\sin\theta[(\xi - c)\cos\beta - (\eta - b)\cos\gamma] \qquad \text{(A-26a)}$$

$$y = \eta - (1-\cos\theta)[(\eta - b) - (\xi - a)\cos\alpha\cos\beta - (\eta - b)\cos^2\beta - (\zeta - c)\cos\beta\cos\gamma]$$

$$+\sin\theta[(\xi - a)\cos\gamma - (\zeta - c)\cos\alpha] \qquad \text{(A-26b)}$$

$$z = \zeta - (1-\cos\theta)[(\zeta - c) - (\xi - a)\cos\alpha\cos\gamma - (\eta - b)\cos\beta\cos\gamma - (\zeta - c)\cos^2\gamma]$$

$$+\sin\theta[(\eta - b)\cos\alpha - (\xi - a)\cos\beta] \qquad \text{(A-26c)}$$

Substituting for ξ, η, and ζ from Eqs. (A-3) to (A-5) into (A-26a) to (A-26c) gives

$$x = \hat{x} + d\cos\alpha - (1-\cos\theta)[(\hat{x}-a)\sin^2\alpha - (\hat{y}-b)\cos a\cos\beta - (\hat{z}-c)\cos\alpha\cos\gamma]$$
$$+\sin\theta[(\hat{z}-c)\cos\beta - (\hat{y}-b)\cos\gamma] \quad \text{(A-27a)}$$

$$y = \hat{y} + d\cos\beta - (1-\cos\theta)[-(\hat{x}-a)\cos a\cos\beta + (\hat{y}-b)\sin^2\beta - (\hat{z}-c)\cos\beta\cos\gamma]$$
$$+\sin\theta[(\hat{x}-a)\cos\gamma - (\hat{z}-c)\cos\alpha] \quad \text{(A-27b)}$$

$$z = \hat{z} + d\cos\gamma - (1-\cos\theta)[-(\hat{x}-a)\cos a\cos\gamma - (\hat{y}-b)\cos\beta\cos\gamma + (\hat{z}-c)\sin^2\gamma]$$
$$+\sin\theta[(\hat{y}-b)\cos\alpha - (\hat{x}-a)\cos\beta] \quad \text{(A-27c)}$$

Eqs. (A-27a) through (A-27c) may be expressed in matrix form as the most general form of the finite displacement transformation given by

$$\begin{bmatrix} x \\ y \\ z \end{bmatrix} = \begin{bmatrix} a \\ b \\ c \end{bmatrix} + \begin{bmatrix} d\cos\alpha \\ d\cos\beta \\ d\cos\gamma \end{bmatrix} + [T_R]\begin{bmatrix} \hat{x}-a \\ \hat{y}-b \\ \hat{z}-c \end{bmatrix} \quad \text{(A-28)}$$

Where

$$[T_R] = \begin{bmatrix} \cos\theta + C\cos^2\alpha & C\cos\alpha\cos\beta - \sin\theta\cos\gamma & C\cos\alpha\cos\gamma + \sin\theta\cos\beta \\ C\cos\alpha\cos\beta + \sin\theta\cos\gamma & \cos\theta + C\cos^2\beta & C\cos\beta\cos\gamma - \sin\theta\cos\alpha \\ C\cos\alpha\cos\gamma - \sin\theta\cos\beta & C\cos\beta\cos\gamma + \sin\theta\cos\alpha & \cos\theta + C\cos^2\gamma \end{bmatrix}$$

(A-29)

And

$$C = 1 - \cos\theta \quad \text{(A-30)}$$

A.5 ROTATION TRANSFORMATION MATRIX

For small rotation transformation, we have $\vec{d}$=0; therefore, Eqs. (A-3) to (A-5) can be simplified to

$$\xi = \hat{x} \tag{A-31a}$$

$$\eta = \hat{y} \tag{A-31b}$$

$$\zeta = \hat{z} \tag{A-31c}$$

Using Eqs. (A-31) in (A-26), we have

$$x = \hat{x} - (1-\cos\theta)[(\hat{x}-a)\sin^2\alpha - (\hat{y}-b)\cos a\cos\beta - (\hat{z}-c)\cos\alpha\cos\gamma]$$
$$+\sin\theta[(\hat{z}-c)\cos\beta - (\hat{y}-b)\cos\gamma] \tag{A-32a}$$

$$y = \hat{y} - (1-\cos\theta)[(\hat{y}-b)\sin^2\beta - (\hat{x}-a)\cos\alpha\cos\beta - (\hat{z}-c)\cos\beta\cos\gamma]$$
$$+\sin\theta[(\hat{x}-a)\cos\gamma - (\hat{z}-c)\cos\alpha] \tag{A-32b}$$

$$z = \hat{z} - (1-\cos\theta)[(\hat{z}-c)\sin^2\gamma - (\hat{x}-a)\cos\alpha\cos\gamma - (\hat{y}-b)\cos\beta\cos\gamma]$$
$$+\sin\theta[(\hat{y}-b)\cos\alpha - (\hat{x}-a)\cos\beta] \tag{A-32c}$$

If the rotation axis AB passes through the origin, then $a = b = c = 0$, and Eqs. (A-32) can be simplified to

$$x = \hat{x} - (1-\cos\theta)[\hat{x}\sin^2\alpha - \hat{y}\cos a\cos\beta - \hat{z}\cos\alpha\cos\gamma] + \sin\theta[\hat{z}\cos\beta - \hat{y}\cos\gamma] \tag{A-33a}$$

$$y = \hat{y} - (1-\cos\theta)[\hat{y}\sin^2\beta - \hat{x}\cos a\cos\beta - \hat{z}\cos\beta\cos\gamma] + \sin\theta[\hat{x}\cos\gamma - \hat{z}\cos\alpha]$$

(A-33b)

$$z = \hat{z} - (1-\cos\theta)[\hat{z}\sin^2\gamma - \hat{x}\cos a\cos\gamma - \hat{y}\cos\beta\cos\gamma] + \sin\theta[\hat{y}\cos\alpha - \hat{x}\cos\beta]$$

(A-33c)

Eqs. (A-33) may be simplified using trigonometric identities and expressed as

$$x = \hat{x} - 2\sin^2\frac{\theta}{2}[\hat{x}\sin^2\alpha - \hat{y}\cos a\cos\beta - \hat{z}\cos\alpha\cos\gamma] + 2\sin\frac{\theta}{2}\cos\frac{\theta}{2}[\hat{z}\cos\beta - \hat{y}\cos\gamma]$$

(A-34a)

$$y = \hat{y} - 2\sin^2\frac{\theta}{2}[\hat{y}\sin^2\beta - \hat{x}\cos a\cos\beta - \hat{z}\cos\beta\cos\gamma] + 2\sin\frac{\theta}{2}\cos\frac{\theta}{2}[\hat{x}\cos\gamma - \hat{z}\cos\alpha]$$

(A-34b)

$$z = \hat{z} - 2\sin^2\frac{\theta}{2}[\hat{z}\sin^2\gamma - \hat{x}\cos a\cos\gamma - \hat{y}\cos\beta\cos\gamma] + 2\sin\frac{\theta}{2}\cos\frac{\theta}{2}[\hat{y}\cos\alpha - \hat{x}\cos\beta]$$

(A-34c)

Eqs. (A-34) may be expressed in the following form

$$x = (1-2\sin^2\frac{\theta}{2}\sin^2\alpha)\hat{x} + (2\sin^2\frac{\theta}{2}\cos\alpha\cos\beta - 2\sin\frac{\theta}{2}\cos\frac{\theta}{2}\cos\gamma)\hat{y}$$
$$+(2\sin^2\frac{\theta}{2}\cos\alpha\cos\gamma + 2\sin\frac{\theta}{2}\cos\frac{\theta}{2}\cos\beta)\hat{z} \quad \text{(A-35a)}$$

$$y = (2\sin^2\frac{\theta}{2}\cos\alpha\cos\beta + 2\sin\frac{\theta}{2}\cos\frac{\theta}{2}\cos\gamma)\hat{x} + (1-2\sin^2\frac{\theta}{2}\sin^2\beta)\hat{y}$$
$$+(2\sin^2\frac{\theta}{2}\cos\beta\cos\gamma - 2\sin\frac{\theta}{2}\cos\frac{\theta}{2}\cos\alpha)\hat{z} \quad \text{(A-35b)}$$

$$z = (2\sin^2\frac{\theta}{2}\cos\alpha\cos\gamma - 2\sin\frac{\theta}{2}\cos\frac{\theta}{2}\cos\beta)\hat{x} + (2\sin^2\frac{\theta}{2}\cos\beta\cos\gamma + 2\sin\frac{\theta}{2}\cos\frac{\theta}{2}\cos\alpha)\hat{y}$$
$$+(1-2\sin^2\frac{\theta}{2}\sin^2\gamma)\hat{z} \quad \text{(A-35c)}$$

For this special case of no translation and the axis of rotation AB passing through the origin o,then point A is at o. If the coordinates systems $oxyz$ rotates with the point P about the line oB and goes to $ox'y'z'$, the coordinates of point Q with respect to the coordinate

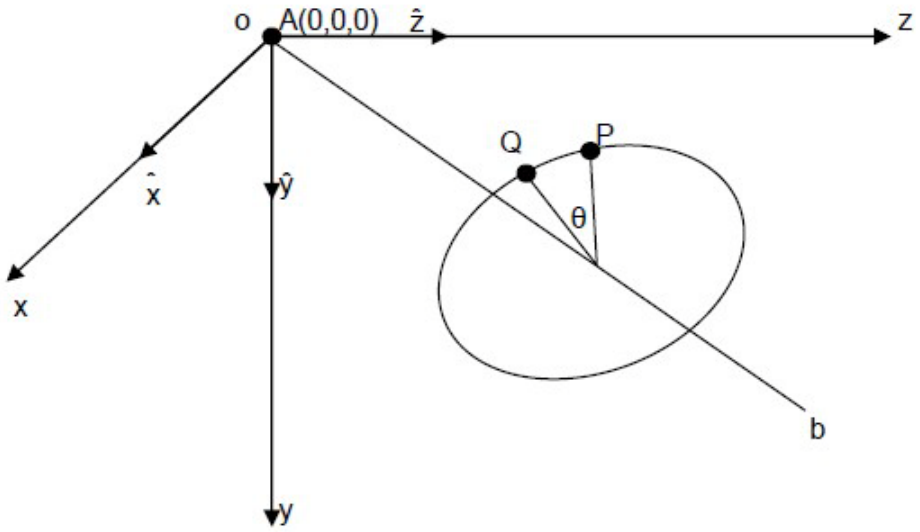

Figure A. 2 Rigid Body Rotation

systems $ox'y'z'$ are $\hat{x}$, $\hat{y}$ and $\hat{z}$, and with respect to the coordinate systems $oxyz$ are x, y and z. Then Eqs. (A-35) represent a rotation transformation coordinate system with the direction cosines for the $ox'y'z'$ system with respect to the $oxyz$ system shown is Table A-1.

Table A-1 Direct Cosines

	x	y	z
$\hat{x}$	l_x	m_x	n_x
$\hat{y}$	l_y	m_y	n_y
$\hat{z}$	l_z	m_z	n_z

Where

$$l_x = 1 - 2\sin^2\frac{\theta}{2}\sin^2\alpha \tag{A-36a}$$

$$l_y = 2\sin^2\frac{\theta}{2}\cos\alpha\cos\beta - 2\sin\frac{\theta}{2}\cos\frac{\theta}{2}\cos\gamma \tag{A-36b}$$

$$l_z = 2\sin^2\frac{\theta}{2}\cos\alpha\cos\gamma + 2\sin\frac{\theta}{2}\cos\frac{\theta}{2}\cos\beta \tag{A-36c}$$

$$m_x = 2\sin^2\frac{\theta}{2}\cos\alpha\cos\beta + 2\sin\frac{\theta}{2}\cos\frac{\theta}{2}\cos\gamma \tag{A-37a}$$

$$m_y = 1 - 2\sin^2\frac{\theta}{2}\sin^2\beta \tag{A-37b}$$

$$m_z = 2\sin^2\frac{\theta}{2}\cos\beta\cos\gamma - 2\sin\frac{\theta}{2}\cos\frac{\theta}{2}\cos\alpha \tag{A-37c}$$

$$n_x = 2\sin^2\frac{\theta}{2}\cos\alpha\cos\gamma - 2\sin\frac{\theta}{2}\cos\frac{\theta}{2}\cos\beta \tag{A-38a}$$

$$n_y = 2\sin^2\frac{\theta}{2}\cos\beta\cos\gamma + 2\sin\frac{\theta}{2}\cos\frac{\theta}{2}\cos\alpha \tag{A-38b}$$

$$n_z = 1 - 2\sin^2\frac{\theta}{2}\sin^2\gamma \tag{A-38c}$$

Equations above can be expressed in a matrix form

$$\begin{bmatrix} x \\ y \\ z \end{bmatrix} = [T_R] \begin{bmatrix} \hat{x} \\ \hat{y} \\ \hat{z} \end{bmatrix} = \begin{bmatrix} l_x & l_y & l_z \\ m_x & m_y & m_z \\ n_x & n_y & n_z \end{bmatrix} \begin{bmatrix} \hat{x} \\ \hat{y} \\ \hat{z} \end{bmatrix} \tag{A-39}$$

If the direction cosine of the unit vector $\vec{N}$ is expressed in terms of the component of the rotation vector $\vec{\theta}$,

$$\vec{\theta} = \theta_x \vec{i} + \theta_y \vec{j} + \theta_z \vec{k} \tag{A-40}$$

And

$$\cos\alpha = \frac{\theta_x}{\theta} \quad , \quad \cos\beta = \frac{\theta_y}{\theta} \quad , \quad \cos\gamma = \frac{\theta_z}{\theta} \tag{A-41}$$

Based on the small rotation assumption, $\sin\theta \approx \theta$ and $\cos\theta \approx 1 - \frac{\theta^2}{2}$, and substituting Eq. (A-41) into Eqs. (A-35), we have

$$\begin{bmatrix} x \\ y \\ z \end{bmatrix} = \begin{bmatrix} 1 - \frac{\theta_y^{\,2}}{2} - \frac{\theta_z^{\,2}}{2} & -\theta_z + \frac{\theta_x\theta_y}{2} & \theta_y + \frac{\theta_x\theta_z}{2} \\ \theta_z + \frac{\theta_x\theta_y}{2} & 1 - \frac{\theta_x^{\,2}}{2} - \frac{\theta_z^{\,2}}{2} & -\theta_x + \frac{\theta_y\theta_z}{2} \\ -\theta_y + \frac{\theta_x\theta_z}{2} & \theta_x + \frac{\theta_y\theta_z}{2} & 1 - \frac{\theta_x^{\,2}}{2} - \frac{\theta_y^{\,2}}{2} \end{bmatrix} \begin{bmatrix} \hat{x} \\ \hat{y} \\ \hat{z} \end{bmatrix} \tag{A-42}$$

APPENDIX B

THE ELASTIC STIFFNESS MATRIX AND THE ELASTIC GEOMETRIC STIFFNESS MATRICES

B. 1

ELASTIC STIFFNESS MATRIX OF A WEB ELEMENT

```
EW[1][1]= 1./2*(hi+hj)*E*pow(tw,3)/pow(L,3);

EW[1][2]= 1./6*(2*hi+hj)*E*pow(tw,3)/pow(L,2);

EW[1][3]=0;

EW[1][4]=0;

EW[1][5]= 1./2*(-hi-hj)*E* pow(tw,3)/ pow(L,3),

EW[1][6]= 1./6*(hi+2*hj)*E* pow(tw,3)/ pow(L,2),

EW[1][7]=0,

EW[1][8]=0;

EW[2][1]= 1./6*(2*hi+hj)*E* pow(tw,3)/ pow(L,2);

EW[2][2]= 1./12*(3*hi+hj)*E* pow(tw,3)/L;

EW[2][3]=0;

EW[2][4]=0;

EW[2][5]= 1./6*(-2*hi-hj)*E* pow(tw,3)/ pow(L,2);

EW[2][6]= 1./12*(hi+hj)*E* pow(tw,3)/L;
```

```
EW[2][7]=0;

EW[2][8]=0;

EW[3][1]=0;

EW[3][2]=0;

EW[3][3]=pow(tw,3)*(2*G*pow(L,2)*hi+2*G*pow(L,2)*hj+7*E*pow(hi,3)+3*E*pow(hi,2)
*hj+3*E*hi*pow(hj,2)+7*E*pow(hj,3))/(10* pow(L,3));

EW[3][4]=pow(tw,3)*(G*pow(L,2)*hj+15*E*pow(hi,3)+6*E*pow(hi,2)*hj+3*E*hi*pow(hj,
2)+6*E* pow(hj,3))/(30* pow(L,2));

EW[3][5]=0;

EW[3][6]=0;

EW[3][7]=-pow(tw,3)*(2*G*pow(L,2)*hi+2*G*pow(L,2)*hj+7*E*pow(hi,3)+3*E*pow(hi,2
)*hj+3*E*hi*pow(hj,2)+7*E*pow(hj,3))/(10* pow(L,3));

EW[3][8]=pow(tw,3)*(G*pow(L,2)*hi+6*E*pow(hi,3)+3*E*pow(hi,2)*hj+6*E*hi*pow(hj,2
)+15*E* pow(hj,3))/(30* pow(L,2));

EW[4][1]=0;

EW[4][2]=0;

EW[4][3]=pow(tw,3)*(G*pow(L,2)*hj+15*E*pow(hi,3)+6*E*pow(hi,2)*hj+3*E*hi*pow(hj,
2)+6*E* pow(hj,3))/(30* pow(L,2));

EW[4][4]=pow(tw,3)*(3*G*pow(L,2)*hi+G*pow(L,2)*hj+33*E*pow(hi,3)+15*E*pow(hi,2)
*hj+6*E*hi* pow(hj,2)+6*E* pow(hj,3))/(90*L);

EW[4][5]=0;

EW[4][6]=0;

EW[4][7]= - pow(tw,3)*(G* pow(L,2)*hj+15*E* pow(hi,3)+6*E* pow(hi,2)*hj+3*E*hi*
pow(hj,2)+6*E* pow(hj,3))/(30* pow(L,2));
```

EW[4][8]=pow(tw,3)*(-G*pow(L,2)*hi-G*pow(L,2)*hj+24*E*pow(hi,3)+6*E*pow(hi,2)*hj +6*E*hi* pow(hj,2)+24*E* pow(hj,3))/(180*L);

EW[5][1]= -(hi+hj)*E* pow(tw,3)/(2*L^3);

EW[5][2]= -(2*hi+hj)*E* pow(tw,3)/(6* pow(L,2));

EW[5][3]=0;

EW[5][4]=0;

EW[5][5]= (hi+hj)*E* pow(tw,3)/(2*L^3);

EW[5][6]= -(hi+2*hj)*E* pow(tw,3)/(6* pow(L,2));

EW[5][7]=0;

EW[5][8]=0;

EW[6][1]= (hi+2*hj)*E* pow(tw,3)/(6* pow(L,2));

EW[6][2]= (hi+hj)*E* pow(tw,3)/(12*L);

EW[6][3]=0;

EW[6][4]=0;

EW[6][5]= -(hi+2*hj)*E* pow(tw,3)/(6* pow(L,2));

EW[6][6]= (hi+3*hj)*E* pow(tw,3)/(12*L);

EW[6][7]=0,

EW[6][8]=0;

EW[7][1]=0;

EW[7][2]= 0;

EW[7][3]=- pow(tw,3)*(2*G* pow(L,2)*hi+2*G* pow(L,2)*hj+7*E* pow(hi,3)+3*E* pow(hi,2)*hj+3*E*hi* pow(hj,2)+7*E* pow(hj,3))/(10*L^3);

EW[7][4]= - pow(tw,3)*(G* pow(L,2)*hj+15*E* pow(hi,3)+6*E* pow(hi,2)*hj+3*E*hi* pow(hj,2)+6*E* pow(hj,3))/(30* pow(L,2)); EW[7][5]=0;

EW[7][6]=0;

EW[7][7]= pow(tw,3)*(2*G* pow(L,2)*hi+2*G* pow(L,2)*hj+7*E* pow(hi,3)+3*E* pow(hi,2)*hj+3*E*hi* pow(hj,2)+7*E* pow(hj,3))/(10*L^3);

EW[7][8]= - pow(tw,3)*(G* pow(L,2)*hi+6*E* pow(hi,3)+3*E* pow(hi,2)*hj+6*E*hi* pow(hj,2)+15*E* pow(hj,3))/(30* pow(L,2));

EW[8][1]=0;

EW[8][2]=0;

EW[8][3]= pow(tw,3)*(G* pow(L,2)*hi+6*E* pow(hi,3)+3*E* pow(hi,2)*hj+6*E*hi* pow(hj,2)+15*E* pow(hj,3))/(30* pow(L,2));

EW[8][4]= pow(tw,3)*(-G* pow(L,2)*hi-G* pow(L,2)*hj+24*E* pow(hi,3)+6*E* pow(hi,2)*hj+6*E*hi* pow(hj,2)+24*E* pow(hj,3))/(180*L);

EW[8][5]=0;

EW[8][6]=0;

EW[8][7]= - pow(tw,3)*(G* pow(L,2)*hi+6*E* pow(hi,3)+3*E* pow(hi,2)*hj+6*E*hi* pow(hj,2)+15*E* pow(hj,3))/(30* pow(L,2));

EW[8][8]= pow(tw,3)*(G* pow(L,2)*hi+3*G* pow(L,2)*hj+6*E* pow(hi,3)+6*E* pow(hi,2)*hj+15*E*hi* pow(hj,2)+33*E* pow(hj,3))/(90*L);

B. 2

ELASTIC STIFFNESS MATRIX OF A FLANGE ELEMENT

```
EF[1][1]= 12.*E*In/ pow(Lf,3);

EF[1][2]= 6.*E*In/ pow(Lf,2);

EF[1][3]=0;

EF[1][4]=0;

EF[1][5]= -12.*E*In/ pow(Lf,3);

EF[1][6]= 6.*E*In/ pow(Lf,2);

EF[1][7]=0,

EF[1][8]=0;

EF[2][1]= 6.*E*In/ pow(Lf,2);

EF[2][2]= 4.*E*In/Lf;

EF[2][3]=0;

EF[2][4]=0;

EF[2][5]= -6.*E*In/ pow(Lf,2),

EF[2][6]= 2.*E*In/Lf,

EF[2][7]=0,

EF[2][8]=0;

EF[3][1]=0;

EF[3][2]=0;

EF[3][3]= 1./5*(6*G*Jf* pow(Lf,2)+60*E*Iwf)/ pow(Lf,3);

EF[3][4]= 1./10*(G*Jf* pow(Lf,2)+60*E*Iwf)/ pow(Lf,2);

EF[3][5]=0,
```

```
EF[3][6]=0,
EF[3][7]= 1./5*(-6*G*Jf* pow(Lf,2)-60*E*Iwf)/ pow(Lf,3),
EF[3][8]= 1./10*(G*Jf* pow(Lf,2)+60*E*Iwf)/ pow(Lf,2);
EF[4][1]=0;
EF[4][2]=0;
EF[4][3]= 1./10*(G*Jf* pow(Lf,2)+60*E*Iwf)/ pow(Lf,2);
EF[4][4]= 1./15*(2*G*Jf* pow(Lf,2)+60*E*Iwf)/Lf;
EF[4][5]=0,
EF[4][6]=0,
EF[4][7]= 1./10*(-G*Jf* pow(Lf,2)-60*E*Iwf)/ pow(Lf,2);
EF[4][8]= 1./30*(-G*Jf* pow(Lf,2)+60*E*Iwf)/Lf;
EF[5][1]= -12.*E*In/ pow(Lf,3);
EF[5][2]= -6.*E*In/ pow(Lf,2);
EF[5][3]=0,
EF[5][4]=0;
EF[5][5]= 12.*E*In/ pow(Lf,3);
EF[5][6]= -6.*E*In/ pow(Lf,2);
EF[5][7]=0;
EF[5][8]=0;
EF[6][1]= 6.*E*In/ pow(Lf,2),
EF[6][2]= 2.*E*In/Lf,
EF[6][3]=0,
EF[6][4]=0;
```

```
EF[6][5]= -6.*E*In/ pow(Lf,2);

EF[6][6]= 4.*E*In/Lf;

EF[6][7]=0;

EF[6][8]=0;

EF[7][1]=0,

EF[7][2]=0,

EF[7][3]= 1./5*(-6*G*Jf* pow(Lf,2)-60*E*Iwf)/ pow(Lf,3);

EF[7][4]= 1./10*(-G*Jf* pow(Lf,2)-60*E*Iwf)/ pow(Lf,2);

EF[7][5]=0;

EF[7][6]=0;

EF[7][7]= 1./5*(6*G*Jf* pow(Lf,2)+60*E*Iwf)/ pow(Lf,3);

EF[7][8]= 1./10*(-G*Jf* pow(Lf,2)-60*E*Iwf)/ pow(Lf,2);

EF[8][1]=0;

EF[8][2]=0;

EF[8][3]= 1./10*(G*Jf* pow(Lf,2)+60*E*Iwf)/ pow(Lf,2);

EF[8][4]= 1./30*(-G*Jf* pow(Lf,2)+60*E*Iwf)/Lf;

EF[8][5]=0;

EF[8][6]=0;

EF[8][7]= 1./10*(-G*Jf* pow(Lf,2)-60*E*Iwf)/ pow(Lf,2);

EF[8][8]= 1./15*(2*G*Jf* pow(Lf,2)+60*E*Iwf)/Lf;
```

B. 3

GEOMETRIC STIFFNESS MATRIX OF A BEAM ELEMENT

```
KG[1][1]=(6.*F)/(5*L);
KG[1][2]=F/10.;
KG[1][3]=(-6.*Mi)/(5*L)-Vi/10.;
KG[1][4]=-Mi/10.;
KG[1][5]=(-6.*F)/(5.*L);
KG[1][6]=F/10;
KG[1][7]=(6.*Mi)/(5.*L)+(11.*Vi)/10.;
KG[1][8]=-Mi/10.-(L*Vi)/10.;
KG[2][1]=KG[1][2];
KG[2][2]=(2.*F*L)/15.;
KG[2][3]=(-11.*Mi)/10.-(L*Vi)/5.;
KG[2][4]=-(2.*L*Mi)/15.-((L*L)*Vi)/30.;
KG[2][5]=-F/10.;
KG[2][6]=-(F*L)/30.;
KG[2][7]=Mi/10.+(L*Vi)/5.;
KG[2][8]=(L*Mi)/30.;
KG[3][1]=KG[1][3];
KG[3][2]=KG[2][3];
KG[3][3]=P*(d+h1/2+zp*0)-(6.*P*(d+h1/2+zp*0)*zp*zp)/(L*L)+(4.*P*(d+h1/2+zp*0)*zp*
zp*zp)/(L*L*L)+(9.*P*(d+h1/2+zp*0)*zp*zp*zp*zp)/(L*L*L*L)-(12.*P*(d+h1/2.+zp*0)*z
p*zp*zp*zp*zp)/(L*L*L*L*L)+(4.*P*(d+h1/2+zp*0)*zp*zp*zp*zp*zp*zp)/(L*L*L*L*L*L
);
KG[3][4]=P*(d+h1/2+zp*0)*zp-(2.*P*(d+h1/2+zp*0)*zp*zp)/L-(2.*P*(d+h1/2+zp*0)*zp*z
p*zp)/(L*L)+(8.*P*(d+h1/2+zp*0)*zp*zp*zp*zp)/(L*L*L)-(7.*P*(d+h1/2.+zp*0)*zp*zp*z
p*zp*zp)/(L*L*L*L)+(2.*P*(d+h1/2+zp*0)*zp*zp*zp*zp*zp*zp)/(L*L*L*L*L);
KG[3][5]=(6.*Mi)/(5.*L)+Vi/10.;
```

```
KG[3][6]=-Mi/10.+(L*Vi)/10.;
KG[3][7]=(3.*P*(d+h1/2+zp*0)*zp*zp)/(L*L)-(2.*P*(d+h1/2+zp*0)*zp*zp*zp)/(L*L*L)-(9
.*P*(d+h1/2+zp*0)*zp*zp*zp*zp)/(L*L*L*L)+(12.*P*(d+h1/2+zp*0)*zp*zp*zp*zp*zp)/(L
*L*L*L*L)-(4.*P*(d+h1/2+zp*0)*zp*zp*zp*zp*zp*zp)/(L*L*L*L*L*L);
KG[3][8]=-(P*(d+h1/2+zp*0)*zp*zp)/L+(P*(d+h1/2+zp*0)*zp*zp*zp)/(L*L)+(3.*P*(d+h1/
2+zp*0)*zp*zp*zp*zp)/(L*L*L)-(5.*P*(d+h1/2.+zp*0)*zp*zp*zp*zp*zp)/(L*L*L*L)+(2.*P
*(d+h1/2+zp*0)*zp*zp*zp*zp*zp*zp)/(L*L*L*L*L);
KG[4][1]=KG[1][4];
KG[4][2]=KG[2][4];
KG[4][3]=KG[3][4];
KG[4][4]=P*(d+h1/2+zp*0)*zp*zp-(4.*P*(d+h1/2.+zp*0)*zp*zp*zp)/L+(6.*P*(d+h1/2.+zp
*0)*zp*zp*zp*zp)/(L*L)-(4.*P*(d+h1/2.+zp*0)*zp*zp*zp*zp*zp)/(L*L*L)+(P*(d+h1/2.+zp
*0)*zp*zp*zp*zp*zp*zp)/(L*L*L*L);
KG[4][5]=Mi/10;
KG[4][6]=(L*Mi)/30.+((L*L)*Vi)/30;
KG[4][7]=(3.*P*(d+h1/2+zp*0)*zp*zp*zp)/(L*L)-(8.*P*(d+h1/2+zp*0)*zp*zp*zp*zp)/(L*
L*L)+(7.*P*(d+h1/2.+zp*0)*zp*zp*zp*zp*zp)/(L*L*L*L)-(2.*P*(d+h1/2.+zp*0)*zp*zp*zp
*zp*zp*zp)/(L*L*L*L*L);
KG[4][8]=-(P*(d+h1/2+zp*0)*zp*zp*zp)/L+(3.*P*(d+h1/2+zp*0)*zp*zp*zp*zp)/(L*L)-(3.*
P*(d+h1/2+zp*0)*zp*zp*zp*zp*zp)/(L*L*L)+(P*(d+h1/2+zp*0)*zp*zp*zp*zp*zp*zp)/(L*
L*L*L);
KG[5][1]=KG[1][5];
KG[5][2]=KG[2][5];
KG[5][3]=KG[3][5];
KG[5][4]=KG[4][5];
KG[5][5]=(6.*F)/(5.*L);
KG[5][6]=-F/10.;
KG[5][7]=(-6.*Mi)/(5.*L)-(11.*Vi)/10.;
```

```
KG[5][8]=Mi/10.+(L*Vi)/10.;
KG[6][1]=KG[1][6];
KG[6][2]=KG[2][6];
KG[6][3]=KG[3][6];
KG[6][4]=KG[4][6];
KG[6][5]=KG[5][6];
KG[6][6]=(2.*F*L)/15;
KG[6][7]=(11.*Mi)/10+(9.*L*Vi)/10;
KG[6][8]=(-2.*L*Mi)/15-((L*L)*Vi)/10.;
KG[7][1]=KG[1][7];
KG[7][2]=KG[2][7];
KG[7][3]=KG[3][7];
KG[7][4]=KG[4][7];
KG[7][5]=KG[5][7];
KG[7][6]=KG[6][7];
KG[7][7]=(9.*P*(d+h1/2+zp*0)*zp*zp*zp*zp)/(L*L*L*L)-(12.*P*(d+h1/2+zp*0)*zp*zp*zp*zp*zp)/(L*L*L*L*L)+(4.*P*(d+h1/2+zp*0)*zp*zp*zp*zp*zp*zp)/(L*L*L*L*L*L);
KG[7][8]=-(3.*P*(d+h1/2+zp*0)*zp*zp*zp*zp)/(L*L*L)+(5.*P*(d+h1/2+zp*0)*zp*zp*zp*zp*zp)/(L*L*L*L)-(2.*P*(d+h1/2+zp*0)*zp*zp*zp*zp*zp*zp)/(L*L*L*L*L);
KG[8][1]=KG[1][8];
KG[8][2]=KG[2][8];
KG[8][3]=KG[3][8];
KG[8][4]=KG[4][8];
KG[8][5]=KG[5][8];
KG[8][6]=KG[6][8];
KG[8][7]=KG[7][8];
KG[8][8]=(P*(d+h1/2)*zp*zp*zp*zp)/(L*L)-(2.*P*(d+h1/2+zp*0)*zp*zp*zp*zp*zp)/(L*L*L)+(P*(d+h1/2+zp*0)*zp*zp*zp*zp*zp*zp)/(L*L*L*L);
```

APPENDIX C

FLEXURAL-TORSIONAL BUCKLING ANALYSIS PROGRAM

This Appendix presents the code written for the LBuck Program.

C.1 PROP.H

```
#if!defined(properties_h)
#define propereties_h
#define MSize 62

class Properties
{
    protected:
        int j1,j2,joint_num;
        float E,G,Jf,Iwf,L,Lf,In,tw,d,zi,zj,hi,hj,tanA0,A0,element_num,length;
        float Fi,Vi,Vj,Mi;
        float z[MSize];
        float h[MSize];
        float v[MSize];
        float mi[MSize];
    public:
        virtual void Fill_Properties(int, int, float)=0;
};

#endif
```

C.2 ELEMENTSTIFF.H

```
#if!defined(element_stiffness_h)
#define element_stiffness_h
#define MSize 62

class Element_Stiffness:public Properties
/* Inheritance */
{
private:
      float KE[MSize][MSize];
      float EW[MSize][MSize];
      float EF[MSize][MSize];
      float P[MSize][MSize];
      float Q[MSize][MSize];
      float PT[MSize][MSize];
      float QT[MSize][MSize];
      float C[MSize][MSize];
      float CT[MSize][MSize];
      float DT[MSize][MSize];
      float D[MSize][MSize];
      float X1[MSize][MSize];
      float X2[MSize][MSize];
      float X3[MSize][MSize];
      float X4[MSize][MSize];
      float Y1[MSize][MSize];
      float Y2[MSize][MSize];
      float Y3[MSize][MSize];
      float Y4[MSize][MSize];
public:
      friend int main();
      friend class Stiffness;
      void Fill_Element_Stiffness(float, int, float);
      void Fill_Properties(int, int, float);
};
#endif
```

C.3 ELEMENTGEOM.H

```
#if!defined(element_geometric_h)
#define element_geometric_h
#define MSize 62

class Element_Geometric:public Properties
{
    private:
        float KG[MSize][MSize];
        float GW[MSize][MSize];
        float GF[MSize][MSize];
        float P[MSize][MSize];
        float Q[MSize][MSize];
        float PT[MSize][MSize];
        float QT[MSize][MSize];
        float C[MSize][MSize];
        float CT[MSize][MSize];
        float DT[MSize][MSize];
        float D[MSize][MSize];
        float X1[MSize][MSize];
        float X2[MSize][MSize];
        float X3[MSize][MSize];
        float X4[MSize][MSize];
        float Y1[MSize][MSize];
        float Y2[MSize][MSize];
        float Y3[MSize][MSize];
        float Y4[MSize][MSize];
    public:
        friend class Geometric;
        void Fill_Element_Geometric(float,int,float);
        void Fill_Properties(int, int, float);
};

#endif
```

C.4 STIFFN.H

```
#if!defined(stiffness_h)
#define stiffness_h
#define MSize 62

class Stiffness
{
private:
     Element_Stiffness stiff;    //Element Stiffness matrix
     int element_num;//number of elements
     float length;
public:
     float A[MSize][MSize];
     Stiffness(int);
     void Assembling_Stiffness_Matrix(float,int,float);
};

#endif
```

C.5 GEOMTR.H

```
#if!defined(geometric_h)
#define geometric_h
#define MSize 62

class Geometric
{
     private:
          Element_Geometric geom;    //element geometric matrix
          int element_num; //number of elements
          float length;
     public:
          float B[MSize][MSize];
          Geometric(int);
          void Assembling_Geometric_Matrix(float,int,float);
};
#endif
```

C.6 SPPRT.H

```
#if!defined(support_h)
#define support_h
#define MSize 62

class Supports
{
private:
     int restrain[MSize];
     int rest;
     int size;          //Total degrees of freedom
     int free_size;     //Free degrees of freedom
public:
     Supports(int);
     void Get_boundary_conditions();
     int Boundary_Condition(float[MSize][MSize],float[MSize][MSize]);
};
#endif
```

C.7 STANDM.H

```
#if!defined(standard_matrix_h)
#define standard_matrix_h
#define MSize 62

class Standard_Matrix
{
     private:
          int size;
          float dia[MSize];
          float C[MSize][MSize];
          float off[MSize];
          float buckling_load;
public:
     Standard_Matrix();
     void standard_matrix(float[MSize][MSize],float[MSize][MSize],int);
     float pythag(float,float);
```

```
    void choldc(float[MSize][MSize]);
    void tred2(float[MSize][MSize]);
    void tqli(float[MSize][MSize]);
    float getBucklingLoad();
};
#endif
```

C.8 PROP. CPP

```
#include<iostream>
#include<fstream>
#include<stdio.h>
#include"math.h"
#include"prop.h"

using namespace std;

//Fill Element Properties
void Properties::Fill_Properties(int j, int element_num, float length)
{    double PI=3.14159265;
            joint_num=element_num+1;
    float P=0.;
    float L=length/element_num;       //in
    float A0=0.0;
  for(int i=1;i<MSize;i++)
    {z[i]=0.0;h[i]=0.;v[i]=0.;mi[i]=0.0;}
  for(int i=1;i<=joint_num;i++)
    {z[i]=(i-1)*L;}
    zi=z[j];
    zj=z[j+1];
  for(int i=2;i<=joint_num;i++)
    {   h[1]=13.12;
        h[i]=h[i-1]+2*L*tan(A0);
        cout<<h[i]<<endl;
      }
    hi=h[j];
    hj=h[j+1];
  for(int i=1;i<=joint_num;i++)
    {v[i]=P;}
    v[joint_num]=0.;
```

```
      Vi=v[j];
      Vj=v[j+1];
  for(int i=1;i<=joint_num;i++)
  { mi[i]=10000;}
    Mi=mi[j];
}
```

C.9 ELEMENTSTIFF. CPP

```
#include<iostream>
#include<fstream>
#include<stdio.h>
#include"math.h"
#include"prop.h"
#include"elementstiff.h"

using namespace std;

static double PI=3.14159265;

void Element_Stiffness::Fill_Properties(int j,int element_num,float length)
{
      Properties::Fill_Properties(j,element_num,length);
}


void Element_Stiffness::Fill_Element_Stiffness(float K, int element_num,float length)
{     ofstream SaveFile("KE.txt");
      float E=30000; //ksi
      float G=12000; //ksi
      float Jf=5.54; //in^4
      float tw=0.71; //in
      float tf=1.105; //in

      float In=172.19; //in^4
      float Iwf;//in^6
      Iwf=In*pow((hi+hj-2*tf)/2,2)/4;
      cout<<"Iwf="<<Iwf<<endl;
      float L=length/element_num;        //in
```

```
    float A0=-0.0; //rad
    float Lf=L/cos(A0);
    for(int i=1;i<MSize;i++)
        for(int j=1;j<MSize;j++)
            {EW[i][j]=0.;EF[i][j]=0;C[i][j]=0;CT[i][j]=0;D[i][j]=0;DT[i][j]=0;P[i][j]=0;
             PT[i][j]=0;Q[i][j]=0;QT[i][j]=0;KE[i][j]=0;X1[i][j]=0;X2[i][j]=0;X3[i][j]=0;
             X4[i][j]=0; Y1[i][j]=0;Y2[i][j]=0;Y3[i][j]=0;Y4[i][j]=0;}

EW[1][1]=1./2*(hi+hj)*E*pow(tw,3)/pow(L,3);
EW[1][2]=1./6*(2*hi+hj)*E*pow(tw,3)/pow(L,2);
EW[1][3]=0;
EW[1][4]=0;
EW[1][5]=1./2*(-hi-hj)*E*pow(tw,3)/pow(L,3);
EW[1][6]=1./6*(hi+2*hj)*E*pow(tw,3)/pow(L,2);
EW[1][7]=0;
EW[1][8]=0;
EW[2][1]=1./6*(2*hi+hj)*E*pow(tw,3)/pow(L,2);
EW[2][2]=1./12*(3*hi+hj)*E*pow(tw,3)/L;
EW[2][3]=0;
EW[2][4]=0;
EW[2][5]=1./6*(-2*hi-hj)*E*pow(tw,3)/ pow(L,2);
EW[2][6]=1./12*(hi+hj)*E*pow(tw,3)/L;
EW[2][7]=0;
EW[2][8]=0;
EW[3][1]=0;
EW[3][2]=0;
EW[3][3]=pow(tw,3)*(2*G*pow(L,2)*hi+2*G*pow(L,2)*hj+7*E*pow(hi,3)+3*E*pow(hi,2
)*hj+3*E*hi*pow(hj,2)+7*E*pow(hj,3))/(10* pow(L,3));
EW[3][4]=pow(tw,3)*(G*pow(L,2)*hj+15*E*pow(hi,3)+6*E*pow(hi,2)*hj+3*E*hi*pow(hj
,2)+6*E*pow(hj,3))/(30*pow(L,2));
EW[3][5]=0;
EW[3][6]=0;
EW[3][7]=-pow(tw,3)*(2*G*pow(L,2)*hi+2*G*pow(L,2)*hj+7*E*pow(hi,3)+3*E*pow(hi,
2)*hj+3*E*hi*pow(hj,2)+7*E*pow(hj,3))/(10*pow(L,3));
EW[3][8]=pow(tw,3)*(G*pow(L,2)*hi+6*E*pow(hi,3)+3*E*pow(hi,2)*hj+6*E*hi*pow(hj,
2)+15*E*pow(hj,3))/(30*pow(L,2));
EW[4][1]=0;
EW[4][2]=0;
EW[4][3]=pow(tw,3)*(G*pow(L,2)*hj+15*E*pow(hi,3)+6*E*pow(hi,2)*hj+3*E*hi*pow(hj
,2)+6*E*pow(hj,3))/(30*pow(L,2));
EW[4][4]=pow(tw,3)*(3*G*pow(L,2)*hi+G*pow(L,2)*hj+33*E*pow(hi,3)+15*E*pow(hi,2
)*hj+6*E*hi*pow(hj,2)+6*E*pow(hj,3))/(90*L);
```

```
EW[4][5]=0;
EW[4][6]=0;
EW[4][7]=-pow(tw,3)*(G*pow(L,2)*hj+15*E*pow(hi,3)+6*E*pow(hi,2)*hj+3*E*hi*pow(h
j,2)+6*E*pow(hj,3))/(30*pow(L,2));
EW[4][8]=pow(tw,3)*(-G*pow(L,2)*hi-G*pow(L,2)*hj+24*E*pow(hi,3)+6*E*pow(hi,2)*hj
+6*E*hi*pow(hj,2)+24*E*pow(hj,3))/(180*L);
EW[5][1]=-(hi+hj)*E*pow(tw,3)/(2*pow(L,3));
EW[5][2]=-(2*hi+hj)*E*pow(tw,3)/(6*pow(L,2));
EW[5][3]=0;
EW[5][4]=0;
EW[5][5]=(hi+hj)*E*pow(tw,3)/(2*pow(L,3));
EW[5][6]=-(hi+2*hj)*E*pow(tw,3)/(6*pow(L,2));
EW[5][7]=0;
EW[5][8]=0;
EW[6][1]=(hi+2*hj)*E*pow(tw,3)/(6*pow(L,2));
EW[6][2]=(hi+hj)*E*pow(tw,3)/(12*L);
EW[6][3]=0;
EW[6][4]=0;
EW[6][5]=-(hi+2*hj)*E*pow(tw,3)/(6*pow(L,2));
EW[6][6]=(hi+3*hj)*E*pow(tw,3)/(12*L);
EW[6][7]=0;
EW[6][8]=0;
EW[7][1]=0;
EW[7][2]=0;
EW[7][3]=-pow(tw,3)*(2*G*pow(L,2)*hi+2*G*pow(L,2)*hj+7*E*pow(hi,3)+3*E*pow(hi,
2)*hj+3*E*hi*pow(hj,2)+7*E*pow(hj,3))/(10*pow(L,3));
EW[7][4]=-pow(tw,3)*(G*pow(L,2)*hj+15*E*pow(hi,3)+6*E*pow(hi,2)*hj+3*E*hi*pow(h
j,2)+6*E*pow(hj,3))/(30*pow(L,2));
EW[7][5]=0;
EW[7][6]=0;
EW[7][7]=pow(tw,3)*(2*G*pow(L,2)*hi+2*G*pow(L,2)*hj+7*E*pow(hi,3)+3*E*pow(hi,2
)*hj+3*E*hi*pow(hj,2)+7*E*pow(hj,3))/(10*pow(L,3));
EW[7][8]=-pow(tw,3)*(G*pow(L,2)*hi+6*E*pow(hi,3)+3*E*pow(hi,2)*hj+6*E*hi*pow(hj,
2)+15*E*pow(hj,3))/(30*pow(L,2));
EW[8][1]=0;
EW[8][2]=0;
EW[8][3]=pow(tw,3)*(G*pow(L,2)*hi+6*E*pow(hi,3)+3*E*pow(hi,2)*hj+6*E*hi*pow(hj,
2)+15*E*pow(hj,3))/(30*pow(L,2));
EW[8][4]=pow(tw,3)*(-G*pow(L,2)*hi-G*pow(L,2)*hj+24*E*pow(hi,3)+6*E*pow(hi,2)*hj
+6*E*hi*pow(hj,2)+24*E*pow(hj,3))/(180*L);
EW[8][5]=0;
EW[8][6]=0;
```

```
EW[8][7]=-pow(tw,3)*(G*pow(L,2)*hi+6*E*pow(hi,3)+3*E*pow(hi,2)*hj+6*E*hi*pow(hj,
2)+15*E*pow(hj,3))/(30*pow(L,2));
EW[8][8]=pow(tw,3)*(G*pow(L,2)*hi+3*G*pow(L,2)*hj+6*E*pow(hi,3)+6*E*pow(hi,2)*
hj+15*E*hi*pow(hj,2)+33*E*pow(hj,3))/(90*L);

EF[1][1]=12.*E*In/pow(Lf,3);
EF[1][2]=6.*E*In/pow(Lf,2);
EF[1][3]=0;
EF[1][4]=0;
EF[1][5]=-12.*E*In/pow(Lf,3);
EF[1][6]=6.*E*In/pow(Lf,2);
EF[1][7]=0;
EF[1][8]=0;
EF[2][1]=6.*E*In/pow(Lf,2);
EF[2][2]=4.*E*In/Lf;
EF[2][3]=0;
EF[2][4]=0;
EF[2][5]=-6.*E*In/pow(Lf,2);
EF[2][6]=2.*E*In/Lf;
EF[2][7]=0;
EF[2][8]=0;
EF[3][1]=0;
EF[3][2]=0;
EF[3][3]=1./5*(6*G*Jf*pow(Lf,2)+60*E*Iwf)/pow(Lf,3);
EF[3][4]=1./10*(G*Jf*pow(Lf,2)+60*E*Iwf)/pow(Lf,2);
EF[3][5]=0;
EF[3][6]=0;
EF[3][7]=1./5*(-6*G*Jf*pow(Lf,2)-60*E*Iwf)/pow(Lf,3);
EF[3][8]=1./10*(G*Jf*pow(Lf,2)+60*E*Iwf)/pow(Lf,2);
EF[4][1]=0;
EF[4][2]=0;
EF[4][3]=1./10*(G*Jf*pow(Lf,2)+60*E*Iwf)/pow(Lf,2);
EF[4][4]=1./15*(2*G*Jf*pow(Lf,2)+60*E*Iwf)/Lf;
EF[4][5]=0;
EF[4][6]=0;
EF[4][7]=1./10*(-G*Jf*pow(Lf,2)-60*E*Iwf)/pow(Lf,2);
EF[4][8]=1./30*(-G*Jf*pow(Lf,2)+60*E*Iwf)/Lf;
EF[5][1]=-12.*E*In/pow(Lf,3);
EF[5][2]=-6.*E*In/pow(Lf,2);
EF[5][3]=0;
EF[5][4]=0;
EF[5][5]=12.*E*In/pow(Lf,3);
```

```
EF[5][6]=-6.*E*In/pow(Lf,2);
EF[5][7]=0;
EF[5][8]=0;
EF[6][1]=6.*E*In/pow(Lf,2);
EF[6][2]=2.*E*In/Lf;
EF[6][3]=0;
EF[6][4]=0;
EF[6][5]=-6.*E*In/pow(Lf,2);
EF[6][6]=4.*E*In/Lf;
EF[6][7]=0;
EF[6][8]=0;
EF[7][1]=0;
EF[7][2]=0;
EF[7][3]=1./5*(-6*G*Jf*pow(Lf,2)-60*E*Iwf)/pow(Lf,3);
EF[7][4]=1./10*(-G*Jf*pow(Lf,2)-60*E*Iwf)/pow(Lf,2);
EF[7][5]=0;
EF[7][6]=0;
EF[7][7]=1./5*(6*G*Jf*pow(Lf,2)+60*E*Iwf)/pow(Lf,3);
EF[7][8]=1./10*(-G*Jf*pow(Lf,2)-60*E*Iwf)/pow(Lf,2);
EF[8][1]=0;
EF[8][2]=0;
EF[8][3]=1./10*(G*Jf*pow(Lf,2)+60*E*Iwf)/pow(Lf,2);
EF[8][4]=1./30*(-G*Jf*pow(Lf,2)+60*E*Iwf)/Lf;
EF[8][5]=0;
EF[8][6]=0;
EF[8][7]=1./10*(-G*Jf*pow(Lf,2)-60*E*Iwf)/pow(Lf,2);
EF[8][8]=1./15*(2*G*Jf*pow(Lf,2)+60*E*Iwf)/Lf;

Q[1][1]=1;
Q[2][2]=1;
Q[3][3]=1;
Q[4][4]=1;
Q[5][5]=1;
Q[6][6]=1;
Q[7][7]=1;
Q[8][8]=1;
/*Q[1][3]=hi/2;
Q[2][3]=tan(A0);
Q[2][4]=hi/2;
Q[5][7]=hj/2;
Q[6][7]=tan(A0);
Q[6][8]=hj/2;*/
```

```
QT[1][1]=1;
QT[2][2]=1;
QT[3][3]=1;
QT[4][4]=1;
QT[5][5]=1;
QT[6][6]=1;
QT[7][7]=1;
QT[8][8]=1;
/*QT[3][1]=hi/2;
QT[3][2]=tan(A0);
QT[4][2]=hi/2;
QT[7][5]=hj/2;
QT[7][6]=tan(A0);
QT[8][6]=hj/2;*/

P[1][1]=1;
P[2][2]=cos(A0);
P[3][3]=cos(A0);
P[4][4]=1;
P[5][5]=1;
P[6][6]=cos(A0);
P[7][7]=cos(A0);
P[8][8]=1;
P[2][3]=sin(A0);
P[3][2]=-sin(A0);
P[6][7]=sin(A0);
P[7][6]=-sin(A0);

PT[1][1]=1;
PT[2][2]=cos(A0);
PT[3][3]=cos(A0);
PT[4][4]=1;
PT[5][5]=1;
PT[6][6]=cos(A0);
PT[7][7]=cos(A0);
PT[8][8]=1;
PT[3][2]=sin(A0);
PT[2][3]=-sin(A0);
PT[7][6]=sin(A0);
PT[6][7]=-sin(A0);
```

```
C[1][1]=1;
C[2][2]=cos(A0);
C[3][3]=cos(A0);
C[4][4]=1;
C[5][5]=1;
C[6][6]=cos(A0);
C[7][7]=cos(A0);
C[8][8]=1;
C[2][3]=-sin(A0);
C[3][2]=sin(A0);
C[6][7]=-sin(A0);
C[7][6]=sin(A0);

CT[1][1]=1;
CT[2][2]=cos(A0);
CT[3][3]=cos(A0);
CT[4][4]=1;
CT[5][5]=1;
CT[6][6]=cos(A0);
CT[7][7]=cos(A0);
CT[8][8]=1;
CT[3][2]=-sin(A0);
CT[2][3]=sin(A0);
CT[7][6]=-sin(A0);
CT[6][7]=sin(A0);

D[1][1]=1;
D[2][2]=1;
D[3][3]=1;
D[4][4]=1;
D[5][5]=1;
D[6][6]=1;
D[7][7]=1;
D[8][8]=1;
/*D[1][3]=-hi/2;
D[2][3]=-tan(A0);
D[2][4]=-hi/2;
D[5][7]=-hj/2;
D[6][7]=-tan(A0);
D[6][8]=-hj/2;*/
```

```
DT[1][1]=1;
DT[2][2]=1;
DT[3][3]=1;
DT[4][4]=1;
DT[5][5]=1;
DT[6][6]=1;
DT[7][7]=1;
DT[8][8]=1;
/*DT[3][1]=-hi/2;
DT[3][2]=-tan(A0);
DT[4][2]=-hi/2;
DT[7][5]=-hj/2;
DT[7][6]=-tan(A0);
DT[8][6]=-hj/2;*/

for(int i=1;i<=8;i++)
    for(int j=1;j<=8;j++)
    {   for(int k=1;k<=8;k++)
            X1[i][j]=X1[i][j]+QT[i][k]*PT[k][j];
    }
for(int i=1;i<=8;i++)
    for(int j=1;j<=8;j++)
    {   for(int k=1;k<=8;k++)
            X2[i][j]=X2[i][j]+X1[i][k]*EF[k][j];
    }
for(int i=1;i<=8;i++)
    for(int j=1;j<=8;j++)
    {   for(int k=1;k<=8;k++)
            X3[i][j]=X3[i][j]+X2[i][k]*P[k][j];
    }
for(int i=1;i<=8;i++)
    for(int j=1;j<=8;j++)
    {   for(int k=1;k<=8;k++)
            X4[i][j]=X4[i][j]+X3[i][k]*Q[k][j];
    }

for(int i=1;i<=8;i++)
    for(int j=1;j<=8;j++)
    {   for(int k=1;k<=8;k++)
            Y1[i][j]=Y1[i][j]+DT[i][k]*CT[k][j];
    }
```

```
for(int i=1;i<=8;i++)
      for(int j=1;j<=8;j++)
      {     for(int k=1;k<=8;k++)
                  Y2[i][j]=Y2[i][j]+Y1[i][k]*EF[k][j];
      }
for(int i=1;i<=8;i++)
      for(int j=1;j<=8;j++)
      {     for(int k=1;k<=8;k++)
                  Y3[i][j]=Y3[i][j]+Y2[i][k]*C[k][j];
      }
for(int i=1;i<=8;i++)
      for(int j=1;j<=8;j++)
      {     for(int k=1;k<=8;k++)
                  Y4[i][j]=Y4[i][j]+Y3[i][k]*D[k][j];
      }

for(int i=1;i<=8;i++)
      {     for(int j=1;j<=8;j++)
                  KE[i][j]=EW[i][j]+X4[i][j]+Y4[i][j];
      }
for(int j=1;j<=8;j++)
            for(int k=1;k<=8;k++)
            {SaveFile<<"KE["<<j<<"]["<<k<<"]="<<KE[j][k]<<endl;}
      SaveFile.close();
}
```

C.10 ELEMENTGEOM. CPP

```
#include<iostream>
#include<fstream>
#include<stdio.h>
#include"math.h"
#include"prop.h"
#include"elementgeom.h"

using namespace std;

static double PI=3.14159265;

void Element_Geometric::Fill_Properties(int j,int element_num,float length)
```

```
{
    Properties::Fill_Properties(j,element_num,length);
}

/* n means the number of elements*/
void Element_Geometric::Fill_Element_Geometric(float n,int element_num,float length)
{   ofstream SaveFile("KG.txt");
    int i=0;

    float L=length/element_num;       //in
    float A0=-0.0; //rad
    float h1=13.12; //inch
    float d=-h1/2; //in    distance of the loading above the flange
    float zp=length;
    float q=0.;
    float P=0.; //kips
    float F=0.;
    for(int i=1;i<MSize;i++)
        for(int j=1;j<MSize;j++)
        {KG[i][j]=0;}
KG[1][1]=(6.*F)/(5*L);
KG[1][2]=F/10.;
KG[1][3]=(-6.*Mi)/(5*L)-Vi/10.;
KG[1][4]=-Mi/10.;
KG[1][5]=(-6.*F)/(5.*L);
KG[1][6]=F/10;
KG[1][7]=(6.*Mi)/(5.*L)+(11.*Vi)/10.;
KG[1][8]=-Mi/10.-(L*Vi)/10.;
KG[2][1]=KG[1][2];
KG[2][2]=(2.*F*L)/15.;
KG[2][3]=(-11.*Mi)/10.-(L*Vi)/5.;
KG[2][4]=-(2.*L*Mi)/15.-((L*L)*Vi)/30.;
KG[2][5]=-F/10.;
KG[2][6]=-(F*L)/30.;
KG[2][7]=Mi/10.+(L*Vi)/5.;
KG[2][8]=(L*Mi)/30.;
KG[3][1]=KG[1][3];
KG[3][2]=KG[2][3];
KG[3][3]=P*(d+h1/2+zp*0)-(6.*P*(d+h1/2+zp*0)*zp*zp)/(L*L)+(4.*P*(d+h1/2+zp*0)*zp*
zp*zp)/(L*L*L)+(9.*P*(d+h1/2+zp*0)*zp*zp*zp*zp)/(L*L*L*L)-(12.*P*(d+h1/2.+zp*0)*z
p*zp*zp*zp*zp)/(L*L*L*L*L)+(4.*P*(d+h1/2+zp*0)*zp*zp*zp*zp*zp*zp)/(L*L*L*L*L*L
);
```

```
KG[3][4]=P*(d+h1/2+zp*0)*zp-(2.*P*(d+h1/2+zp*0)*zp*zp)/L-(2.*P*(d+h1/2+zp*0)*zp*zp*zp)/(L*L)+(8.*P*(d+h1/2+zp*0)*zp*zp*zp*zp)/(L*L*L)-(7.*P*(d+h1/2.+zp*0)*zp*zp*zp*zp*zp)/(L*L*L*L)+(2.*P*(d+h1/2+zp*0)*zp*zp*zp*zp*zp*zp)/(L*L*L*L*L);
KG[3][5]=(6.*Mi)/(5.*L)+Vi/10.;
KG[3][6]=-Mi/10.+(L*Vi)/10.;
KG[3][7]=(3.*P*(d+h1/2+zp*0)*zp*zp)/(L*L)-(2.*P*(d+h1/2+zp*0)*zp*zp*zp)/(L*L*L)-(9.*P*(d+h1/2+zp*0)*zp*zp*zp*zp)/(L*L*L*L)+(12.*P*(d+h1/2+zp*0)*zp*zp*zp*zp*zp)/(L*L*L*L*L)-(4.*P*(d+h1/2+zp*0)*zp*zp*zp*zp*zp*zp)/(L*L*L*L*L*L);
KG[3][8]=-(P*(d+h1/2+zp*0)*zp*zp)/L+(P*(d+h1/2+zp*0)*zp*zp*zp)/(L*L)+(3.*P*(d+h1/2+zp*0)*zp*zp*zp*zp)/(L*L*L)-(5.*P*(d+h1/2.+zp*0)*zp*zp*zp*zp*zp)/(L*L*L*L)+(2.*P*(d+h1/2+zp*0)*zp*zp*zp*zp*zp*zp)/(L*L*L*L*L);
KG[4][1]=KG[1][4];
KG[4][2]=KG[2][4];
KG[4][3]=KG[3][4];
KG[4][4]=P*(d+h1/2+zp*0)*zp*zp-(4.*P*(d+h1/2.+zp*0)*zp*zp*zp)/L+(6.*P*(d+h1/2.+zp*0)*zp*zp*zp*zp)/(L*L)-(4.*P*(d+h1/2.+zp*0)*zp*zp*zp*zp*zp)/(L*L*L)+(P*(d+h1/2.+zp*0)*zp*zp*zp*zp*zp*zp)/(L*L*L*L);
KG[4][5]=Mi/10;
KG[4][6]=(L*Mi)/30.+((L*L)*Vi)/30;
KG[4][7]=(3.*P*(d+h1/2+zp*0)*zp*zp*zp)/(L*L)-(8.*P*(d+h1/2+zp*0)*zp*zp*zp*zp)/(L*L)+(7.*P*(d+h1/2.+zp*0)*zp*zp*zp*zp*zp)/(L*L*L*L)-(2.*P*(d+h1/2.+zp*0)*zp*zp*zp*zp*zp*zp)/(L*L*L*L*L);
KG[4][8]=-(P*(d+h1/2+zp*0)*zp*zp*zp)/L+(3.*P*(d+h1/2+zp*0)*zp*zp*zp*zp)/(L*L)-(3.*P*(d+h1/2+zp*0)*zp*zp*zp*zp*zp)/(L*L*L)+(P*(d+h1/2+zp*0)*zp*zp*zp*zp*zp*zp)/(L*L*L*L);
KG[5][1]=KG[1][5];
KG[5][2]=KG[2][5];
KG[5][3]=KG[3][5];
KG[5][4]=KG[4][5];
KG[5][5]=(6.*F)/(5.*L);
KG[5][6]=-F/10.;
KG[5][7]=(-6.*Mi)/(5.*L)-(11.*Vi)/10.;
KG[5][8]=Mi/10.+(L*Vi)/10.;
KG[6][1]=KG[1][6];
KG[6][2]=KG[2][6];
KG[6][3]=KG[3][6];
KG[6][4]=KG[4][6];
KG[6][5]=KG[5][6];
KG[6][6]=(2.*F*L)/15;
KG[6][7]=(11.*Mi)/10+(9.*L*Vi)/10;
KG[6][8]=(-2.*L*Mi)/15-((L*L)*Vi)/10.;
```

```
KG[7][1]=KG[1][7];
KG[7][2]=KG[2][7];
KG[7][3]=KG[3][7];
KG[7][4]=KG[4][7];
KG[7][5]=KG[5][7];
KG[7][6]=KG[6][7];
KG[7][7]=(9.*P*(d+h1/2+zp*0)*zp*zp*zp*zp)/(L*L*L*L)-(12.*P*(d+h1/2+zp*0)*zp*zp*z
p*zp*zp)/(L*L*L*L*L)+(4.*P*(d+h1/2+zp*0)*zp*zp*zp*zp*zp*zp)/(L*L*L*L*L*L);
KG[7][8]=-(3.*P*(d+h1/2+zp*0)*zp*zp*zp*zp)/(L*L*L)+(5.*P*(d+h1/2+zp*0)*zp*zp*zp*
zp*zp)/(L*L*L*L)-(2.*P*(d+h1/2+zp*0)*zp*zp*zp*zp*zp*zp)/(L*L*L*L*L);
KG[8][1]=KG[1][8];
KG[8][2]=KG[2][8];
KG[8][3]=KG[3][8];
KG[8][4]=KG[4][8];
KG[8][5]=KG[5][8];
KG[8][6]=KG[6][8];
KG[8][7]=KG[7][8];
KG[8][8]=(P*(d+h1/2)*zp*zp*zp*zp)/(L*L)-(2.*P*(d+h1/2+zp*0)*zp*zp*zp*zp*zp)/(L*L*
L)+(P*(d+h1/2+zp*0)*zp*zp*zp*zp*zp*zp)/(L*L*L*L);

for(int j=1;j<=8;j++)
        for(int k=1;k<=8;k++)
        {SaveFile<<"KG["<<j<<"]["<<k<<"]="<<KG[j][k]<<endl;}
         SaveFile.close();
}
```

C.11 STIFFN. CPP

```
#include "prop.h"
#include "elementstiff.h"
#include "stiffn.h"
#include<iostream>

using namespace std;

//Constructor
Stiffness::Stiffness(int e)
{
    for(int i=1;i<MSize;i++)
```

```
            for(int j=1;j<MSize;j++)
                A[i][j]=0.0;
        element_num=e;
}

//Assemble element stiffness matrices,KE,
//to a structural stiffness matrix, A

void Stiffness::Assembling_Stiffness_Matrix(float K, int element_num,float length)
{   int j1=1;int j2=2;

    for(int i=1;i<=element_num;i++) //for each element
    {   stiff.Fill_Properties(i,element_num,length);//Read in properties
        //Fill element matrix;
        stiff.Fill_Element_Stiffness(K,element_num,length);
        for(int j=1;j<=4;j++)           //Fill Global Matrix
        {
            for(int k=1;k<=4;k++)
            {
                A[4*(j1-1)+j][4*(j1-1)+k]+=stiff.KE[j][k];
                A[4*(j2-1)+j][4*(j2-1)+k]+=stiff.KE[j+4][k+4];
                A[4*(j2-1)+j][4*(j1-1)+k]+=stiff.KE[j+4][k];
                A[4*(j1-1)+j][4*(j2-1)+k]+=stiff.KE[j][k+4];
                //Get the stiffness matrix for each element(two nodes)
                //in global matrix
            }
        }
        j1=j1+1;j2=j2+1;
    }

}
```

C.12 GEOMTR. CPP

```
#include<iostream>
#include"prop.h"
#include"elementgeom.h"
#include"geomtr.h"

using namespace std;
```

```
Geometric::Geometric(int e)
{
    for(int i=0;i<MSize;i++)        //Clear Geometric Matrix
        for(int j=0;j<MSize;j++)
            B[i][j]=0.0;
    element_num=e;
}

//Assemble element geometric matrices to
//a global geometric matrix


void Geometric::Assembling_Geometric_Matrix(float K,int element_num,float length)
{   int j1=1;int j2=2;
    for(int i=1;i<=element_num;i++)   //for each element
    {
        geom.Fill_Properties(i,element_num,length);          //Fill element matrix and rotate
        geom.Fill_Element_Geometric(K,element_num,length);
        for(int j=1;j<=4;j++)       //Fill Global Matrix
        {
            for(int k=1;k<=4;k++)
            {   B[4*(j1-1)+j][4*(j1-1)+k]+=geom.KG[j][k];
                B[4*(j2-1)+j][4*(j2-1)+k]+=geom.KG[j+4][k+4];
                B[4*(j2-1)+j][4*(j1-1)+k]+=geom.KG[j+4][k];
                B[4*(j1-1)+j][4*(j2-1)+k]+=geom.KG[j][k+4];
                //Get the stiffness matrix for each element(two nodes)
                //in global matrix
            }

        }
        ++j1;++j2;
    }
}
```

C.13 SPPRT. CPP

```
#include<iostream>
#include"spprt.h"
```

```
using namespace std;


Supports::Supports(int s)
{
	size=s;
	rest=0;
	for(int i=1;i<MSize;i++)
		restrain[i]=0;
}

//Read the Boundary condition
void Supports::Get_boundary_conditions()
{
	/*restrain[1]=1;
	restrain[2]=1;
	restrain[3]=1;
	restrain[4]=1;*/
	restrain[1]=1;
	restrain[3]=1;
	/*restrain[size]=1;
	restrain[size-1]=1;
	restrain[size-2]=1;
	restrain[size-3]=1;*/
	rest=2;				//number of restraints
}

//Apply BCs to the stiffness matrix and geometric stiffness matrix

int Supports::Boundary_Condition(float X[MSize][MSize], float Y[MSize][MSize])
{
	int r=0;
	for(int i=1;i<=size;i++)
		if(restrain[i]==1)
		{
			for(int j=1;j<=size;j++)
				for(int k=i-r;k<=size-r;k++)
					X[k][j]=X[k+1][j];
			r++;
		}
	r=0;
	for(int i=1;i<=size;i++)
```

```
        if(restrain[i]==1)
        {
            for(int j=1;j<=size-rest;j++)
                for(int k=i-r;k<=size-r;k++)
                    X[j][k]=X[j][k+1];
            r++;
        }
    r=0;
    for(int i=1;i<=size;i++)
        if(restrain[i]==1)
        {
            for(int j=1;j<=size;j++)
                for(int k=i-r;k<=size-r;k++)
                    Y[k][j]=Y[k+1][j];
            r++;
        }
    r=0;
    for(int i=1;i<=size;i++)
        if(restrain[i]==1)
        {
            for(int j=1;j<=size-rest;j++)
                for(int k=i-r;k<=size-r;k++)
                    Y[j][k]=Y[j][k+1];
            r++;
        }
    cout<<"rest="<<rest<<endl;
    free_size=size-rest;
    return free_size;

}
```

C.14 STANDM. CPP

```
#include<iostream>
#include<fstream>
#include<stdio.h>
#include"math.h"
#include"prop.h"
#include"elementstiff.h"
#include"stiffn.h"
```

```
#include"elementgeom.h"
#include"geomtr.h"
#include"standm.h"
using namespace std;

#define SIGN(a,b)((b)>=0.0?fabs(a):-fabs(a))

Standard_Matrix::Standard_Matrix()
{
      for(int i=1;i<MSize;i++)
            for(int j=1;j<MSize;j++)
            {C[i][j]=0.0;}
}
//Standard_Matrix: Decompose the stiffness matrices to
//a standard matrix, and solve the eigenvalues
void Standard_Matrix::standard_matrix(float A[MSize][MSize], float B[MSize][MSize], int
s)
{ofstream SaveFile("Standm.txt");
  size=s;
  choldc(A);    //Cholevski  Decomposition
  for(int i=1;i<=size;i++)
        for(int j=1;j<=size;j++)
        {   C[i][j]=0.0;
            for(int k=1;k<=size;k++)
                  C[i][j]=C[i][j]+A[i][k]*B[k][j];    //A=L(-1)
        }
      for(int i=1;i<=size;i++)
            for(int j=1;j<=size;j++)
            SaveFile<<"L(-1)["<<i<<"]["<<j<<"]="<<A[i][j]<<endl;
      for(int i=1;i<=size;i++)
            for(int j=1;j<=size;j++)
                  if(i>j)
                  {
                        A[j][i]=A[i][j];    //A=LT(-1)
                        A[i][j]=0.0;
                  }
      for(int i=1;i<=size;i++)
            for(int j=1;j<=size;j++)
            SaveFile<<"LT(-1)["<<i<<"]["<<j<<"]="<<A[i][j]<<endl;
    for(int i=1;i<=size;i++)
          for(int j=1;j<=size;j++)
          {   B[i][j]=0.0;
```

```
            for(int k=1;k<=size;k++)
              B[i][j]=B[i][j]+C[i][k]*A[k][j];
              SaveFile<<"S["<<i<<"]["<<j<<"]="<<B[i][j]<<endl;
        }
   tred2(B);
      for(int i=1;i<=size;i++)
        for(int j=1;j<=size;j++)
            SaveFile<<"After_TRED2_B["<<i<<"]["<<j<<"]="<<B[i][j]<<endl;
   tqli(B);
       for(int i=1;i<=size;i++)
        for(int j=1;j<=size;j++)
            SaveFile<<"After_TQLI_B["<<i<<"]["<<j<<"]="<<B[i][j]<<endl;
}

void Standard_Matrix::choldc(float A[MSize][MSize])
{    int i=0,j=0,k=0;
     double sum=0.0, p[MSize];
     for(int i=1;i<=size;i++)
     {
          p[i]=0.0;
          for(int j=i;j<=size;j++)
          {
               sum=(double)A[i][j];
               for(k=i-1;k>=1;k--)                    {
                    sum-=(double)A[i][k]*A[j][k];
               }
               if(i==j)
               {
                    if(sum<=0.0)
                    {
                         cout<<"choldc failed"<<endl;
                         exit(0);
                    }
                    p[i]=sqrt(sum);
                    }
               else A[j][i]=(float)sum/p[i];
          }
     }

     for(int i=1;i<=size;i++)
     {
          for(int j=1;j<=size;j++)
```

```
        {
            if(i>j) A[i][j]=A[i][j];
            else  A[i][j]=(i==j?p[i]:0.0);
        }
    }
    for(int i=1;i<=size;i++)
    {
        A[i][i]=1.0/p[i];
        for(int j=i+1;j<=size;j++)
        {
            sum=0.0;
            for(int k=i;k<j;k++)
                sum-=A[j][k]*A[k][i];
            A[j][i]=(float)sum/p[j];
        }
    }
}

    /*(C) Copr.1986-92 Numerical Recipes Software 5.){2p491&0X43''52'(.*/

    //Apply Householder's method to change the standard matrix
    //to Tridiagonal matrix,and calculate eigenvalue by QL iteration

    void Standard_Matrix::tred2(float B[MSize][MSize])
    {
        int i,l,k,j,n=size;
        float scale,hh,h,g,f;
        for(int i=n;i>=2;i--)
        {
            l=i-1;
            h=scale=0.0;
            if(l>1)
            {
                for(k=1;k<=l;k++)
                    scale+=(float)fabs(B[i][k]);
                if(scale==0.0)
                    off[i]=B[i][l];
                else{
                        for(k=1;k<=l;k++)
                        {
                            B[i][k]/=scale;
                            h+=B[i][k]*B[i][k];
```

```
                    }
                    f=B[i][l];
                    g=(f>0.0?(float)-sqrt(h):(float)sqrt(h));
                    off[i]=scale*g;
                    h-=f*g;
                    B[i][l]=f-g;
                    f=0.0;
                    for(j=1;j<=l;j++)
                    {
                        B[j][i]=B[i][j]/h;
                        g=0.0;
                        for(k=1;k<=j;k++)
                            g+=B[j][k]*B[i][k];
                        for(k=j+1;k<=l;k++)
                            g+=B[k][j]*B[i][k];
                        off[j]=g/h;
                        f+=off[j]*B[i][j];
                    }
                    hh=(float)f/(h+h);
                    for(j=1;j<=l;j++)
                    {
                        f=B[i][j];
                        off[j]=g=off[j]-hh*f;
                        for(k=1;k<=j;k++)
                            B[j][k]-=(f*off[k]+g*B[i][k]);
                    }
                }
            }
            else
                off[i]=B[i][l];
            dia[i]=h;
        }
        dia[1]=0.0;off[1]=0.0;
        /*contents of this loop can be omitted if eigenvectors not wanted
        except for statement d[i]=B[i][j];*/

        for(int i=1;i<=n;i++)
        {
            l=i-1;
            if(dia[i])
            {
                for(j=1;j<=l;j++)
```

```
                {
                    g=0.0;
                    for(k=1;k<=l;k++)
                        g+=B[i][k]*B[k][j];
                    for(k=1;k<=l;k++)
                        B[k][j]-=g*B[k][i];
                }
            }
                dia[i]=B[i][i];
            B[i][i]=1.0;
                for (j=1;j<=l;j++) B[j][i]=B[i][j]=0.0;
        }
}
/*(C) Copr.1986-92 Numerical Recipes Software 5.){2p491&0X43''52'(.*/

// tqli:Solve eigenvalues from the tridiagonal matrix
void Standard_Matrix::tqli(float B[MSize][MSize])
{
    int i,l,k,m,iter,n=size;
    float s,r,p,g,f,dd,c,b,bkp;
    float chkmin=99999999.9;

    for(i=2;i<=n;i++)
        off[i-1]=off[i];
    off[n]=0.0;

    for(l=1;l<=n;l++)
    {
        iter=0;
        do
        {
            for(m=l;m<=n-1;m++)
            {
                dd=(float)fabs(dia[m])+(float)fabs(dia[m+1]);
                if(((float)fabs(off[m])+dd==dd)) break;
            }
            if(m!=l)
            {
                if(iter++==30)
                {
                    cout<<"Too many iterations in tqli"<<endl;
                    exit(0);
```

```
                }
                g=(dia[l+1]-dia[l])/(2.0*off[l]);
                r=pythag(g,1.0);
                g=dia[m]-dia[l]+off[l]/(g+(float)SIGN(r,g));
                s=c=1.0;
                p=0.0;

                for(i=m-1;i>=l;i--)
                {
                    f=s*off[i];
                    b=c*off[i];
                    if(fabs(f)>=fabs(g))
                    {
                        c=g/f;
                        r=pythag(c,1.0);
                        off[i+1]=f*r;
                        c*=(s=1.0/r);
                    }
                    else
                    {
                        s=f/g;
                        r=pythag(s,1.0);
                        off[i+1]=g*r;
                        s*=(c=1.0/r);
                    }
                    g=dia[i+1]-p;
                    r=(dia[i]-g)*s+2.0*c*b;
                    p=s*r;
                    dia[i+1]=g+p;
                    g=c*r-b;
                }
                dia[l]-=p;
                off[l]=g;
                off[m]=0.0;
            }
        }while(m!=l);
}
for(int i=1;i<n;i++)
{
    if(dia[i]!=0)
    {   cout<<"dia["<<i<<"]="<<dia[i]<<endl;
        bkp=fabs(float(1.0/dia[i]));
```

```
                cout<<"bkp="<<bkp<<endl;
                if(bkp>0.0001)
                    if(chkmin>bkp)
                        chkmin=bkp;
            }
        }
        buckling_load=chkmin;
    }

    /*(C) Copr.1986-92 Numerical Recipes Software 5.){2p491&0X43''52'(.*/

    //Pythagorus function
    float Standard_Matrix::pythag(const float a,const float b)
    {
        float c;
        float fabsa=fabs(a);
        float fabsb=fabs(b);
        c=(fabsa>fabsb?fabsa*sqrt(1.0+(fabsb*fabsb)/(fabsa*fabsa)):
            (fabsb==0.0?0.0:fabsb*sqrt(1.0+(fabsa*fabsa)/(fabsb*fabsb))));
        return c;
    }

    float Standard_Matrix::getBucklingLoad()
    {
        return buckling_load;

    }
```

C. 15 LBUCK. CPP

```
#include<iostream>
#include<stdio.h>
#include<fstream>
#include"process.h"
#include"prop.h"
#include"elementstiff.h"
#include"stiffn.h"
#include"spprt.h"
#include"elementgeom.h"
#include"geomtr.h"
```

```
#include"standm.h"

using namespace std;

int main(void)
{       ofstream SaveFile("buckling.txt");
        int joint_num,element_num; //number of joints and elements
        float P=10000.,length;
        cout<<"Please input beam length:";
        cin>>length;
        cout<<"Please input element number:";
        cin>>element_num;
        joint_num=element_num+1;
        SaveFile<<"Element number is:"<<element_num<<endl;
        SaveFile<<"Joint number is:"<<joint_num<<endl;
        joint_num=element_num+1;
        int size=joint_num*4;

        Stiffness global_stiff(element_num); //Create global stiffness matrix
        Geometric global_geom(element_num); //Create global geometric matrix
        Standard_Matrix std;                    //Create standard matrix
        Supports sp(size);                      //Create support object

        //Call the stiffness matrix and the
        //geometric stiffness matrix
        global_stiff.Assembling_Stiffness_Matrix(0.,element_num,length);
        global_geom.Assembling_Geometric_Matrix(0.,element_num,length);

        //Apply Boundary Conditions
        sp.Get_boundary_conditions();
        int s=sp.Boundary_Condition(global_stiff.A,global_geom.B);
        for(int j=1;j<=size;j++)            //Read Global Matrix
        {
            for(int k=1;k<=size;k++)
            {
              SaveFile<<"A["<<j<<"]["<<k<<"]="<<global_stiff.A[j][k]<<endl;
              }
        }
       for(int j=1;j<=size;j++)             //Read Global Matrix
        {
            for(int k=1;k<=size;k++)
            {
```

```
            SaveFile<<"B["<<j<<"]["<<k<<"]="<<global_geom.B[j][k]<<endl;
            }
        }
        //Find Standard Matrix
        sd.standard_matrix(global_stiff.A,global_geom.B,s);
        //Print Buckling Load
        float buck_load=sd.getBucklingLoad();
        SaveFile<<"BucklingLoad is "<<buck_load*P<<endl;
        cout<<"BucklingLoad is "<<buck_load*P<<endl;
        SaveFile.close();
        system("pause");

}
```

BIBLIOGRAPHY

American Institute of Steel Construction (1994). *Steel Construction Manual*, American Institute of Steel Construction, Chicago, IL.

American Institute of Steel Construction (2009). *Steel Construction Manual*, American Institute of Steel Construction, Chicago, IL.

Anderson, J. M., and Trahair, N. S. (1972). Stability of Monosymmetric Beams and Cantilevers. *Journal of the Structural Division, ASCE, 98*(1), 269-285.

Andrade A., and Camotim D. (2005). Lateral-torsional buckling of singly-symmetric tapered beams: Theory and application. *Journal of Engineering Mechanics; 131*(6): 586-97.

Andrade A, Camotim D., and Dinis P. B. (2007). Lateral-torsional buckling of singly-symmetric web-tapered thin-walled I-beams: 1D model vs. shell FEA. *Computers and Structures*, 85 (2007), 1343–1359.

Assadi, M., and Roeder, C. W. (1985). Stability of Continuously Restrained Cantilevers. *Journal of Engineering Mechanics, 111*(12), 1440-1456.

Barsoum, R. S., and Gallagher, R. H. (1970). Finite Element Analysis of Torsional and Torsional-flexural Stability Problems. *International Journal for Numerical Method in Engineering*, *2*(3), 335-352.

Bazant, Z. P. (1965). Nonuniform torsion of thin-walled bars of variable cross section. *International Association of Bridge Structural Engineering 25* 17–39.

Bazeos, N., and Xykis, C. (2002). Elastic Buckling Analysis of 3-D Trusses and Frames with Thin-Walled Members. *Computational Mechanics, 29*(6), 459-470.

Bleich, F. (1952). *Buckling Strength of Metal Structures*. McGraw-Hill, New York.

Boresi, A. P., Schmidt, R. J., and Sidebottom, O. M. (1993). *Advanced Mechanics of Materials (5th edition).* John Wiley&Sons, New York.

Bradford, M. A., and Ronagh, H. R. (1997). Generalized Elastic Buckling of Restrained I-Beams by FEM. *Journal of Structural Engineering, ASCE, 123*(12), 1631-1637.

Bradford M.A., and Cuk P.E. (1988). Elastic buckling of tapered monosymmetric I-beams. *Journal of Structural Engineering, 114*(5), 977-996.

Chajes, A. (1993). *Principles of Structural Stability Theory*. Englewood Cliffs, Prentice-Hall, New Jersey.

Cywinski, Z. (1964). Theory of torsion of thin-walled bars with variable rigidity. *Arch. Inzynieru Ladovej* 10 (2) 161–183.

Fowler, M. (1999). *Refactoring, Improving the Design of Existing Code*. Addison-Wesley, Massachusetts.

Fowler, M. and Scott, K. (2000). *UML Distilled Second Edition: A Brief Guide to the Standard Object Modeling Languag.* Addison-Wesley, Massachusetts.

Galambos, T. V. (1963). Inelastic Lateral Buckling of Beams. *Journal of the Structural Division, ASCE, 89*(ST5), 217-242.

Griffiths, D. V. and Smith, I. M. (1991). *Numerical Methods for Engineers*. London, England: Blackwell Scientific Publications.

Hancock, G. J., and Trahair, N. S. (1978). Finite Element Analysis of Lateral Buckling of Continuously Restrained Beam-Columns. *Civil Engineering Transations, Institution of Engineering, Australia, CE20*(2), 120-127.

Horne, M. R. (1950). *Critical Loading Condition of Engineering Struc*tures. *PhD Dissertation*, Cambridge University, Cambridge, England.

Jacobson, I. (2000). *The Road to the Unified Software Development Process.* Cambridge University Press, New York.

Jacobson, I., Booch, G., and Rumbaugh, J. (1999). *The Unified Software Development Process*. Reading, Addison-Wesley, Massachusetts.

Kitipornchai, S., and Trahair, N.S. (1972). Elastic stability of tapered I-beams. *Journal of the Structural Division, ASCE, 98* (3) 713–728.

Kitipornchai, S., and Trahair, N. S. (1975). Elastic Behavior of Tapered Monosymmetric I-Beams Under Moment Gradient. *Journal of the Structural Division, ASCE*, *101*(8), 1661-1678.

Lafore, R. (2002). *Object-Oriented Programming in C++* (4th ed.). Sams Publishing, Indiana.

Lee, L. H. N. (1959). On the Lateral Buckling of a Tapered Narrow Rectangular Beam. *Journal of Applied Mechanics*, 1959(26) 457-458.

Lee, G. C. (1960). Literature Survey on Lateral Instability and Lateral Bracing Requirements. *Technical Report 62, Welding Research Council Bulletin*, August.

Lee, G.C., Szabo, B.A. (1967). Torsional response of tapered I-girders. *Journal of the Structural Division, ASCE*, *93* (5) 233–252.

Love, A. E. H. (1944). *A Treatise on the mathematical Theory of Elasticity (4th edition)*, Dover Publication, New York.

Mezini, M. (1998). *Variational Object-Oriented Programming Beyond Classes and Inheritance*. Kluwer Academic Publishers, Massachusetts.

Michell, A. G. M. (1899). Elastic Stability of Long Beams under Transverse Forces. *Philosophical Magazine*, *48*, 298-309.

Mohri F., Noureddine D., and Michel P. F. (2008). Large torsion finite element model for thin-walled beams. *Computers and Structures 86*(7-8) 671-683.

Mohri, F., Brouki, A. and Roth, J.C. (2003). Theoretical and numerical stability analyses of unrestrained, mono-symmetric thin-walled beams. *J Construct Steel Res.* v59. 63-90.

Papangelis, J. P., Trahair, N. S., and Hancock, G. L. (1998). Elastic flexural-torsional buckling of structures by computer. *Computers and Structures*, *68*(1-3), 125-137.

Pasquino M., and Marotti-de-Sciarra F. (1992). Buckling of thin-walled beams with open and generically variable section. *Computers and Structures*, *44*(4), 843-849.

Phusit Dontree (1994). *Elatic flexural-torsional buckling analysis using object-oriented technology and C/C++*. Master Thesis, University of Pittsburgh, Pittsburgh, Pennsylvania.

Pilkey, W. D., and Wunderlich, W. (1994). *Mechanics of Structures Variational and Computational Methods*, CRC Press Inc., Boca Patom, Florida.

Pi, Y. L., and Trahair, N. S. (1992a). Prebuckling Deflections and Lateral Buckling. *Journal of Structural Engineering*, ASCE, Vol. 118, No. 11, pp. 2949-2966.

Pi, Y. L., Trahair, N. S., and Rajasekaran, S. (1992b). Energy equation for beam lateral buckling. *Journal of Structural Engineering*, ASCE, Vol. 118, No. 6, June 1992, pp.1462-1479.

Powell, G., and Klingner, R. (1970). Elastic lateral buckling of steel beams. *Journal of the Structural Division, ASCE*, 96(9), 1919-1932.

Prandtl, L. (1899). *Kipperscheinungen*. Munich, Germany: PhD Dissertation.

Press, W. H. (1992). *Numerical Recipes in C: The Art of Scientific Computing*. Cambridge: Cambridge University Press.

Lee G. C., Morell M. L. (1975). Application of AISC Design Provisions for Tapered Members. *Engineering Journal*, Volume 12, pp. 1-13.

Rajasekaran, S. (1994). Equations for tapered thin-walled beams of generic open cross section. *Journal of Engineering Mechanics, ASCE, 120* (8) 1607–1629.

Roberts, E.R.(2004). *Elatic flexural-torsional buckling analysis using finite element method and object-oriented technology with C/C++*. Master Thesis, University of Pittsburgh, Pittsburgh, Pennsylvania.

Ronagh, H. R., Bradford, M. A., and Attard, M. M. (2000). Nonlinear analysis of thin-walled members of variable cross-section, Part I: theory. *Computer Structures 77* 285–299.

Ronagh, H. R., Bradford, M. A., and Attard, M. M. (2000). Nonlinear analysis of thin-walled members of variable cross-section, Part II: application. *Computer Structures 77* 301–313.

Rumbaugh, J., Michael, B., William, P., Frederick, E., and William, L. (1991). *Object-Oriented Modeling and Design*, Prentice Hall, New York.

Sallstrom, J. H. (1996). Accurate Calculation of Elastic Buckling Loads for Space Frames Built up of Uniform Beams of Open Thin-Walled Cross-Section. *International Journal of Numerical Methods in Engineering, 39,* 2319-2333.

Stroustrup, B. (1991). *The C++ Programming Language* (2nd ed.). Reading, Addison-Wesley, Massachusetts.

Timoshenko, S. P., and Gere, J. M. (1961). *Theory of Elastic Stability (2nd ed.).* McGraw-Hill, New York.

Tong, G., and Zhang, L. (2003a). A General Theory for the Flexural-Torsional Buckling of Thin-Walled Members I: Energy Method. *Advances in Structural Engineering, 6*(4), 293-298.

Tong, G., and Zhang, L. (2003b). A General Theory for the Flexural-Torsional Buckling of Thin-Walled Members I: Fictitious Load Method. *Advances in Structural Engineering, 6*(4), 299-308.

Torkamani, M. A. M. (1998). Transformation matrices for finite and small rotations. *Journal of Engineering Mechanics, ASCE*, 124(3), 359-362.

Torkamani, M. A. M., and Erin R. R. (2009)**.** Energy equations for elastic flexural–torsional buckling analysis of plane structures. *Thin-Walled Structures, 47*(4), 463-473.

Trahair, N. S. (1968). Elastic Stability of Propped Cantilevers. *Civil Engineering Transations, Institution of Engineering, Australia*, *CE10* (1), 94-100.

Trahair, N. S. (1983). Lateral buckling of overhanging beams. *Proceedings International Conference On Instability And Plastic Collapse Of Steel Structures*, (ed. L. J. Morris), Granada, London, pp. 503-18.

Trahair, N. S. (1993). *Flexural-Torsional Buckling of Structures.* CRC Press, Boca Raton, Florida.

Vlasov, V. Z. (1961). *Thin-walled Elastic Beams (2nd edition)*. Israel Program for Scientific Translation, Jerusalem, Israel.

Wagner, H. (1929). Torsion and buckling of open sections. in *25th Anniversary Publication*, Technische Hochschule, Danzig.

Wang, C. M., Wang, L., and Ang, K. K. (1994). Beam-Buckling Analysis via Automated Rayleigh-Ritz Method. *Journal of Structural Engineering, ASCE, 120*(1), 200-211.

Wekezer, J. (1985). Instability of thin-walled bars. *Journal of Engineering Mechanics (ASCE)*, 111(7), 923-935.

White, M. W. (1956). *The Lateral Torsional Buckling of Yielded Structural Steel Members*. PhD Dissertation, Lehigh University, Bethlehem, Pennsylvania.

Wilde, P. (1968). The torsion of thin-walled bars with variable cross section. *Arch. Mech. Stosowanej 4* (20) 431–443.

Wittrick, W. H. (1952). Lateral Instability of Rectangular Beams of Strain Hardening Material under Uniform Bending. *Journal of Aeronautical Science, 19*(12).

Yang,Y.B., and Kuo, S.R. (1994). *Theory and Analysis of Nonlinear Framed Structures*, Prentice-Hall, Singapore.

Yang,Y.B., Yau,J.D., and Yin, S.H. (1996). Theory of buckling for tapered beams. *International Conference on Advances in Steel Structures*, Hong Kong, December 11–14, pp. 91–96.

Yang, Y.B., and Yau, J.D. (1987). Stability of beams with tapered I-sections. *Journal of Engineering Mechanics, ASCE, 113* (9) 1337–1357.

Yau, J.D., Yang, Y.B., and Kuo, S.R. (1992). Stability of tapered bars of circular cross-sections under semi- and quasi-tangential torques. *International Journal of Mechanics Science 34*(1) 31–40.

Zhang, L., and Tong, G. S. (2008). Lateral buckling of web-tapered I-beams: A new theory. *Journal of Constructional Steel Research*, 2008.01.014.